(resulting from equilibrium of rain with rock minerals) in polluted and unpolluted regions. Although the questions are obviously related, most of them can be answered independently.

a. What is the pH of the rain in an unpolluted region if it can be considered simply as distilled water in equilibrium with the atmosphere ($P_{CO_2} = 10^{-3.5}$ atm)? What is its buffer capacity?

b. In this case, what are the pH and alkalinity of the groundwater ($P_{CO_2} = 10^{-1.5}$ atm) in a calcite region? In a dolomite region? In an albite region?

c. In a polluted region the rain is actually acidic, pH = 3.7, as a result of equimolar concentrations of nitric and sulfuric acids. What is the mineral acidity of the polluted rainwater? What is its buffer capacity?

d. In the case of acidic precipitation, what are the pH and the alkalinity of the groundwater ($P_{CO_2} = 10^{-1.5}$ atm) in a calcite region? In a dolomite region? In an albite region?

CHAPTER 6

COMPLEXATION

In Chapters 4 and 5 we examined chemical processes that control the geochemical cycles of major elements. The dissolution and dissociation of weakly acidic gases and the weathering and sedimentation of rocks control the gross chemical composition of natural waters. Complex formation—defined here loosely as the reversible reaction of two dissolved species to form a third one—plays a relatively minor role in these major element cycles. Nonetheless, as we shall see, the solubility of a solid such as $CaCO_3$(s) is markedly increased by complexation reactions in seawater compared to freshwater.

For many trace elements, however, the situation is quite different. Their global geochemical cycles may also be controlled by precipitation and dissolution of minerals, but their chemistry in the water column is dominated by complexation, biological uptake, and sorption on suspended solids. All three of these processes, which are particularly important in surface waters where biological activity is most intense, are controlled by the same coordinative mechanisms, all obeying the principles expounded in this chapter. We shall briefly discuss biological uptake at the end of this chapter and leave a detailed study of sorption reactions for Chapter 8.

The topic of aquatic complexation is in a paradoxical state. We know a great deal about coordination chemistry and we can make many chemical models that predict the existence of complexes in natural waters. Yet it is so difficult to analyze for individual chemical species under the conditions prevailing in aquatic systems where the concentrations are very low and the constituents very many, that we can rarely demonstrate the existence of these complexes unambiguously. The elucidation of the chemical speciation of trace elements in natural waters

is probably the greatest remaining challenge to analytical chemists; the objective is to demonstrate and quantify the existence of fractions of chemical constituents as picomolar concentrations of perhaps ephemeral species. Thus, seemingly simple questions are yet unanswered: what are the principal dissolved species of the major and minor components of natural waters? What are the concentrations or the activities of free ions in comparison to the total (analytical) concentrations of chemical constituents?

Besides irrepressible chemical curiosity, a major motivation for asking these questions arises from our interest in the aquatic biota. Chemical constituents of natural waters affect the biota as essential nutrients and as potential toxicants. It is now firmly established that these interactions are directly dependent on the chemical speciation of the constituents. For example, the availability and toxicity of many trace metals to planktonic microorganisms are determined by their free concentrations rather than their total concentrations and are thus decreased by complexation. Trace metal availability and toxicity are not just matters of academic exercises or pollution control; they are thought to be natural controlling environmental factors for aquatic ecosystems. We need to understand the speciation of elements in water if we want to understand the interactions of aquatic organisms with their external milieu. Although the role of complexation in natural waters may be more subtle than geochemists typically care about or than analysts can presently measure, it is a dominant aspect of aquatic chemistry for biologists. Thus, much of this chapter will focus on "biologically interesting" elements such as Fe, Mn, Zn, Co, Ni, Cu, and Cd.

In keeping with the thermodynamic view that we have taken so far, we say little in this chapter regarding the fundamental theories of coordination chemistry. Questions relating to the nature of coordination bonds or comparisons among the coordinative properties of elements and compounds are addressed only briefly. For the most part, we describe chemical species by their stoichiometries and their free energies. Electronic interactions in metal–ligand complexes are discussed primarily to provide some basis for macroscopic observations of the structure and reactivity of these species.

Chemical complexes in natural waters can be conveniently classified into three groups: ion pairs of major constituents, inorganic complexes of trace elements, and organic complexes. These are discussed briefly at the beginning of the chapter where necessary definitions are provided. From simple mole balance considerations, the speciation of abundant aquatic constituents such as Ca^{2+}, Na^+, Cl^-, and HCO_3^- cannot be affected by complexation with those present in trace amounts. Although the nature of the coordination processes may not be very different, the topics of inorganic complexation of major and of trace constituents are thus effectively separate and are presented in consecutive sections. Owing to our relative ignorance of the nature and properties of the dissolved organic matter in natural waters, the question of organic complexation must be addressed largely at a theoretical level. To make the presentation more tangible the scant available data are thus generalized liberally and perhaps speculatively. We close the chapter with the subjects of complexation kinetics and biological uptake, the former serving as a conceptual framework for the latter.

1. AQUEOUS COMPLEXES

Consider a metal ion such as Cu^{2+} in water. Although we commonly talk of the "free cupric ion" in solution, this is really a misnomer, for the metal ion is actually associated with its surrounding water molecules. Inorganic chemists distinguish four solvent regions around a metal ion[1] (see Figure 6.1):

1. A primary solvation shell in which the water molecules are considered chemically bound to the ion. In the case of copper (and many other metals) there are six such water molecules, leading to the more refined chemical symbolism $Cu(H_2O)_6^{2+}$ instead of Cu^{2+} for the hydrated cupric ion.
2. A secondary solvation shell in which the water molecules are ordered by the electrostatic influence of the ion. The volume of this shell increases with the charge of the ion and is inversely related to its size.
3. A transition region separating the hydrated metal ion from the bulk

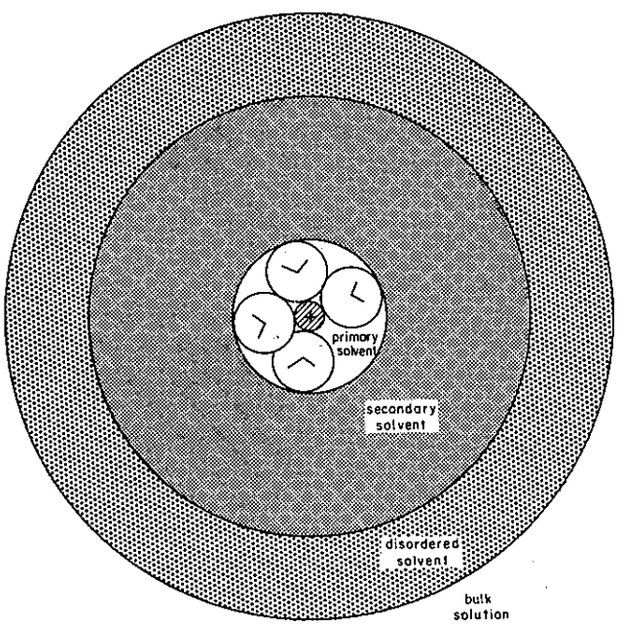

Figure 6.1 The various solvent regions around a metal ion. Adapted from Burgess, 1978.[1]

solution. In this region the water molecules are less ordered than in either the solvation shell or the bulk solution.

4. The bulk solution where the presence of the metal ion is not felt.

From a thermodynamic point of view, the energy of hydration of an ion is critical to its very existence. Ionization of a metal or separation of cations and anions from a crystal lattice are energetically very unfavorable processes. For example, it takes some 2700 kJ mol^{-1} to ionize Cu to Cu^{2+} in the gas phase. The presence of the cupric ion in solution is thus made possible only by a considerable energy of solvation which exceeds the unfavorable ionization energy. Of course, the energetics of the metal–solvent interactions do not normally concern us when we study the thermodynamics of complex formation in aqueous solution and consider only the differences among the free energies of aquated species. However, the large energy of solvation is important for the kinetics of complex formation which are often controlled by the rate of dissociation of the coordinated water molecules, an energetically unfavorable process. Free metal ions in solutions are really aquo complexes, the water itself is a *ligand* that binds metals, and every complexation reaction in water is effectively a *ligand-exchange* reaction.

Other ligands that can replace water molecules around the *central atom* (metal ion) are chemical species that have a nonbonding pair of electrons to share with the metal. These include simple anions such as the halides Cl^-, F^-, Br^-, I^-, more complex inorganic compounds such as NO_3^-, CO_3^{2-}, SO_4^{2-}, NH_3, S^{2-}, PO_4^{3-}, SO_3^{2-}, CN^-, and a great variety of organic molecules with suitable functional groups, usually containing oxygen, nitrogen, or sulfur atoms as purveyors of electron pairs (e.g., R—COO^-; R—OH; R—NH_2; R—SH). For the sake of generality, it is convenient to consider H^+ as a metal and OH^- as a ligand, thus including all acid–base reactions as a subset of coordination reactions.

The reaction of a metal with a ligand can be of an electrostatic or covalent nature or both. When it is primarily electrostatic and the reactants retain some water of hydration between them, the product is called an *ion pair* or an *outer sphere complex*. In natural waters this type of interaction is particularly important among the major ions in high ionic stength media such as seawater. When the reaction of a metal with a ligand involves coordination at several positions, one speaks of *chelation* (in Greek, *chelos* = crab—has two binding claws). Such a reaction requires the combination of a metal with a *coordination number* greater than 1 (i.e., more than one site for coordination), and a *multidentate* ligand, an organic compound with several reactive functional groups. These organic compounds are called *chelators*, *chelating agents*, or *complexing agents*. Among metals, only H^+ has a coordination number of 1; most metals of interest in aquatic chemistry have a coordination number of 6 and thus form octahedral complexes[2] (see Table 6.1). In natural waters, *polynuclear complexes*, those involving more than one metal, are probably rare except for polymeric hydroxide species. In this chapter, we use the word complex somewhat loosely

TABLE 6.1 Common Coordination Numbers and Geometries for Some Metals

Metal Species	CN[a]	Geometry[a]	Example
Li(I)	4	Tetrahedral	$Li(H_2O)_4^+$
Cr(II)	6	Octahedral	$Cr(H_2O)_6^{2+}$
Cr(III)	6	Octahedral	$Cr(H_2O)_6^{3+}$
Cr(VI)	4	Tetrahedral	CrO_4^{2-}
Mn(II)	6	Octahedral	$Mn(H_2O)_6^{2+}$
Mn(III)	6	Octahedral	$Mn(oxalate)_3^{3-}$
Mn(IV)	6	Octahedral	$MnCl_6^{2-}$
Fe(II)	6	Octahedral	$Fe(H_2O)_6^{2+}$
Fe(III)	6	Octahedral	$Fe(H_2O)_6^{3+}$
	(4)	(Tetrahedral)	$FeCl_4^-$
Co(II)	6	Octahedral	$Co(H_2O)_6^{2+}$
	4	Tetrahedral	$CoCl_4^{2-}$
Co(III)	6	Octahedral	$Co(NH_3)_6^{3+}$
Ni(II)	6	Octahedral	$Ni(H_2O)_6^{2+}$
	4	Square planar	$Ni(CN)_4^{2-}$
	(4)	(Tetrahedral)	$NiCl_4^{2-}$
Cu(I)	4	Tetrahedral	$Cu(CN)_4^{3-}$
	(2)	(Linear)	$CuCl_2^-$
Cu(II)	6	Octahedral (distorted)	$Cu(H_2O)_6^{2+}$
	(4)	(Square planar)	$CuCl_4^{2-}$

[a]Less common CN and geometries indicated by parentheses. Based on Cotton and Wilkinson (1972).[2]

to cover all dissolved species resulting from the metal–ligand combinations illustrated in Figure 6.2, including ion pairs and chelates.

Our primary interest is to use thermodynamic data describing metal–ligand interactions, specifically equilibrium constants, to predict the distribution of metal species and the reactivity of metals in natural waters. For this purpose, it is not strictly necessary to understand the factors determining the magnitude of the equilibrium constants for a particular complex or the details of the interaction between metals and ligands. Nonetheless, a brief discussion of the fundamentals of metal–ligand interactions may lend some insight into the chemical characteristics (particularly the stability and reactivity) of metal complexes. We thus now examine the relative importance of enthalpic and entropic factors in determining the thermodynamics of metal–ligand interactions and the effects of electronic interactions and overlap of metal and ligand electron orbitals on the structure and reactivity of metal complexes.

1.1 Thermodynamics of Complex Formation

The changes in standard free energy, ΔG°, upon formation of metal complexes and the corresponding stability constants, $K = \exp(-\Delta G^\circ/RT)$, are due, in large

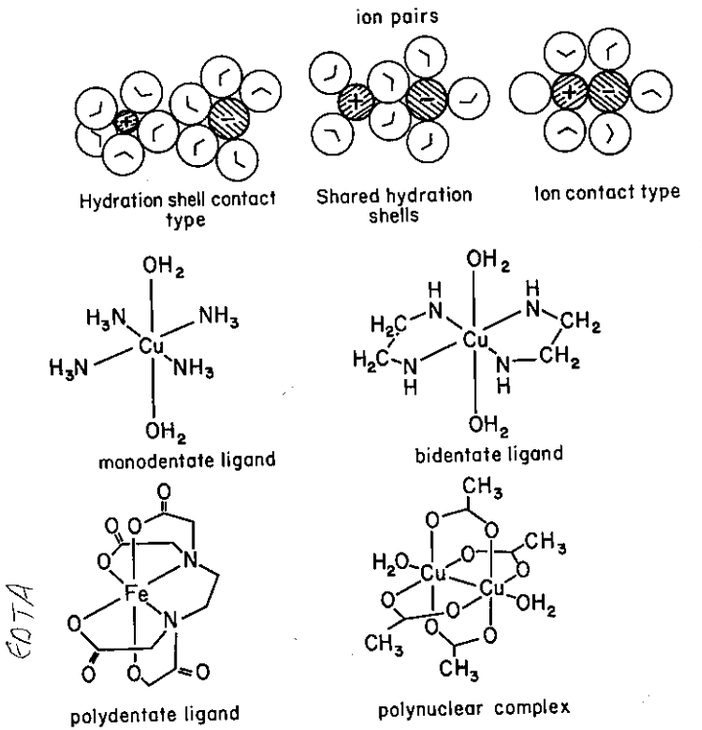

Figure 6.2 Various types of aqueous complexes.

part, to entropic factors. In some cases, for example the hydrolysis of Ca^{2+} or Fe^{3+}, the enthalpy change is actually unfavorable and the reaction proceeds solely because of the favorable change in entropy[3] (Table 6.2). As already mentioned, formation of a complex between a metal ion in solution and a ligand requires displacement of one or more coordinated water molecules from the initial aquo complex. The release of coordinated waters from the relatively constrained metal complex results in a significant increase in entropy. This may be compared to the entropy gained when ice melts as the water molecules are freed from the rigid structure of the solid. The increase in entropy associated with complex formation depends on the strength of the initial interaction between the metal and the coordinated water—the stronger the initial association, the greater the entropy increase as the water is displaced. Decreasing entropic effects would be expected with decreasing charge on the central metal ion or with the stepwise addition of subsequent ligands (cf. Table 6.2). The increased stability of multidentate ligands over monodentate ligands with the same donor atoms (the chelate effect) is also due to entropic factors[2]. This effect may be illustrated by comparing the stability of nickel complexes with NH_3 and ethylenediamine

TABLE 6.2 Enthalpy and Entropy of Complex Formation[a]

Ligand = OH^- Metal	ΔH° ($kJ \cdot mol^{-1}$)	ΔS° ($J \cdot mol^{-1} K^{-1}$)	log K	Ionic Strength
Ca^{2+}	8.4	51.5	1.2	0
	5.0	43.5	1.4	0
Fe^{3+}	5.0	209	11.7	0
Ligand = malonate complex	**ΔH° ($kJ \cdot mol^{-1}$)**	**ΔS° ($J \cdot mol^{-1} K^{-1}$)**	**log K**	**Ionic Strength**
FeL/Fe.L	11.3	181.4	7.5	1
FeL_2/FeL.L	3.1	117	5.54	1
FeL_3/FeL_2.L	−4.6	53	3.56	1

[a]Data for 25°C from Christensen and Izatt (1983).[3]

(en = $H_2NCH_2CH_2NH_2$). In the reaction

$$Ni(NH_3)_6^{2+} + 3(en) = Ni(en)_3^{2+} + 6NH_3$$

the chelate complex is favored ($\Delta G^\circ = -67\ kJ\ mol^{-1}$) predominantly by entropy ($-T\Delta S^\circ = -55\ kJ\ mol^{-1}$). The chelate effect has also been rationalized in terms of the increased probability of binding additional donor atoms of a multidentate ligand, subsequent to attachment of the first donor atom, as compared to the stepwise binding of monodentate ligands.

These thermodynamic arguments, however, cannot be used to rationalize the effects of specific ligands on the characteristics of metal–organic complexes, particularly the spectroscopic characteristics of the complexes, their coordination number and geometry, or the stabilization of different oxidation states of the metal. To understand these aspects of coordination chemistry, we must consider the electronic structure of metals and the electronic interactions between metals and ligands.

1.2 Electronic Configurations of Metals

The chemical and physical properties of the metallic elements depend on their electron configurations, that is, the occupancy of their electron orbitals. Most of the elements (roughly three-fourths) are metals, characterized by their luster, high electrical conductivity (decreasing with increasing temperature), high thermal conductivity, and mechanical properties such as strength and ductility. The metallic elements fall into several groups: *main group* elements, whose outer electron (or *valence*) shells consist solely of s and p electrons; the *transition* elements, which have, either as the neutral atom or as an important ion or both, an incomplete set of d electrons; and the *post-transition* elements, Zn, Cd, and Hg. (Note: The designations s, p, and d refer to electron orbitals of different

shape and symmetry. Superscripts, e.g., s^2, are used to denote the number of electrons in an orbital or occupancy. The maximum occupancy is 2 for s orbitals, 6 for p orbitals, and 10 for d orbitals; the higher orbitals are not of much concern for our purposes.)

Metal chemistry is strongly influenced by the ease with which one or more electrons can be removed from the neutral metal atom. For example, the alkali metals (Li, Na, K, etc.) have only a single electron outside a noble-gas core (corresponding to the very stable electron configuration of the inert or noble gases, e.g. $1s^2$ for He, $1s^2 2s^2 p^6$ for Ne, etc.). Thus, of all the elements, the alkali metals have the lowest first ionization energies, defined as the energies required to remove an electron from the metals as isolated gaseous atoms. These metals react violently with water, the resulting alkali hydroxides are strong bases, and the chemistry of the alkali metals is essentially that of their +1 ions. It is a common feature of the main group and post-transition metals that they occur as ionic species only in a single oxidation state.

In contrast, most transition metals exhibit variable valence, such as +2 and +3 for Fe or +2, +3, +4, +6 and +7 for Mn. Transition metal ions with partially filled d shells are strongly influenced by their surroundings, particularly by their coordinated ligands, because the d orbitals project well out to the periphery of the ions. (Note: We do not consider here the lanthanide or actinide elements, which have partially filled f orbitals, although these elements are formally included among the transition elements.)

1.3 Electronic Interactions in Metal Complexes

The specific influence of ligands on transition metals may be treated in two ways. The first and simpler treatment, ligand field theory (LFT, also called crystal field theory), considers the perturbation of the atomic orbitals of the metal, specifically the d orbitals, by the electrostatic effect of the ligands. The second, molecular orbital theory (MOT), allows for overlap between the metal and ligand orbitals.

In LFT the approach of the ligands, considered as point charges, toward the metal affects the stability of the metal d orbitals because of electrostatic repulsion. As a result, some ions with partially filled d orbitals are energetically more (or less) stable than they would be if the d orbitals were unperturbed. This difference in stability is the ligand field stabilization energy (LFSE). Specifically, for octahedral complexes, the stability of the d orbitals oriented along axes (i.e., $d_{x^2-y^2}$ and d_{z^2}) is decreased and the stability of the d orbitals oriented off the axes (d_{xy}, d_{xz}, d_{yz}) is increased due to the approach of the ligands along the axes (Figure 6.3). An energy diagram (Figure 6.4*a*) then shows the five degenerate levels of the d orbitals split into two higher-energy levels (with the symmetry designation e_g) and three lower-energy levels (with the symmetry designation t_{2g}). Since the geometry of the complex, which is most often either octahedral or tetrahedral, affects the interaction of the coordinating ligands with the metal d orbitals, the different contributions of LFSE partly determine which geometries are favored for various metal complexes (cf. Table 6.1).

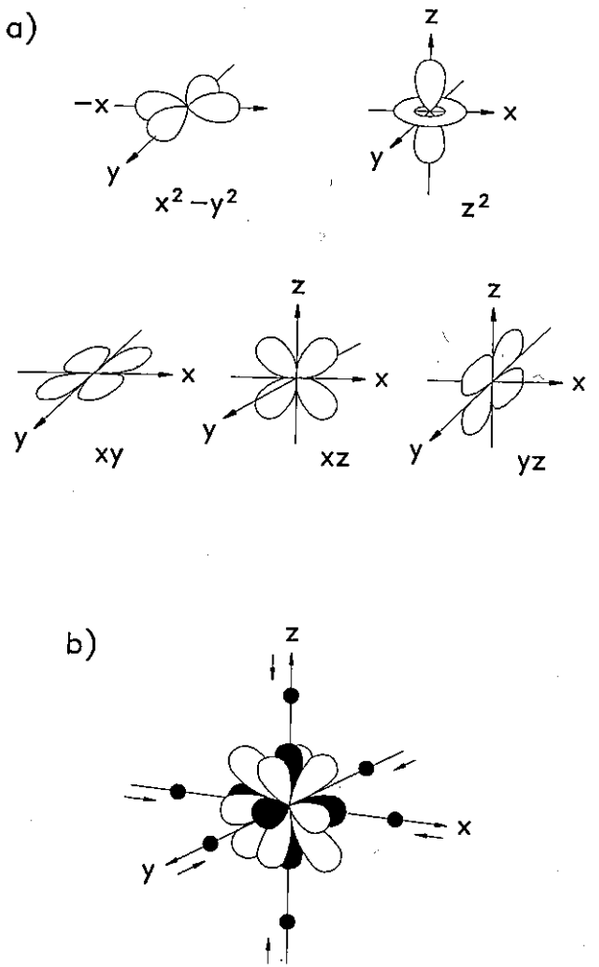

Figure 6.3 Representations of the five d orbitals (xy, xz, yz, z^2, and $x^2 - y^2$). As shown in *a*, two of the orbitals (z^2 and $x^2 - y^2$) are oriented along the axes and the other three orbitals (xy, xz, and yz) are oriented off the axes. Because of these different orientations, the interactions of the d orbitals with the ligands approaching along the axes, shown in *b* for an octahedral complex, destabilizes the z^2 and $x^2 - y^2$ orbitals and stabilizes the xy, xz, and yz orbitals. Adapted from Huheey (1983).[4]

The contribution of LFSE to hydration energies of the +2 ions in the first transition series, corresponding to the reaction

$$M^{2+}(g) + \infty H_2O = M(H_2O)_6^{2+}(aq)$$

can be seen in Figure 6.5. The ions $Ca^{2+}(d^0)$, $Mn^{2+}(d^5)$, and $Zn^{2+}(d^{10})$ have

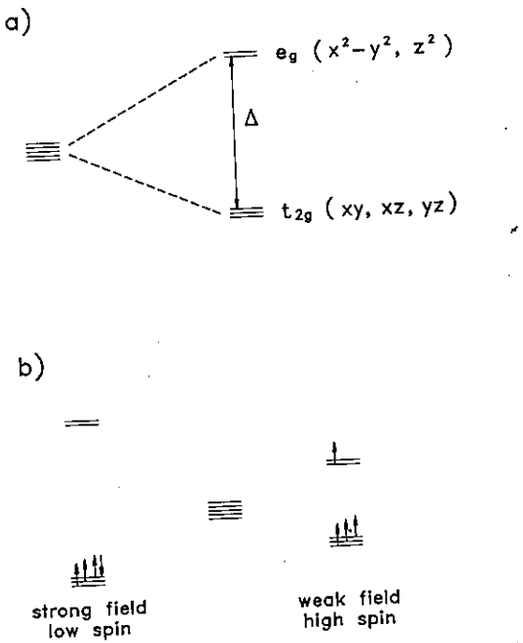

Figure 6.4 (*a*) Splitting of the energy of the five d orbitals as a result of interactions with ligands in an octahedral complex. The energies of the z^2 and $x^2 - y^2$ orbitals (with symmetry designation e_g) are increased and the energies of the *xy*, *xz*, and *yz* orbitals (with symmetry designation t_{2g}) are decreased. The energy gap between the e_g and t_{2g} orbitals is indicated by Δ. (*b*) The occupancy of the orbitals, shown for metals with four d electrons, depends on the nature of the ligand. Interactions with strong field ligands produce a large energy gap (Δ) and favor the low spin configuration. With all four d electrons in the three t_{2g} orbitals, two of the electrons must have opposite spin (indicated by the directions of the arrows). In contrast, weak field ligands produce only a small energy gap and favor the high spin configuration in which all four electrons have the same spin.

no LFSE and their hydration energies lie along a smooth curve. The hydration energies of the other ions lie above this curve; the difference corresponds to the spectroscopically determined LFSE. Although the values of LFSE for divalent ions are on the order of 100 kJ mol^{-1} and thus comparable to the energies of many chemical changes, they are small (ca. 5–10%) compared to the total binding energies involved in metal complexation.[2] Thus, the LFSE is mostly important in explaining the difference in reactivity of various metal complexes.

Spectroscopic evidence, such as the absorbance of ultraviolet or visible light by metal complexes, demonstrates the effects of specific ligands on the metal d orbitals. Differences in the spectra of metal complexes indicate a consistent pattern in the extent to which metal orbitals are perturbed by ligands; this

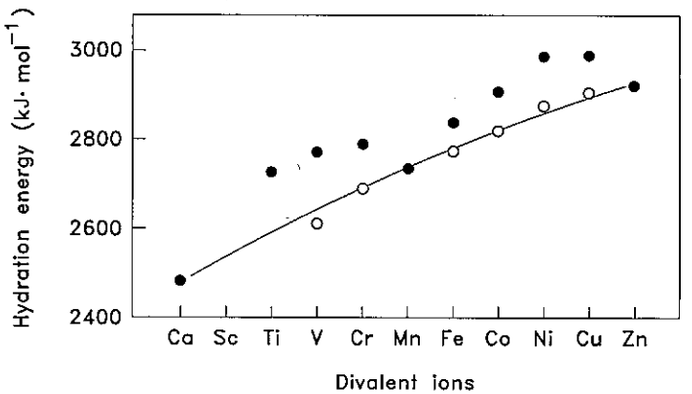

Figure 6.5 Hydration energies of the divalent cations including the first row of the transition metals. Solid symbols indicate measured hydration energies. Open symbols are corrected for the contributions of LFSE (ligand field stabilization energies). With this correction, hydration energies increase smoothly across the row. From Cotton and Wilkinson, 1972.[2]

ranking of ligands is termed the "spectrochemical series." Strong field ligands generate a large energy gap (Δ) between the t_{2g} and e_g levels and weak field ligands a small energy gap. In the case of a d^4 metal (e.g., Cr^{2+}), there can be either one electron in the higher-energy e_g level or a pair of electrons in the lower-energy t_{2g}. Then, the electron configuration (see Figure 6.4*b*) will depend on how the energy gap (Δ) between the t_{2g} and e_g levels compares with the spin-pairing energy, which arises from the inherent repulsion between the electrons within one orbital. Thus the ligands in a metal complex affect the distribution of electrons among the d orbitals, which influences both the chemical reactivity and magnetic and spectroscopic properties of the complexes.

Some metal–ligand interactions, however, cannot be explained simply in terms of electrostatics. In MOT overlap between metal and ligand orbitals is considered explicitly. For our purposes, the important difference between MOT and LFT is seen if the ligand has either extra lone pairs of electrons (π donor ligands) or empty orbitals of energy comparable to the metal d orbital energies (π acceptor ligands). Then interaction of the ligand p or d orbitals and the metal d orbitals (see Figure 6.6) results in formation of π bonds. In metal complexes with π donor ligands, there is increased electron density at the metal center and with π acceptor ligands, decreased electron density at the metal center. These variations in electron density influence the relative stability of metal oxidation states in the complexes. Figure 6.7 shows that Fe(II) is stabilized by π acceptor ligands and Fe(III) is stabilized by π donor ligands.[5]

Although necessarily brief, this discussion of the fundamentals of metal–ligand interactions provides some context for the discussion of (equilibrium) metal speciation in natural waters. Complexation kinetics have also been

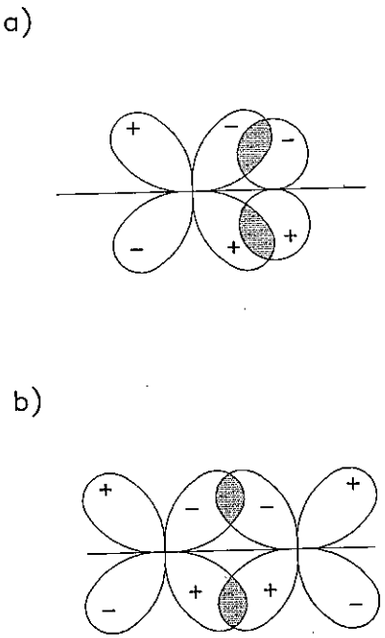

Figure 6.6 Overlap between metal and ligand orbitals that results in π bonds between the metal and ligand described by molecular orbital theory (MOT). (*a*) Overlap between metal d orbital and ligand p orbital. (*b*) Overlap between metal and ligand d orbitals.

interpreted, to some extent, on the basis of electronic interactions in metal complexes, particularly on the basis of the changes in LFSE in the transition state of the reaction. This is discussed in more detail in Section 5.

1.4 Prediction of Metal Speciation

Metal–ligand interactions are a particularly convenient framework within which to organize the reactions of interest in natural waters, including acid–base reactions, complexation, and solid formation. Equilibrium constants and the stoichiometric coefficients for reactions among some 20 metals and 32 ligands are presented, in a compact way, in Table 6.3. The first 15 ligands represent practically all reactive inorganic constituents commonly encountered in natural waters; they are roughly arranged in order of decreasing abundance. The other 17 ligands are chosen as representative compounds containing the types of functionalities present in aquatic organic matter, all of them being actually present as individual species at trace concentrations in natural waters. The metals are also roughly organized in order of decreasing abundance, the list of trace metals being biased toward the more reactive elements.

The logs of equilibrium constants given in Table 6.3 correspond to a general

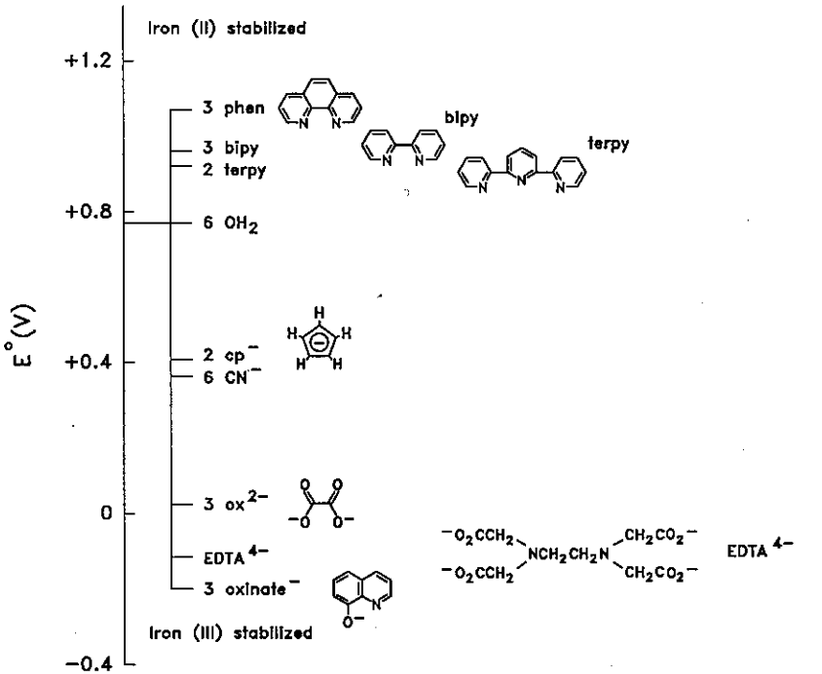

Figure 6.7 Standard reduction potentials for iron complexes. Iron(II) is stabilized by π acceptor ligands such as phenanthroline (phen) and iron(III) is stabilized by π donor ligands such as EDTA. Adapted from Burgess (1988).[5]

complexation or precipitation reaction of the type

$$mM + lL + hH^+ = M_mL_lH_h$$

$$\beta_{mlh} = \frac{[M_mL_lH_h]}{[M]^m[L]^l[H^+]^h}$$

For any given complex or solid, several different reactions of formation or dissociation can be written making it necessary to specify the reaction considered when giving an equilibrium constant. This is achieved implicitly by standardizing the notation for the constants themselves as shown in Table 6.4.

An important caveat must accompany any compilation of thermodynamic data such as that of Table 6.3. Although the choice of constants has been made with some care, there might still be some glaring errors or omissions. The original references have been examined only in a few instances, and previous compilations, particularly those of Smith and Martell, and Martell and Smith,[6] have been relied upon extensively. A major issue is that of data consistency: for example, a complex formation constant reported by one author may have been calculated

Read p. 331 before using this table to be sure which mass actions are associated w/ the β's

Consider these to be thermodynamic betas

TABLE 6.3 Stability Constants for Formation of Complexes and Solids from Metals and Ligands[a]

	OH^-	CO_3^{2-}	SO_4^{2-}	Cl^-	Br^-	F^-	NH_3	$B(OH)_4$
H^+	HL·w 14.00	HL 10.33 H_2L 16.68 H_2L·g 18.14	HL 1.99			HL 3.2	HL 9.24 L·g −1.8	HL 9.24 HL_3 10.4 H_2L_3 20.4 H_2L_4 21.0 H_4L_5 38.8
Na^+		NaL 1.27 NaHL 10.08	NaL 1.06					
K^+			KL 0.96					
Ca^{2+}	CaL 1.15 CaL_2·s 5.19	CaL 3.2 CaHL 11.59 CaL·s 8.22 CaL·s 8.35	CaL 2.31 CaL·s 4.62			CaL 1.1 CaL_2·s 10.4		
Mg^{2+}	MgL 2.56 Mg_4L_4 16.28 MgL_2·s 11.16	MgL 3.4 MgHL 11.49 MgL·s 4.54 MgL·s 7.45	MgL 2.36			MgL 1.8 MgL_2·s 8.2		
Sr^{2+}		SrL·s 9.0	SrL 2.6 SrL·s 6.5			SrL_2·s 8.5		
Ba^{2+}		BaL 2.8 BaL·s 8.3	BaL 2.7 BaL·s 10.0			BaL_2·s 5.8		
Cr^{3+}	CrL 10.0 CrL_2 18.3 CrL_3 24.0 CrL_4 28.6 Cr_3L_4 47.8 CrL_3·s 30.0		CrL 3.0	CrL .23		CrL 5.2 CrL_2 9.2 CrL_3 12.0		

$\beta = \frac{[NaHCO_3^\circ]}{[Na^+][H^+][CO_3^{2-}]}$

$Na^+ + H^+ + CO_3^{2-} = NaHCO_3^\circ$ + 10.08

$HCO_3^- = H^+ + CO_3^{2-}$ + −10.33

$Na^+ + HCO_3^- = NaHCO_3^\circ$ −0.25

Al^{3+}	AlL 9.0 AlL_2 18.7 AlL_3 27.0 AlL_4 33.0 Al_3L_4 42.1 AlL_3·s 33.5									AlL 7.0 AlL_2 12.6 AlL_3 16.7 AlL_4 19.1		
Fe^{3+}	FeL 11.8 FeL_2 22.3 FeL_4 34.4 Fe_2L_2 25.0 FeL_3·s 42.7 FeL_3·s 38.8		FeL 4.0 FeL_2 5.4	FeL 1.5 FeL_2 2.1	FeL 0.6	FeL 6.0 FeL_2 10.6 FeL_3 13.7						
Mn^{2+}	MnL 3.4 MnL_2 5.8 MnL_3 7.2 MnL_4 7.7 MnL_2·s 12.8	MnHL 12.1 MnL·s 9.3	MnL 2.3	MnL 0.6		MnL 1.3	MnL 1.0 MnL_2 1.5					
Fe^{2+}	FeL 4.5 FeL_2 7.4 FeL_3 11.0 FeL_2·s 15.1	FeL·s 10.7	FeL 2.2			FeL 1.4						
Co^{2+}	CoL 4.3 CoL_2 9.2 CoL_3 10.5 CoL_2·s 15.7	CoL·s 10.0	CoL 2.4	CoL 0.5		CoL 1.0	CoL 2.0 CoL_2 3.5 CoL_3 4.4 CoL_4 5.0					
Ni^{2+}	NiL 4.1 NiL_2 9.0 NiL_3 12.0 NiL_2·s 17.2	NiL·s 6.9	NiL 2.3	NiL 0.6		NiL 1.1	NiL 2.7 NiL_2 4.9 NiL_3 6.6 NiL_4 7.7 NiL_5 8.3					

TABLE 6.3 (*Continued*)

	OH^-	CO_3^{2-}	SO_4^{2-}	Cl^-	Br^-	F^-	NH_3	$B(OH)_4$
Cu^{2+}	CuL 6.3 CuL_2 11.8 CuL_4 16.4 Cu_2L_2 17.7 $CuL_2{\cdot}s$ 19.3 $CuL_2{\cdot}s$ 20.4	CuL 6.7 CuL_2 10.2 $CuL{\cdot}s$ 9.6 $Cu_2(OH)_2L{\cdot}s$ 33.8 $Cu_3(OH)_2L_2{\cdot}s$ 46.0	CuL 2.4 $Cu_4(OH)_6L{\cdot}s$ 68.6	CuL 0.5		CuL 1.5	CuL 4.0 CuL_2 7.5 CuL_3 10.3 CuL_4 11.8	
Zn^{2+}	ZnL 5.0 ZnL_2 11.1 ZnL_3 13.6 ZnL_4 14.8 $ZnL_2{\cdot}s$ 15.5 $ZnL_2{\cdot}s$ 16.8	$ZnL{\cdot}s$ 10.0	ZnL 2.1 ZnL_2 3.1	ZnL 0.4 ZnL_2 0.2 ZnL_3 0.5 $Zn_2(OH)_3L{\cdot}s$ 26.8		ZnL 1.2	ZnL 2.2 ZnL_2 4.5 ZnL_3 6.9 ZnL_4 8.9	
Pb^{2+}	PbL 6.3 PbL_2 10.9 PbL_3 13.9 $PbL_2{\cdot}s$ 15.3	$PbL{\cdot}s$ 13.1	PbL 2.8 $PbL{\cdot}s$ 7.8	PbL 1.6 PbL_2 1.8 PbL_3 1.7 PbL_4 1.4 $PbL_2{\cdot}s$ 4.8	PbL 1.8 PbL_2 2.6 PbL_3 3.0 $PbL_2{\cdot}s$ 5.7	PbL 2.0 PbL_2 3.4 $PbL_2{\cdot}s$ 7.4		
Hg^{2+}	HgL 10.6 HgL_2 21.8 HgL_3 20.9 $HgL_2{\cdot}s$ 25.4	$HgL{\cdot}s$ 16.1	HgL 2.5 HgL_2 3.6	HgL 7.2 HgL_2 14.0 HgL_3 15.1 HgL_4 15.4 HgOHL 18.1	HgL 9.6 HgL_2 18.0 HgL_3 20.3 HgL_4 21.6 $HgL_2{\cdot}s$ 19.8	HgL 1.6	HgL 8.8 HgL_2 17.4 HgL_3 18.4 HgL_4 19.1	
Cd^{2+}	CdL 3.9 CdL_2 7.6 $CdL_2{\cdot}s$ 14.3	$CdL{\cdot}s$ 13.7	CdL 2.3 CdL_2 3.2 CdL_3 2.7	CdL 2.0 CdL_2 2.6 CdL_3 2.4 CdL_4 1.7	CdL 2.1 CdL_2 3.0	CdL 1.0 CdL_2 1.4	CdL 2.6 CdL_2 4.6 CdL_3 5.9 CdL_4 6.7	
Ag^+	AgL 2.0 AgL_2 4.0 $AgL{\cdot}s$ 7.7	$Ag_2L{\cdot}s$ 11.1	AgL 1.3 $Ag_2L{\cdot}s$ 4.8	AgL 3.3 AgL_2 5.3 AgL_3 6.4 $AgL{\cdot}s$ 9.7	AgL 4.7 AgL_2 6.9 AgL_3 8.7 AgL_4 9.0 $AgL{\cdot}s$ 12.3	AgL 0.4	AgL 3.3 AgL_2 7.2	AgL 0.6 $AgHL_2{\cdot}s$ 22.9

	SiO_3^{2-}	S^{2-}	$S_2O_3^{2-}$	PO_4^{3-}	$P_2O_7^{4-}$	$P_3O_{10}^{5-}$	CN^-
H^+	HL 13.1 H_2L 23.0 H_2L_2 26.6 H_4L_4 55.9 H_6L_4 78.2 $H_2L{\cdot}s$ 25.7	HL 13.9 H_2L 20.9 $H_2L{\cdot}g{\cdot}$ 21.9	HL 1.6 H_2L 2.2	HL 12.35 H_2L 19.55 H_3L 21.70	HL 9.4 H_2L 16.1 H_3L 18.3 H_4L 19.7	HL 9.3 H_2L 18.8 H_3L 21.3 H_4L 22.3	HL 9.2
Na^+			NaL 0.5	NaHL 13.5	NaL 2.3 Na_2L 4.2 NaHL 10.8	NaL 2.7 NaHL 11.6	
K^+			KL 1.0	KHL 13.4	KL 2.1	KL 2.8	
Ca^{2+}	CaL 4.2 CaHL 14.1 CaH_2L_2 29.9		CaL 2.0	CaL 6.5 CaHL 15.1 CaH_2L 21.0 $CaHL{\cdot}s$ 19.0	CaL 6.8 CaHL 13.4 CaOHL 8.9 $Ca_2L{\cdot}s$ 14.7	CaL 8.1 CaHL 14.1 CaOHL 10.4	
Mg^{2+}	MgL 5.3 MgHL 14.3 MgH_2L_2 30.8		MgL 1.8	MgL 4.8 MgHL 15.3 MgH_2L 20.0 $Mg_3L_2{\cdot}s$ 25.2 $MgHL{\cdot}s$ 18.2	MgL 7.2 MgHL 14.1 MgOHL 9.3	MgL 8.6 MgHL 14.5 MgOHL 11.0	
Sr^{2+}			SrL 2.0	SrL 5.5 SrHL 14.5 SrH_2L 20.3 $SrHL{\cdot}s$ 19.3	SrL 5.4 SrOHL 7.7 $Sr_2L{\cdot}s$ 12.9	SrL 7.2 SrHL 13.6 SrOHL 9.3	
Ba^{2+}			BaL 2.3 $BaL{\cdot}s$ 4.8	$BaHL{\cdot}s$ 19.8		BaL 6.3 BaHL 12.9 $Ba_2L{\cdot}s$ 16.1	
Cr^{3+}							
Al^{3+}							

TABLE 6.3 (*Continued*)

	SiO_3^{2-}	S^{2-}	$S_2O_3^{2-}$	PO_4^{3-}	$P_2O_7^{4-}$	$P_3O_{10}^{5-}$	CN^-
Fe^{3+}	FeHL 22.7		FeL 3.3	FeHL 22.5 FeH_2L 23.9 FeL·s 26.4			FeL_6 43.6
Mn^{2+}		MnL·s 10.5 13.5	MnL 2.0			MnL 9.9 MnHL 14.8	
Fe^{2+}		FeL·s 18.1		FeHL 16.0 FeH_2L 22.3 Fe_3L_2·s 36.0			FeL_6 35.4
Co^{2+}		CoL·s 21.3 CoL·s 25.6	CoL 2.1	CoHL 15.5	CoL 7.9 CoHL 14.1	CoL 9.7 CoHL 14.8	
Ni^{2+}		NiL·s 19.4 NiL·s 24.9 NiL·s 26.6	NiL 2.1	NiHL 15.4	NiL 7.7 NiHL 14.4	NiL 9.5 NiHL 14.7	NiL 7.3 NiL_4 30.2 NiH_2L_4 40.8 $NiHL_4$ 36.1
Cu^{2+}		CuL·s 36.1		CuHL 16.5 CuH_2L 21.3	CuL 9.8 CuHL 15.5 CuL_2 12.5 CuH_2L 19.2	CuL 11.1 CuHL 15.5	CuL_2 16.3 CuL_3 21.6 CuL_4 23.1
Zn^{2+}		ZnL 16.6 ZnL·s 24.7	ZnL 2.4 ZnL_2 2.5 ZnL_3 3.3 Zn_2L_2 7.0	ZnHL 15.7 ZnH_2L 21.2 Zn_3L_2 35.3	ZnL 8.7 ZnL_2 11.0 ZnOHL 13.1	ZnL 10.3 ZnHL 14.9 ZnOHL 13.6	ZnL 5.7 ZnL_2 11.1 ZnL_3 16.1 ZnL_4 19.6 ZnL_2·s 15.9
Pb^{2+}		PbL·s 27.5	PbL 3.0 PbL_2 5.5 PbL_3 6.2 PbL_4 7.3	PbHL 15.5 PbH_2L 21.1 Pb_3L_2·s 43.5 PbHL·s 23.8	PbL 9.5 PbL_2 10.2		
Hg^{2+}		HgL 7.9 HgL_2 14.3 HgOHL 18.5 HgL·s 52.7 HgL·s 53.3	HgL_2 29.2 HgL_3 30.6		HgOHL 18.6		HgL 17.0 HgL_2 32.8 HgL_3 36.3 HgL_4 39.0 HgOHL 29.6
Cd^{2+}		CdL 19.5 CdHL 22.1 CdH_2L_2 43.2 CdH_3L_3 59.0 CdH_4L_4 75.1 CdL·s 27.0	CdL 3.9 CdL_2 6.3 CdL_3 6.4 CdL_4 8.2 Cd_2L_2 12.3		CdL 8.7 CdOHL 11.8	CdL 9.8 CdHL 14.6 CdOHL 12.6	CdL 6.0 CdL_2 11.1 CdL_3 15.7 CdL_4 17.9
Ag^+		AgL 19.2 AgHL 27.7 $AgHL_2$ 35.8 AgH_2L_2 45.7 Ag_2L·s 50.1	AgL 8.8 AgL_2 13.7 AgL_3 14.2 Ag_2L_4 26.3 Ag_3L_5 39.8 Ag_6L_8 78.6	Ag_3L·s 17.6			AgL_2 20.5 AgL_3 21.4 AgOHL 13.2 AgL·s 15.7

TABLE 6.3 *(Continued)*

	Ethylene-diamine		NTA		EDTA		CDTA		IDA		Picolinate		Cysteine		Desferri-ferrioxamine B	
H^+	HL	9.93	HL	10.33	HL	11.12	HL	13.28	HL	9.73	HL	5.39	HL	10.77	HL	10.1
	H_2L	16.78	H_2L	13.27	H_2L	17.8	H_2L	20.0	H_2L	12.63	H_2L	6.40	H_2L	19.13	H_2L	19.4
			H_3L	14.92	H_3L	21.04	H_3L	23.98	H_3L	14.51			H_3L	20.84	H_3L	27.8
			H_4L	16.02	H_4L	23.76	H_4L	26.62								
					H_5L	24.76	H_5L	28.34								
Na^+			NaL	1.9	NaL	2.5			NaL	0.8						
K^+					KL	1.7										
Ca^{2+}			CaL	7.6	CaL	12.4	CaL	15.0	CaL	3.5	CaL	2.2			CaL	3.5
					CaHL	16.0					CaL_2	3.8				
Mg^{2+}	MgL	0.4	MgL	6.5	MgL	10.6	MgL	12.8	MgL	3.8	MgL	2.6			MgL	5.2
					MgHL	15.1					MgL_2	4.0				
Sr^{2+}			SrL	6.3	SrL	10.5	SrL	12.4	SrL	3.1	SrL	1.8			SrL	3.1
					SrHL	14.9					SrL_2	3.0				
Ba^{2+}			BaL	5.9	BaL	9.6	BaL	10.5	Ba	2.5	BaL	1.6				
					BaHL	14.6	BaHL	17.8								
Cr^{3+}					CrL	26.0			CrL	12.2						
					CrHL	28.2			CrL	23.2						
					CrOHL	32.2										
Al^{3+}			AlL	13.4	AlL	18.9	AlL	22.1	AlL	9.9						
			AlOHL	22.1	AlHL	21.6	AlHL	24.3	AlL_2	17.5						
					AlOHL	26.6	AlOHL	28.1								
					$Al(OH)_2L$	30.0										
Fe^{3+}			FeL	17.9	FeL	27.7	FeL	32.6	FeL	12.5	FeL_2	13.9			FeL	31.9
			FeL_2	26.3	FeHL	29.2	FeOHL	36.5			$FeOHL_2$	24.9			FeHL	32.6
					FeOHL	33.8										
					$Fe(OH)_2L$	37.7										
Mn^+	MnL	2.8	MnL	8.7	MnL	15.6	MnL	19.2			MnL	4.0	MnL	5.6		
	MnL_2	3.7	MnL_2	11.6	MnHL	19.1	MnHL	22.4			MnL_2	7.1				
	MnL_3	5.8									MnL_3	8.8				
Fe^{2+}	FeL	4.3	FeL	9.6	FeL	16.1	FeL	20.8	FeL	6.7	FeL	5.3			FeHL	18.7
	FeL_2	7.7	FeL_2	13.6	FeHL	19.3	FeHL	23.9	FeL_2	11.0	FeL_2	9.7			FeH_2L	21.0
	FeL_3	9.7	FeOHL	12.6	FeOHL	20.4					FeL_3	13.0				
					$Fe(OH)_2L$	23.7										
Co^{2+}	CoL	6.0	CoL	11.7	CoL	18.1	CoL	21.4	CoL	7.9	CoL	6.4			CoL	11.2
	CoL_2	10.8	CoL_2	15.0	CoHL	21.5	CoHL	24.7	CoL_2	13.2	CoL_2	11.3			CoHL	18.0
	CoL_3	14.1	CoOHL	14.5							CoL_3	14.8			CoHL	23.6
Ni^{2+}	NiL	7.4	NiL	12.8	NiL	20.4	NiL	22.1	NiL	9.1	NiL	7.2	NiL	10.7	NiL	11.8
	NiL_2	13.6	NiL_2	17.0	NiHL	24.0	NiHL	25.4	NiL_2	15.7	NiL_2	12.5	NiL_2	20.9	NiHL	18.3
	NiL_3	17.9	NiOHL	15.5	NiOHL	21.8					NiL_3	17.9			NiH_2L	23.8
Cu^{2+}	CuL	10.5	CuL	14.2	CuL	20.5	CuL	23.7	CuL	11.5	CuL	8.4	Cu(II)→Cu(I)		CuL	15.0
	CuL_2	19.6	CuL_2	18.1	CuHL	23.9	CuHL	27.3	CuL_2	17.6	CuL_2	15.6			CuHL	24.1
	CuOHL	11.8	CuOHL	18.6	CuOHL	22.6									CuH_2L	27.0
Zn^{2+}	ZnL	5.7	ZnL	12.0	ZnL	18.3	ZnL	21.1	ZnL	8.2	ZnL	5.7	ZnL	10.1	ZnL	11.0
	ZnL_2	10.6	ZnL_2	14.9	ZnHL	21.7	ZnHL	24.4	ZnL_2	13.5	ZnL_2	10.3	ZnL	19.1	ZnHL	17.5
	ZnL_3	13.9	ZnOHL	15.5	ZnOHL	19.9					ZnL_3	13.6	ZnHL	16.4	ZnH_2L	22.9
Pb^{2+}	PbL	7.0	PbL	12.6	PbL	19.8	PbL	22.1	PbL	8.3	PbL	5.0	PbL	12.5		
	PbL_2	8.5			PbHL	23.0	PbHL	25.3			PbL_2	8.6				
Hg^{2+}	HgL	14.3	HgL	15.9	HgL	23.5	HgL	26.8	HgL	11.7	HgL	8.1	HgL	15.3		
	HgL_2	23.2			HgHL	27.0	HgHL	30.3			HgL_2	16.2				
	HgOHL	24.2			HgOHL	27.7	HgOHL	29.7								
	$HgHL_2$	28.0														
Cd^{2+}	CdL	5.4	CdL	11.1	CdL	18.2	CdL	21.7	CdL	6.6	CdL	5.0			CdL	8.8
	CdL_2	9.9	CdL_2	15.1	CdHL	21.5	CdHL	25.1	CdL_2	11.1	CdL_2	8.3			CdHL	16.2
	CdL_3	11.7	CdOHL	13.4							CdL_3	11.4			CdH_2L	22.7
Ag^+	AgL	4.7	AgL	5.8	AgL	8.2	AgL	9.9			AgL	3.6				
	AgL_2	7.7			AgHL	14.9					AgL_2	6.1				
	AgHL	11.9														

TABLE 6.3 (*Continued*)

	Glycine	Glutamate	Acetate	Glycolate	Citrate	Malonate	Salicylate	Phthalate
H^+	HL 9.78 H_2L 12.13	HL 9.95 H_2L 14.47 H_3L 16.70	HL 4.76	HL 3.83	HL 6.40 H_2L 11.16 H_3L 14.29	HL 5.70 H_2L 8.55	HL 13.74 H_2L 16.71	HL 5.51 H_2L 8.36
Na^+					NaL 1.4	NaL 0.7		NaL 0.7
K^+					KL 1.3			
Ca^{2+}	CaL 1.4	CaL 2.1	CaL 1.2	CaL 1.6	CaL 4.7 CaHL 9.5 CaH_2L 12.3	CaL 2.4 CaHL 6.6	CaL 0.4	CaL 2.4
Mg^{2+}	MgL 2.7	MgL 2.8	MgL 1.3	MgL 1.3	MgL 4.7 MgHL 9.2	MgL 2.9 MgHL 7.1		
Sr^{2+}	SrL 0.9	SrL 2.3	SrL 1.1	SrL 1.2	SrL 4.1	SrL 2.1 SrHL 6.5		
Ba^{2+}	BaL 0.8	BaL 2.2	BaL 1.1	BaL 1.1	BaL 4.1 BaHL 9.0 BaH_2L 12.4	BaL 2.1	BaL 0.2	BaL 2.3
Cr^{3+}			CrL 5.4 CrL_2 8.4 CrL_3 11.2			CrL 9.6		
Al^{3+}			AlL 2.4				AlL 14.2 AlL_2 25.1 AlL_3 31.1	AlL 5.0 AlL_2 8.7
Fe^{3+}	FeL 10.8	FeL 13.8	FeL 4.0 FeL_2 7.6 FeL_3 9.6	FeL 3.7 FeOHL 19.6 $FeOHL_2$ 22.3 $FeOHL_3$ 23.8	FeL 13.5 $Fe_2(OH)_2L_2$ 56.3	FeL 9.3	FeL 17.6 FeL_2 28.6 FeL_3 36.2	

Mn^{2+}	MnL 3.2		MnL 1.4	MnL 1.6	MnL 5.5 MnHL 9.4	MnL 3.3	MnL 6.8 MnL_2 10.7	MnL 2.7
Fe^{2+}	FeL 4.3	FeL 4.6	FeL 1.4	FeL 1.9	FeL 5.7 FeHL 9.9		FeL 7.4 FeL_2 12.1	
Co^{2+}	CoL 5.1 CoL_2 9.0 CoL_3 11.6	CoL 5.4 CoL_2 8.7	CoL 1.5	CoL 2.0 CoL_2 3.0	CoL 6.3 CoHL 10.3 CoH_2L 12.9	CoL 3.7 CoL_2 5.1 CoHL 7.0	CoL 7.5 CoL_2 12.3	CoL 2.8 CoHL 7.2
Ni^{2+}	NiL 6.2 NiL_2 11.1 NiL_3 14.2	NiL 6.5 NiL_2 10.6	NiL 1.4	NiL 2.3 NiL_2 3.4 NiL_3 3.7	NiL 6.7 NiHL 10.5 NiH_2L 12.9	NiL 4.1 NiL_2 5.8 NiHL 7.2	NiL 7.8 NiL_2 12.6	NiL 3.0 NiHL 6.6
Cu^{2+}	CuL 8.6 CuL_2 15.6	CuL 8.8 CuL_2 15.0	CuL 2.2 CuL_2 3.6	CuL 2.9 CuL_2 4.7 CuL_3 4.7	CuL 7.2 CuHL 10.7 CuH_2L 13.8 CuOHL 16.4 Cu_2L_2 16.3	CuL 5.7 CuL_2 8.2 CuHL 8.3	CuL 11.5 CuL_2 19.3	CuL 4.0 CuHL 7.1
Zn^{2+}	ZnL 5.4 ZnL_2 9.8 ZnL_3 12.3	ZnL 5.8 ZnL_2 9.5 ZnL_3 9.8	ZnL 1.6 ZnL_2 1.8	ZnL 2.4 ZnL_2 3.6 ZnL_3 3.9	ZnL 6.1 ZnL_2 6.8 ZnHL 10.3 ZnH_2L 13.3	ZnL 3.8 ZnL_2 5.4 ZnHL 7.1	ZnL 7.7	ZnL 2.9 ZnL_2 4.2
Pb^{2+}	PbL 5.5 PbL_2 8.9		PbL 2.7 PbL_2 4.1	PbL 2.5 PbL_2 3.7 PbL_3 3.6	PbL 5.4 PbL_2 8.1 PbHL 10.2 PbH_2L 13.1	Pb 4.0 PbL_2 4.5		
Hg^{2+}	HgL 10.9 HgL_2 20.1		HgL 6.1 HgL_2 10.1 HgL_3 14.1 HgL_4 17.6		HgL 12.2			

TABLE 6.3 (*Continued*)

	Glycine	Glutamate	Acetate	Glycolate	Citrate	Malonate	Salicylate	Phthalate
Cd^{2+}	CdL 4.7 CdL_2 8.4 CdL_3 10.7	CdL 4.8	CdL 1.9 CdL_2 3.2	CdL 1.9 CdL_2 2.7	CdL 5.0 CdL_2 7.2 CdHL 9.5 CdH_2L 12.6	CdL 3.2 CdL_2 4.0 CdHL 6.9	CdL 6.4	CdL 3.4
Ag^+	AgL 3.5 AgL_2 6.9		AgL 0.7 AgL_2 0.6	AgL 0.4 AgL_2 0.5				

[a] *Note:* Constants are given as logarithms of the overall formation constants, β, for complexes and as logarithms of the overall precipitation constants for solids, at zero ionic strength and 25°C [From Smith and Martell 1975, 1976 and Martell and Smith 1974, 1977.[6] Exceptions are major ion interaction constants (Na^+, K^+, Ca^{2+}, Mg^{2+}, CO_3^{2-}, SO_4^{2-}, Cl^-) taken from Whitfield;[7] hydrolysis (OH^-) and some carbonate (CO_3^{2-}) formation constants taken from Baes and Mesmer;[8] Cu^{2+}—CO_3^{2-} complexes constants taken from Sunda and Hanson;[9] the ZnS(aq) constant recalculated from the data of Sainte Marie et al.[10]; the $MnCO_3$(s) constant taken from Morgan.[11]] When necessary, constants have been extrapolated to $I = 0\,M$ using the following values of (−log of) activity coefficients (applied to all ions including H^+ and tri- and tetravalent ions):

I \ z	1	2	3	4
0.1 *M*, 2 *M*	0.11	0.44	0.99	1.76
0.3 *M*	0.13	0.52	1.17	2.08
0.5 *M*	0.15	0.60	1.35	2.40
1.0 *M*	0.14	0.56	1.26	2.24
3.0 *M*	0.07	0.28	0.63	1.12
4.0 *M*	0.03	0.12	0.27	0.48

TABLE 6.4 Formulation of Stability Constant[a]

Mononuclear Complexes

Addition of ligand

$$M \xrightarrow[K_1]{L} ML \xrightarrow[K_2]{L} ML_2 \cdots \xrightarrow[K_i]{L} ML_i \cdots \xrightarrow[K_n]{L} ML_n$$

$$\beta_2 \longrightarrow$$
$$\beta_i \longrightarrow$$
$$\beta_n \longrightarrow$$

$$K_i = \frac{[ML_i]}{[ML_{(i-1)}][L]}$$

$$\beta_i = \frac{[ML_i]}{[M][L]^i}$$

Addition of protonated ligands

$$M \xrightarrow[{}^*K_1]{HL} ML \xrightarrow[{}^*K_2]{HL} ML_2 \cdots \xrightarrow[{}^*K_i]{HL} ML_i \cdots \xrightarrow{HL} ML_n$$

$${}^*\beta_2 \longrightarrow$$
$${}^*\beta_i \longrightarrow$$
$${}^*\beta_n \longrightarrow$$

$${}^*K_i = \frac{[ML_i][H^+]}{[ML_{(i-1)}][HL]}$$

$${}^*\beta_i = \frac{[ML_i][H^+]^i}{[M][HL]^i}$$

Polynuclear Complexes

In β_{nm} and ${}^*\beta_{nm}$ the subscripts n and m denote the composition of the complex M_mL_n formed. [If $m = 1$, the second subscript (= 1) is omitted.]

$$\beta_{nm} = \frac{[M_mL_n]}{[M]^m[L]^n}$$

$${}^*\beta_{nm} = \frac{[M_mL_n][H^+]^n}{[M]^m[HL]^n}$$

Source: Adapted from Stumm and Morgan (1981).[12]

[a] *Note:* The notation given above is the same as that used by Sillén and Martell (1964, 1971).[13] In the text the notation β_i or K_i is used indifferently to indicate the constants of formation of M_1L_i complexes. β' or K' indicate mixed acidity constants expressed as a function of the activity of H^+ and of the concentrations of other reactants and products.

on the basis of a solubility constant that is not the same as that chosen in the compilation. For precise calculations it is essential to examine the original literature and crosscheck the methods for estimating the constants from experimental data. Note also that the absence of a reported constant for a metal–ligand combination in Table 6.3 does not rule out the existence of a complex. It is in fact the value of such a table to make the missing information particularly visible. (The price paid for such advantage is that mixed complexes, such as HgClGly, cannot be accommodated in the format of the table.)

Some simple generalities about coordination chemistry can be deduced by inspection of Table 6.3. Consider first the sulfate column. The similarities among stability constants for metals of like charge is striking (e.g., $\log K = 2.2$–2.8 for divalent metal ions). This is a reflection of the principally electrostatic binding of the sulfate ion pair complexes (see Section 5.1). Similarly low equilibrium constants for complex formation, correlated with ionic charge, are also observed for carbonate (and bicarbonate) and halides (Cl^-, Br^-, and F^-).

A dominant feature of Table 6.3 is the high degree of similarity among organic ligands having the same donor atoms in their relative affinities for various metals. The absolute values of the stability constants may be different from one ligand to another but their relative values from metal to metal are highly correlated. A good example is the complex stability sequence of the transition metals, $Mn^{2+} < Fe^{2+} < Co^{2+} < Ni^{2+} < Cu^{2+} > Zn^{2+}$, well known as the Irving–Williams series.[14] This empirical observation is related to both the increase in effective nuclear charge with atomic number (which is due to imperfect shielding by the electrons) and the LFSE effects described previously. On the basis of such empirical observations, the metals can be organized into various groups exhibiting similar coordinative properties. Table 6.3 has been organized to highlight some of these correlations; the grouping of the metals reflects their coordination properties which can be explained by the configurations of their electron shells.[15]

Most of the organic ligands in Table 6.3 coordinate metals through oxygen donor atoms. A marked difference in the affinity of ligands for various metals may be noted when ligands with O, N, and S donor atoms are compared. Both metals and ligands may be categorized in terms of their polarizability. Interactions between "soft" (easily polarizable) donors and acceptors or between "hard" (usually compact) donors and acceptors are more favorable than hard–soft interactions. The empirically observed order of ligand affinities for "hard" metals (typically, alkali and alkaline earth metal ions and smaller, highly charged ions such as Fe^{3+}, Co^{3+}, or Al^{3+}) and for "soft" metals (typically, heavier transition metal ions such as Hg^{2+}) may be summarized as follows:[15]

strongest	⟶		weakest	complexes with "hard" metals
F^-	Cl^-	Br^-	I^-	
R_2O	R_2S	R_2Se	R_2Te	
R_3N	R_3P	R_3As	R_3Sb	
weakest	⟵		strongest	complexes with "soft" metals

where R indicates that the heteroatoms (O, N, S, P, Te, Se, As, and Sb) are bonded to organic carbon. Although useful, this classification is entirely empirical.

It is apparent that trivalent metals are typically more reactive than divalent ones, but this is largely offset by the greater insolubility of their corresponding oxides and hydroxides. For example, many ligands have a relatively high affinity for Fe^{3+}, but the very high stability of the ferric hydroxides, including the solid $Fe(OH)_3$, keeps the free ferric ion activity so low that the extent of Fe complexation is limited. As a result, Cu^{2+} and Hg^{2+}, the most reactive of the divalent metals, are most apt to form complexes in natural waters. Copper complexation is one of the major foci of experimental studies of trace metal speciation in aquatic systems and will serve as one of our principal examples throughout this chapter.

2. ION ASSOCIATION AMONG MAJOR AQUATIC CONSTITUENTS

If two constituents are present in widely differing concentrations, say, by a factor of 100 or more, the less abundant constituent can affect the activity of the other only negligibly through complex formation. To study the complexation of the major constituents of natural waters, it is then sufficient to consider the components that account for 99% or so of the dissolved solids. For most natural waters, including seawater, these components are the metals Na^+, Ca^{2+}, Mg^{2+}, K^+ and the ligands Cl^-, SO_4^{2-}, and CO_3^{2-}. (H^+ and OH^- are included implicitly and so is HCO_3^- as a "complex" of H^+ and CO_3^{2-}.) Our objective is to describe quantitatively to what degree these seven major aquatic constituents are bound to each other as complexes. For the purpose of comparison, let us consider a freshwater and a seawater model, both at pH = 8.1.

Example 1. Ion Association in Freshwater; pH = 8.1*

$$TOT\mathrm{Na} = 2.8 \times 10^{-4}\,M = 10^{-3.55} \qquad TOT\mathrm{Cl} = 2.0 \times 10^{-4}\,M = 10^{-3.70}$$
$$TOT\mathrm{Ca} = 3.7 \times 10^{-4}\,M = 10^{-3.43} \qquad TOT\mathrm{SO_4} = 1.0 \times 10^{-4}\,M = 10^{-4.00}$$
$$TOT\mathrm{Mg} = 1.6 \times 10^{-4}\,M = 10^{-3.80} \qquad TOT\mathrm{CO_3} = 1.0 \times 10^{-3}\,M = 10^{-3.00}$$
$$TOT\mathrm{K} = 6.0 \times 10^{-5}\,M = 10^{-4.22}$$

Example 2. Ion Association in Seawater; pH = 8.1*

$$TOT\mathrm{Na} = 4.68 \times 10^{-1}\,M = 10^{-0.33} \qquad TOT\mathrm{Cl} = 5.45 \times 10^{-1}\,M = 10^{-0.26}$$
$$TOT\mathrm{Ca} = 1.02 \times 10^{-2}\,M = 10^{-1.99} \qquad TOT\mathrm{SO_4} = 2.82 \times 10^{-2}\,M = 10^{-1.55}$$
$$TOT\mathrm{Mg} = 5.32 \times 10^{-2}\,M = 10^{-1.27} \qquad TOT\mathrm{CO_3} = 2.38 \times 10^{-3}\,M = 10^{-2.62}$$
$$TOT\mathrm{K} = 1.02 \times 10^{-2}\,M = 10^{-1.99}$$

The upper left corner of Table 6.3 provides the necessary list of species and thermodynamic constants and the equilibrium problems can be formulated with

*Total concentrations from Holland (1978).[16]

TABLE 6.5 Free Single Ion Activity Coefficients Used in the Ion Association Model for Seawater

Ion	γ	$-\log\gamma$
H^+	0.95	0.02
Na^+	0.71	0.15
K^+	0.63	0.20
All other +1 ions	0.68	0.17
Ca^{2+}	0.26	0.59
Mg^{2+}	0.29	0.54
OH^-	0.65	0.19
Cl^-	0.63	0.20
All other −1 ions	0.68	0.17
SO_4^{2-}	0.17	0.77
CO_3^{2-}	0.20	0.70
Uncharged species	1.13	−0.05

Source: After Whitfield (1974).[7]

appropriate mole balance and mass law equations. The complexation effects that we wish to study are reasonably subtle, however, since the formation constants of the complexes are only on the order of 10^0–10^2. To achieve precision in the seawater model, it is imperative that proper ionic strength corrections be made. In this spirit of precision, we choose from the literature activity coefficients that are considered most appropriate for seawater[7] (see Table 6.5) rather than applying a general empirical expression such as the Davies equation. Concentration equilibrium constants are then readily calculated and choosing H^+, Na^+, Ca^{2+}, Mg^{2+}, K^+, Cl^-, SO_4^{2-}, and HCO_3^- as components yields Tableau 6.1 in which the constants are expressed for the formation of the species from the components.

Hand calculations corresponding to our two examples are a bit tedious and require some iterative solution scheme. For example, as shown in Tables 6.6 and 6.7 one can (1) start the calculation by assuming the principal component concentrations to be equal to the total concentrations, (2) calculate each of the species from the corresponding mass law, and (3) compare the sum of species in each mole balance equation to the imposed total concentration and increase or decrease accordingly the concentration for the next iteration. The calculation converges in two iterations for the freshwater model, and in four iterations for the seawater model. The test of convergence is of course the satisfaction of the mole balance equations.

In the freshwater example, the complexes are of little importance for the speciation of the major constituents. Complexation is most significant for sulfate which is calculated to be 10% bound to calcium and magnesium. By contrast, in the seawater example the effect of association among major ions is quite important; major fractions of both sulfate (60%) and carbonate (34%) are complexed by the metals, and some 10% of the calcium and magnesium bound to the ligands. The results of Example 2 are by and large comparable to those of the historical

TABLEAU 6.1

	H^+	Na^+	K^+	Ca^{2+}	Mg^{2+}	HCO_3^-	SO_4^{2-}	Cl^-	Freshwater	Seawater
H^+	1									+0.02
OH^-	−1								−14.0	−13.81
CO_3^{2-}	−1					1			−10.33	−9.80
HCO_3^-						1				
H_2CO_3	1					1			+6.35	+6.13
SO_4^{2-}							1			
HSO_4^-	1						1		+1.99	+1.39
Cl^-								1		
Na^+		1								
$NaCO_3^-$	−1	1				1			−9.06	−9.21
$NaHCO_3$		1				1			−0.25	−0.62
$NaSO_4^-$		1					1		+1.06	+0.31
K^+			1							
KSO_4^-			1				1		+0.96	+0.16
Ca^{2+}				1						
$CaOH^+$	−1			1					−12.85	−13.27
$CaCO_3$	−1			1					−7.13	−7.94
$CaHCO_3^+$				1		1			+1.26	+0.67
$CaSO_4$				1			1		+2.31	+0.90
Mg^{2+}					1					
$MgOH^+$	−1				1				−11.44	−11.81
$MgCO_3$	−1				1	1			−6.93	−7.69
$MgHCO_3^+$					1	1			+1.16	+0.62
$MgSO_4$					1		1		+2.36	+1.00

TABLE 6.6 Calculation of Major Ion Interactions in Freshwater

	Iteration		Metal	Ligand
	1st	2nd	(%)	(%)
H^+	8.1	8.1		
Na^+	3.55	3.55	100	
K^+	4.22	4.22	100	
Ca^{2+}	3.43	3.45	95	
Mg^{2+}	3.80	3.82	95	
HCO_3^-	3.00	3.02		96
SO_4^{2-}	4.00	4.05		90
Cl^-	3.70	3.70		100
OH^-	5.9	5.9		
CO_3^{2-}	5.23	5.25		1
H_2CO_3	4.75	4.77		2
HSO_4^-	10.11	10.16		
$NaCO_3^-$	7.51	7.53		
$NaHCO_3$	6.80	6.82		
$NaSO_4^-$	6.49	6.54		
KSO_4^-	7.26	7.31		
$CaOH^+$	8.18	8.20		
$CaCO_3$	5.46	5.50	3	1
$CaHCO_3^+$	5.17	5.21		
$CaSO_4$	5.12	5.19	2	6
$MgOH^+$	7.14	7.16		
$MgCO_3$	5.63	5.67	3	
$MgHCO_3^+$	5.64	5.68		
$MgSO_4$	5.44	5.51	2	3
ΣNa	$10^{-3.55}$	$10^{-3.55}$		
ΣK	$10^{-4.22}$	$10^{-4.22}$		
ΣCa	$10^{-3.41}$	$10^{-3.43}$		
ΣMg	$10^{-3.78}$	$10^{-3.80}$		
ΣHCO_3	$10^{-2.98}$	$10^{-3.00}$		
ΣSO_4	$10^{-3.95}$	$10^{-4.00}$		
ΣCl	$10^{-3.7}$	$10^{-3.7}$		

Garrels and Thompson[17] model for seawater, and of course similar to those of Whitfield[7] since most of the same constants and activity coefficients have been selected. The differences that exist among these various calculations point out the difficulty in estimating stability constants and activity coefficients in a system as complex as seawater.

In all these traditional models of ion interactions in seawater, chloride complexes are considered unimportant. However, there is evidence that species such

TABLE 6.7 Calculation of Major Ion Interactions in Seawater

	Iteration				Metal	Ligand
	1st	2nd	3rd	4th	(%)	(%)
H^+	8.1	8.1	8.1	8.1		
Na^+	0.33	0.35	0.34	0.34	98	
K^+	1.99	2.01	2.00	2.00	98	
Ca^{2+}	1.99	2.08	2.03	2.03	91	
Mg^{2+}	1.27	1.38	1.32	1.32	89	
HCO_3^-	2.62	2.83	2.80	2.81		64
SO_4^{2-}	1.55	1.96	1.93	1.95		40
Cl^-	0.26	0.26	0.26	0.26		100
OH^-	5.71	5.71	5.71			
CO_3^{2-}	4.32	4.53	4.50	4.51		1
H_2CO_3	4.59	4.80	4.77	4.78		1
HSO_4^-	8.26	8.67	8.64	8.66		
$NaCO_3^-$	4.06	4.29	4.25	4.26		2
$NaHCO_3$	3.57	3.80	3.76	3.77		7
$NaSO_4^-$	1.57	2.00	1.96	1.98	2	37
KSO_4^-	3.38	3.81	3.78	3.80	2	1
$CaOH^+$	7.16	7.25	7.20	7.20		
$CaCO_3$	4.45	4.75	4.67	4.68		1
$CaHCO_3^+$	3.94	4.24	4.16	4.17	1	3
$CaSO_4$	2.64	3.14	3.06	3.08	8	3
$MgOH^+$	4.98	5.09	5.03	5.03		
$MgCO_3$	3.48	3.80	3.71	3.72		8
$MgHCO_3^+$	3.27	3.59	3.50	3.51	1	13
$MgSO_4$	1.82	2.34	2.25	2.27	10	19
ΣNa	$10^{-0.31}$	$10^{-0.34}$	$10^{-0.33}$	$10^{-0.33}$		
ΣK	$10^{-1.97}$	$10^{-2.00}$	$10^{-1.99}$	$10^{-1.99}$		
ΣCa	$10^{-1.90}$	$10^{-2.04}$	$10^{-1.99}$	$10^{-1.99}$		
ΣMg	$10^{-1.16}$	$10^{-1.33}$	$10^{-1.27}$	$10^{-1.27}$		
ΣHCO_3	$10^{-2.41}$	$10^{-2.65}$	$10^{-2.61}$	$10^{-2.62}$		
ΣSO_4	$10^{-1.14}$	$10^{-1.58}$	$10^{-1.53}$	$10^{-1.55}$		
ΣCl	$10^{-0.26}$	$10^{-0.26}$	$10^{-0.26}$	$10^{-0.26}$		

as NaCl, KCl, $MgCl^+$, and $CaCl^+$ may represent a significant fraction (13, 17, 43, 47%, respectively) of the total metal concentrations.[18] The recalculation of the ion-pairing model with the additional chloride constants is straightforward. However, the extension of these results to trace elements (see Section 3) would require a reinterpretation of the original experimental coordination data with equilibrium constants that are consistent with the new ion-pairing model.

As discussed in Chapter 2, interactions among ions in complex systems span

the whole spectrum from unspecific long-range electrostatic interactions (of the type accounted for by the Debye–Hückel theory) to specific complex formation. In the *ion-association model* of seawater (Example 2), the mutual interactions among major ions are divided into these two types, utilizing simultaneously single ion activity coefficients and formation constants for the ion pair complexes. Such division between ideal and nonideal interactions among ions is largely arbitrary, particularly in the case of ion pairs. As is the case for nonideal effects, the major part of the energy for ion pair formation is electrostatic and may be considered "long range" since the primary solvation shell is thought to be intact. Still, we have chosen to consider that these long-range electrostatic interactions, but not others, result in the formation of independent chemical entities. To paraphrase Horne,[19] we have chosen to bless some liaisons into marriages and considered the others to be outside the ideality laws.

A different approach is clearly possible, and all electrostatic interactions among ions, including what we have taken to be ion pair formation, can be considered as nonideal interactions. In such a case, a *total activity coefficient*, γ_i^T, is defined for each ion as the ratio of the free ion activity to the *total* ion concentration:

$$\gamma_i^T = \frac{\{C_i\}}{[C_i]_T} \tag{1}$$

For example, according to Example 2, the total activity coefficients for the major seawater ions are

$$\gamma_{Na}^T = \frac{\{Na^+\}}{Na_T} = \gamma_{Na}\frac{[Na^+]}{Na_T} = 0.71 \times 0.98 = 0.70 \tag{2}$$

$$\gamma_K^T = \frac{\{K^+\}}{K_T} = \gamma_K\frac{[K^+]}{K_T} = 0.63 \times 0.98 = 0.62 \tag{3}$$

$$\gamma_{Ca}^T = \frac{\{Ca^{2+}\}}{Ca_T} = \gamma_{Ca}\frac{[Ca^{2+}]}{Ca_T} = 0.26 \times 0.91 = 0.24 \tag{4}$$

$$\gamma_{Mg}^T = \frac{\{Mg^{2+}\}}{Mg_T} = \gamma_{Mg}\frac{[Mg^{2+}]}{Mg_T} = 0.29 \times 0.89 = 0.26 \tag{5}$$

$$\gamma_{SO_4}^T = \frac{\{SO_4^{2-}\}}{[SO_4]_T} = \gamma_{SO_4}\frac{[SO_4^{2-}]}{[SO_4]_T} = 0.17 \times 0.4 = 0.068 \tag{6}$$

$$\gamma_{Cl}^T = \frac{\{Cl^-\}}{Cl_T} = \gamma_{Cl}\frac{[Cl^-]}{Cl_T} = 0.63 \times 1.0 = 0.63 \tag{7}$$

For the carbonate system, the coefficients are defined for each acid–base species:

$$\gamma_{H_2CO_3}^T = \frac{\{H_2CO_3^*\}}{[H_2CO_3]_T} = \gamma_{H_2CO_3}\frac{[H_2CO_3^*]}{[H_2CO_3]_T} = 1.13 \tag{8}$$

$$\gamma_{HCO_3}^T = \frac{\{HCO_3^-\}}{[HCO_3]_T} = \gamma_{HCO_3}\frac{[HCO_3^-]}{[HCO_3^-]+[NaHCO_3]+[CaHCO_3^+]+[MgHCO_3^+]}$$
$$= 0.68 \times 0.74 = 0.50 \tag{9}$$

$$\gamma_{CO_3}^T = \frac{\{CO_3^{2-}\}}{[CO_3]_T} = \gamma_{CO_3}\frac{[CO_3^{2-}]}{[CO_3^{2-}]+[NaCO_3^-]+[CaCO_3]+[MgCO_3]}$$
$$= 0.20 \times 0.10 = 0.020 \tag{10}$$

Such total activity coefficients are of course dependent on the ionic composition of the system and they must be defined anew for each different system. It is important to realize that total activity coefficients rather than ion pair formation constants are the quantities most directly amenable to experimental determination. Our calculation of total activity coefficients on the basis of the ion pair model is essentially a reversal of the process by which the parameters of the ion pair model are estimated in the first place.

In the same way that concentration equilibrium constants can be defined for any ionic strength by including activity coefficients into thermodynamic constants, *apparent equilibrium constants* can be defined for a particular solution by incorporation of total activity coefficients. For example, for the carbonate system in seawater, the first and second apparent mixed acidity constants are defined as

$$(K_1^{app})' = \frac{\{H^+\}[HCO_3]_T}{[H_2CO_3]_T} = K_1'\frac{\gamma_{H_2CO_3}^T}{\gamma_{HCO_3}^T} = 10^{-6.00} \tag{11}$$

$$(K_2^{app})' = \frac{\{H^+\}[CO_3]_T}{[HCO_3]_T} = K_2'\frac{\gamma_{HCO_3}^T}{\gamma_{CO_3}^T} = 10^{-8.93} \tag{12}$$

[These apparent constants vary somewhat depending on the chosen ion pair formation model. For example, Stumm and Morgan[20] report: $(pK_1^{app})' = 6.035$; $(pK_2^{app})' = 9.09$.] In the same way, we obtain the apparent solubility product of calcite:

$$K_s^{app} = [Ca^{2+}]_T[CO_3^{2-}]_T = \frac{K_s}{\gamma_{Ca}^T\gamma_{CO_3}^T} = 10^{-6.03} \tag{13}$$

Much of the interest in quantifying the extent of major ion association in seawater centers on its effects on the carbonate system and particularly calcium carbonate

solubility. [Note that $CaCO_3$(s) has not been considered in Example 2, thus allowing for calcite supersaturation in the seawater.]

In reference to the ion pair model of Example 2, apparent acidity and solubility constants effectively lump together the various ion pairs for each carbonate species, much in the way that H_2CO_3 and CO_2(aq) are lumped together to define $H_2CO_3^*$. This is a very convenient convention to study carbonate chemistry in seawater: by simple redefinition of the acidity constants, $pK_{a1} = 6.0$, $pK_{a2} = 8.9$, we can consider seawater as a typical CO_2, C_T, Alk, pH system, ignoring the complications of major ion interactions. Calculations with apparent constants for the carbonate system in seawater and complete ion-pairing calculations are equivalent only because the major cations are little affected by ion pairing. Otherwise, the free concentrations of the metals and hence their effects on the carbonate speciation would be affected by the pH through carbonate complexation and the apparent constants would vary with pH.

The two approaches—total activity coefficients or ion pair complexes—provide equally valid thermodynamic representations of ion interactions in water. Whether or not we wish to consider major ion interactions as actual complex formation is more a matter of philosophy and terminology than a matter of fact. In the end, it is really a matter of practicality. If one is considering systems with highly variable ionic strength and composition, then it seems more convenient to use a universal description of ion association according to the ion pairing approach. (For concentrated brines, the ion pairing model is insufficient and other ion interaction models including first and second order effects among all major ions must be considered; see Chapter 2.) On the contrary, if one is dealing exclusively with seawater composition, then the total activity coefficient approach becomes very efficient. The whole major seawater ion model of Tableau 6.1 can then be reduced to 12 lines, eliminating all ion pairs and including the proper total activity coefficients in the last column.

3. INORGANIC COMPLEXATION OF TRACE ELEMENTS

Unlike the question of interactions among major ions, in which everything depends on everything, the question of the inorganic speciation of minor constituents of natural waters can be treated one element at a time, independently of the other constituents. This is because the important complexes are formed with constituents in large excess whose free concentrations (activities) are unaffected by complexation with a trace element.

To focus this discussion, let us consider a divalent trace metal M^{2+}. The inorganic ligands that may form important complexes with this metal in natural waters are relatively few: OH^-, Cl^-, SO_4^{2-}, CO_3^{2-}, S^{2-} (HCO_3^- and HS^- are included implicitly). Other reactive inorganic ligands (e.g., F^-, Br^-, NH_3, PO_4^{3-}, CN^-) are usually present at concentrations too low to result in any significant metal binding.

Consider the following complex formation reactions with ligands A^- and B^-:

$$M^{2+} + mA^- = MA_m^{(m-2)-}; \qquad \beta_m \tag{14}$$

$$M^{2+} + nB^- = MB_n^{(n-2)-}; \qquad \beta_n \tag{15}$$

Introducing the mass laws for Reactions 14 and 15 into the mole balance equation for M^{2+} allows the separation of the metal and ligand concentrations into the two factors of a product:

$$TOTM = [M^{2+}] + [MA_m^{(m-2)-}] + [MB_n^{(n-2)-}] + \cdots \tag{16}$$

$$TOTM = [M^{2+}](1 + \beta_m[A^-]^m + \beta_n[B^-]^n + \cdots) \tag{17}$$

Such separation is possible as long as there are no polynuclear species, which would introduce higher exponents for $[M^{2+}]$. To resolve the question of metal speciation it is then sufficient to evaluate the term in brackets which depends exclusively on the ligand concentrations.

Since the inorganic ligands are normally in large excess of the trace metals that they bind, the problem of evaluating the free ligand concentrations is independent of the nature and concentration of the metals. Only two considerations then enter in the calculation: (1) at high ionic strength the possible effect of major ion interactions on the ligand speciation as discussed in Section 2, and (2) the acid–base chemistry of weak acid ligands as a function of pH. The use of apparent constants accounting for all ion-pairing effects allows the resolution of the acid–base speciation independently of the major ion interactions. For example, using the ionization fraction formalism for carbonate in seawater one can write

$$[CO_3^{2-}] = \alpha_2 C_T$$

in which α_2 is calculated on the basis of the appropriate apparent acidity constants.

In general, Equation 17 can thus be rewritten:

$$TOTM = [M^{2+}](1 + \beta_m(\alpha_A)^m(A_T)^m + \beta_n(\alpha_B)^n(B_T)^n + \cdots) \tag{18}$$

where the coefficients α are uniquely determined for a given pH and a given extent of major ion association.

In most cases, only a few of the terms inside the parentheses are important, most typically only one:

if $1 \gg \beta_m(\alpha_A)^m(A_T)^m, \beta_n(\alpha_B)^n(B_T)^n, \ldots$
then M^{2+} is the dominant species;
if $\beta_m(\alpha_A)^m(A_T)^m \gg 1, \beta_n(\alpha_B)^n(B_T)^n, \ldots$
then $MA_m^{(m-2)-}$ is the dominant species, and so on.

Species that are not dominant, but may be significant in the speciation of M^{2+}, are those for which the expression in parentheses is not too small compared to the largest one (say > 1%). Since L_T is an upper limit on $[L]$, the coefficients α are always smaller than 1; thus ligands for which $\beta_n(L_T)^n$ is less than 1 can never form dominant complexes.

The methodology to calculate the inorganic complexation of a trace metal is thus remarkably simple:

1. List all the species considered.
2. Calculate the free ligand concentrations on the basis of some ion interaction model and of the acid–base speciation of the weak acids—most simply by using apparent acidity constants that include the effects of major ion interactions.
3. Calculate the various terms in brackets and retain only those that are significant.
4. Obtain the distribution of the trace metal among its major inorganic species by division.

Example 3. Inorganic Speciation of Copper and Cadmium in Freshwater Let us consider the freshwater system of Example 1 and the following data from Table 6.3:

$CuOH^+$; $\log\beta_1 = 6.3$	$CuCO_3$; $\log\beta_1 = 6.7$	$CuSO_4$; $\log\beta_1 = 2.4$
$Cu(OH)_2$; $\log\beta_2 = 11.8$	$Cu(CO_3)_2^{2-}$; $\log\beta_2 = 10.2$	$CuCl^+$; $\log\beta_1 = 0.5$
$CdOH^+$; $\log\beta_1 = 3.9$	$Cd(SO_4)$; $\log\beta_1 = 2.3$	$CdCl^+$; $\log\beta_1 = 2.0$
$Cd(OH)_2$; $\log\beta_2 = 7.6$	$Cd(SO_4)_2^{2-}$; $\log\beta_2 = 3.2$	$CdCl_2$; $\log\beta_2 = 2.6$
	$Cd(SO_4)_3^{4-}$; $\log\beta_3 = 2.7$	$CdCl_3^-$; $\log\beta_3 = 2.4$
		$CdCl_4^{2-}$; $\log\beta_4 = 1.7$

From the calculations of Example 1, we already know the free ligand concentrations:

$$[OH^-] = 10^{-5.9}$$
$$[CO_3^{2-}] = 10^{-5.3}$$
$$[SO_4^{2-}] = 10^{-4.0}$$
$$[Cl^-] = 10^{-3.7}$$

A rapid examination of the thermodynamic data shows the predominant complexes to be the following.

For copper:

$$CuOH^+: \quad \beta_1[OH^-] = 10^{+0.4} \tag{19}$$

$$Cu(OH)_2: \quad \beta_2[OH^-]^2 = 10^{0.0} \tag{20}$$

$$CuCO_3: \quad \beta_1[CO_3^{2-}] = 10^{1.4} \tag{21}$$

$$Cu(CO_3)_2^{2-}: \quad \beta_2[CO_3^{2-}]^2 = 10^{-0.4} \tag{22}$$

For cadmium:

$$CdOH^+: \beta_1[OH^-] = 10^{-2.0} \tag{23}$$

$$CdSO_4: \beta_1[SO_4^{2-}] = 10^{-1.7} = 2 \times 10^{-2.0} \tag{24}$$

$$CdCl^+: \beta_1[Cl^-] = 10^{-1.7} = 2 \times 10^{-2.0} \tag{25}$$

Other complexes are negligible. The copper is thus mostly present as carbonate and hydroxide complexes and only about 3% as the free (hydrated) cupric ion:

$$\begin{aligned} TOTCu &= [Cu^{2+}](1 + 10^{0.4} + 10^{0.0} + 10^{1.4} + 10^{-0.4}) \\ &= [Cu^{2+}] \times 10^{1.5} = [Cu^{2+}] \times 30 = Cu_T \end{aligned} \tag{26}$$

therefore

$$\frac{[Cu^{2+}]}{Cu_T} = \frac{1}{30} = 3\%$$

$$\frac{[CuOH^+]}{Cu_T} = \frac{10^{0.4}}{30} = 8\%$$

$$\frac{[Cu(OH)_2]}{Cu_T} = \frac{10^{0.0}}{30} = 3\%$$

$$\frac{[CuCO_3]}{Cu_T} = \frac{10^{1.4}}{30} = 84\%$$

$$\frac{[Cu(CO_3)_2^{2-}]}{Cu_T} = \frac{10^{-0.4}}{30} = 1\%$$

On the other hand, only about 5% of the cadmium is complexed, and the major species is, by far, the free cadmium ion, Cd^{2+}:

$$\begin{aligned} TOTCd &= [Cd^{2+}](1 + 10^{-2} + 2 \times 10^{-2} + 2 \times 10^{-2}) \\ &= [Cd^{2+}] \times 1.05 = Cd_T \end{aligned} \tag{27}$$

therefore

$$\frac{[Cd^{2+}]}{Cd_T} \cong \frac{1}{1.05} = 95\%$$

$$\frac{[CdOH^+]}{Cd_T} = \frac{0.01}{1.05} = 1\%$$

$$\frac{[CdSO_4]}{Cd_T} = \frac{0.02}{1.05} = 2\%$$

$$\frac{[CdCl^+]}{Cd_T} = \frac{0.02}{1.05} = 2\%$$

Example 4. Inorganic Speciation of Copper and Cadmium in Seawater Consider the seawater model of Example 2; the free ligand concentrations are

$$[OH^-] = 10^{-5.7}$$
$$[CO_3^{2-}] = 10^{-4.5}$$
$$[SO_4^{2-}] = 10^{-2.0}$$
$$[Cl^-] = 10^{-0.26}$$

Extrapolation of the previous copper and cadmium constants to $I = 0.5\ M$ according to the Davies equation yields (concentration β's) [$^c\beta_1$]

$CuOH^+$; $\log \beta_{1c} = 5.7$	$CuCO_3$; $\log \beta_{1c} = 5.5$	$CuSO_4$; $\log \beta_{1c} = 1.2$
$Cu(OH)_2$; $\log \beta_{2c} = 10.9$	$Cu(CO_3)_2^{2-}$; $\log \beta_{2c} = 9.0$	$CuCl^+$; $\log \beta_{1c} = -0.2$
$CdOH^+$; $\log \beta_{1c} = 3.3$	$CdSO_4$; $\log \beta_{1c} = 1.1$	$CdCl^+$; $\log \beta_{1c} = 1.4$
$Cd(OH)_2$; $\log \beta_{2c} = 6.7$	$Cd(SO_4)_2^{2-}$; $\log \beta_{2c} = 2.0$	$CdCl_2$; $\log \beta_{2c} = 1.7$
	$Cd(SO_4)_3^{4-}$; $\log \beta_{3c} = 2.7$	$CdCl_3^-$; $\log \beta_{3c} = 1.5$
		$CdCl_4^{2-}$; $\log \beta_{4c} = 1.1$

For copper, the hydroxide and carbonate complexes are still the most important and the speciation of copper is changed from that of Example 3, mostly because of ionic strength effects:

$$CuOH^+: \quad \beta_1[OH^-] = 10^{0.0} \tag{28}$$

$$Cu(OH)_2: \quad \beta_2[OH^-]^2 = 10^{-0.5} \tag{29}$$

$$CuCO_3: \quad \beta_1[CO_3^{2-}] = 10^{1.0} \tag{30}$$

$$Cu(CO_3)_2^{2-}: \quad \beta_2[CO_3^{2-}]^2 = 10^{0.0} \tag{31}$$

$$CuSO_4: \quad \beta_1[SO_4^{2-}] = 10^{-0.8} \tag{32}$$

$$CuCl^+: \quad \beta_1[Cl^-] \cong 10^{-0.5} \tag{33}$$

Copper is now about 7% in the free ionic form:

$$TOTCu = [Cu^{2+}](1 + 10^{0.0} + 10^{-0.5} + 10^{1.0} + 10^{0.0} + 10^{-0.8} + 10^{-0.5})$$
$$= Cu_T$$

$$\frac{[Cu^{2+}]}{Cu_T} = \frac{1}{13.8} = 10^{-1.14} = 0.07 \tag{34}$$

For cadmium, the chloride complexes are now obviously the most important:

$$CdCl^+: \quad \beta_1[Cl^-] = 10^{1.14} \tag{35}$$

$$CdCl_2: \quad \beta_2[Cl^-]^2 = 10^{1.18} \tag{36}$$

$$CdCl_3^-: \quad \beta_3[Cl^-]^3 = 10^{0.72} \tag{37}$$

$$CdCl_4^{2-}: \quad \beta_4[Cl^-]^4 = 10^{0.06} \tag{38}$$

Since the constants are not very precisely known, we can consider that cadmium is present in seawater predominantly as chloro complexes and that the free cadmium ion is roughly 3% of the total metal:

$$TOTCd = [Cd^{2+}](1 + 10^{1.14} + 10^{1.18} + 10^{0.72} + 10^{0.06}) = Cd_T \tag{39}$$

therefore

$$\frac{[Cd^{2+}]}{Cd_T} = 10^{-1.56} = 0.03$$

Considering the results of Examples 3 and 4, we note that the speciation of metals that form important carbonate or hydroxide complexes (e.g., Cu^{2+}) varies strongly with pH. For metals that form important chloride or sulfate complexes (e.g., Cd^{2+}, Hg^{2+}) in seawater, their speciation in estuaries as freshwater mixes with seawater provides an interesting, though somewhat tedious, case study of inorganic complexation, as illustrated in Figure 6.8.

Hydroxide complexes, which may be considered to be produced by the dissociation of the weakly acidic hydrated metal ions, are of course important for many metals in natural waters, as illustrated in our study of ferric hydroxide precipitation (see Example 1 in Chapter 5). Many metal hydroxides form polymers [e.g., $Fe_n(OH)_n^{2n+}$] on the way to precipitation as hydrous oxide solids. These polynuclear complexes are poorly studied and often metastable. Note also that the presence of stoichiometric coefficients greater than 1 for the metal complicates the speciation calculations. At the limit there is a continuum between large metal hydroxide polymers and small suspended colloids of hydrous oxides.

From examination of the thermodynamic data in Table 6.3 it appears that apart from the hydroxides there are relatively few inorganic complexes of trace metals that are expected to be dominant in oxic waters. The major exceptions

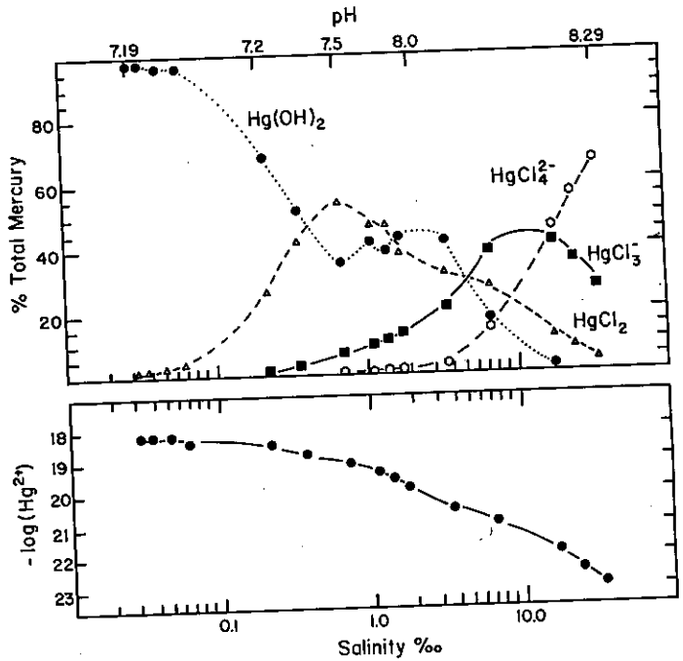

Figure 6.8 Inorganic speciation of mercury in an estuary as a function of salinity. This example has been calculated by considering the mixture of a freshwater ($[Cl^-]$) = 5×10^{-4} *M*; Alk = 1.3×10^{-4} *M*; pH = 7.2) with seawater (salinity = 36‰, pH = 8.20) and maintaining the total mercury concentration at 1 n*M*. Note the complicated changes in the inorganic mercuric species [(●)$Hg(OH)_2$, (Δ)$HgCl_2$, (■)$HgCl_3^-$, (○)$HgCl_4^{2-}$] due to concomitant variations in pH (see top scale) and major ion (chiefly Cl^-) concentrations.

are the carbonate complex of copper in sufficiently alkaline systems and the chloride complexes of cadmium, silver, and mercury in the presence of high chlorinity. Generalizing to all species that account for a few percent of the total metal concentrations, Table 6.8 shows—for the trace metals of Table 6.3—the inorganic species that are expected to be important in natural waters.

In anoxic waters the formation of bisulfide (HS^-), thiosulfate ($S_2O_3^{2-}$), and polysulfide (S_n^{2-}) complexes is important in maintaining a fraction of some trace metals in solution despite the low solubility of metal sulfides.[21,22]

4. ORGANIC COMPLEXATION

The concentration of dissolved organic matter in natural waters is typically in the range 1–100 mg $C\,L^{-1}$ (dissolved organic carbon, DOC). Typical average values in freshwater are 1 mg L^{-1} in ground- and rainwater, 2–10 mg L^{-1} in lakes

TABLE 6.8 Predominant Inorganic Species for Selected Trace Metals in Aquatic Systems

Ba
Ba^{2+}
$BaSO_4(s)$, $BaCO_3(s)$

Cr
$Cr(OH)_2^+$, $Cr(OH)_3$, $Cr(OH)_4^-$, $HCrO_4^-$, CrO_4^{2-}
$Cr(OH)_3(s)$

Al
$Al(OH)_3$, $Al(OH)_4^-$, AlF^{2+}, AlF_2^+
$Al(OH)_3(s)$, $Al_2O_3(s)$, $Al_2Si_2O_5(OH)_4(s)$, Al-silicates

Fe
Fe^{2+}, $FeCl^+$, $FeSO_4$, $Fe(OH)_2^+$, $Fe(OH)_4^-$
$FeS(s)$, $FeS_2(s)$, $FeCO_3(s)$, $Fe(OH)_3(s)$, $Fe_2O_3(s)$, $Fe_3O_4(s)$, $FePO_4(s)$, $Fe_3(PO_4)_2(s)$, Fe-silicates

Mn
Mn^{2+}, $MnCl^+$
$MnS(s)$, $MnCO_3(s)$, $Mn(OH)_2(s)$, $MnO_2(s)$

Co
Co^{2+}, $CoCl^+$, $CoSO_4$
$CoS(s)$, $Co(OH)_2(s)$, $CoCO_3(s)$, $Co(OH)_3(s)$

Ni
Ni^{2+}, $NiCl^+$, $NiSO_4$
$NiS(s)$, $Ni(OH)_2(s)$

Cu
Cu^{2+}, $CuCO_3$, $CuOH^+$
$CuS(s)$, $CuFeS_2(s)$, $Cu_2CO_3(OH)_2(s)$, $Cu_3(CO_3)_2(OH)_2(s)$, $Cu(OH)_2(s)$, $CuO(s)$

Zn
Zn^{2+}, $ZnCl^+$, $ZnSO_4$, $ZnOH^+$, $ZnCO_3$, ZnS
$ZnS(s)$, $ZnCO_3(s)$, $ZnSiO_3(s)$

Pb
Pb^{2+}, $PbCl^+$, $PbCl_2$, $PbCl_3^-$, $PbOH^+$, $PbCO_3$
$PbS(s)$, $PbCO_3(s)$, $Pb(OH)_2(s)$, PbO_2

Hg
Hg^{2+}, $HgCl^+$, $HgCl_2$, $HgCl_3^-$, $HgOHCl$, $Hg(OH)_2$, HgS_2^{2-}, $HgOHS^-$
$HgS(s)$, $Hg(liq)$, $Hg(OH)_2(s)$

Cd
Cd^{2+}, $CdCl^+$, $CdCl_2$, $CdCl_3^-$, $CdOH^+$, CdS, $CdHS^+$, $Cd(HS)_2$, $Cd(HS)_3^-$, $Cd(HS)_4^{2-}$
$Cd(s)$, $CdCO_3(s)$, $Cd(OH)_2(s)$

Ag
Ag^+, $AgCl$, $AgCl_2^-$, AgS^-, $AgHS$, $AgHS_2^{2-}$, $Ag(HS)_2^-$
$Ag_2S(s)$, $AgCl(s)$, $AgBr(s)$

and rivers, 10–50 mg L^{-1} in bogs and marshes. In the ocean, DOC varies from 1 mg C L^{-1} in deep waters to as much as 10 times this value in highly productive surface waters. Recent determinations of DOC by high temperature catalytic oxidation have given values two to three times those of earlier methods.[23] These controversial data exhibit strong vertical DOC gradients whose correlation with oxygen utilization suggests significant respiration of DOC in deep waters.[24]

The chemical nature of dissolved organic matter is poorly characterized. For example, in attempts to fractionate organic compounds in seawater, 50–90% of the DOC could not be identified and is thus broadly classified as humic and fulvic material[25,26] (Table 6.9). The term *humic acids* is normally used to indicate the fraction (ca. 10%) of DOC that precipitates at very low pH. The term *fulvic acids*

TABLE 6.9 Composition of Dissolved Organic Matter in Surface and Deep Ocean Water[a]

Compound Class[b] (Units)	Surface Ocean		Deep Ocean	
	Concentration	DOC-C[c] (%)	Concentration	DOC-C[c] (%)
DOC (μg/L)	400–2500		400–1600	
TFAA (n*M*)	50–500	0.4–1.8	25–40	0.3–0.4
THAA (n*M*)	50–1600	0.4–5.9	50–200	0.6–2.4
Hexosamines (n*M*)	10–30	0.1–0.2		
Urea (n*M*)	30–1700	0.05–1.4	< 70	< 0.17
TFMS (n*M*)	90–1700	1.0–8.7	51–120	0.8–1.8
THMS (n*M*)	600–4700	6.5–24	1000–1400	15–21
Combined uronic acids (n*M*)	75–260	0.8–1.3		
THFA (n*M*)	19–190	0.5–2.5	37–80	1.4–3.0
Chlorophyll (ng L^{-1})	10–2000	0.001–0.1	< 100	< 0.02
Indoles (μg L^{-1})	1	0.1		
Glycollic acid (n*M*)	260–520	0.9		
Phenols (μg L^{-1})	1–2	0.2		
Nucleic acids (μg L^{-1})	13–80	1.8–5.0		
Sterols (μg L^{-1})	0.2–0.4	0.02		
Hydrocarbons (μg L^{-1})	0.3–30	0.04–2.0	0–4	0–0.8
Vitamin B12 (ng L^{-1})	0.1–6.0		1	
Thiamine (ng L^{-1})	8.0–100			
Biotin (ng L^{-1})	1.6–4.6			
Unidentified		46–87[d]		70–82[d]

[a] Adapted from Buffle (1988).[25]

[b] TFAA—total free amino acids; THAA—total hydrolyzable amino acids; TFMS—total free monosaccharides; THMS—total hydrolyzable monosaccharides; THFA—total hydrolyzable fatty acids.

[c] Percentage contribution of carbon in the compound class to DOC estimated based on surface DOC = 0.7–1.5 mg L^{-1}, mean deep DOC = 0.5 mg L^{-1}.

[d] Estimated by difference based on other values in this table.

refers to acid-soluble compounds, usually of lower molecular weight (ca. 40% of DOC). Both of these fractions are generally defined operationally by a method of extraction, most often as what is retained on a particular type of chromatographic column. Thus humic and fulvic acids are those compounds that are sufficiently hydrophobic to be retained on acrylic-ester resins (XAD-8). A more hydrophilic fraction that passes through such columns can be extracted on others (e.g., XAD-4). This fraction (ca. 30% of DOC) has been less extensively studied than the more hydrophobic one but appears to have generally the same coordination properties. Here we shall use the general terms humate, humic acid, or humic compounds to designate all fractions: humic, fulvic, and hydrophilic acids.

One could undoubtedly identify a myriad of other trace organic compounds from natural and pollution sources in all natural waters, but the compounds in Table 6.9 may in fact account for the bulk of the DOC in the samples. A majority of the organic matter is put into the ill-defined class of humic acids because it possesses the inherent complexity and structural variability characteristic of this class, probably not because we ignore the existence of some well-defined substance that accounts for a sizeable fraction of the dissolved organic pool.

There is a major difference between the geochemical behavior of the humic organic fraction and the rest. Relatively small and reactive molecules such as sugars, amino acids, urea, or phenols provide readily available energy or nitrogen sources to aquatic microorganisms and are rapidly degraded. Their concentrations are maintained in the water column by an equally rapid production rate from microorganisms. One should visualize this fraction of the total DOC as turning over very rapidly—on a time scale of minutes to days. The rapid turnover time of this material makes it analytically elusive; some researchers believe that compounds such as carbohydrates may represent a sizeable fraction of the DOC.[27,28] The polymeric compounds that compose the humic fraction are refractory (a good definition for dissolved humic material is the acidic fraction of the DOC that is resistant to oxidation), and they are eliminated, at least in part, by eventual incorporation into the sediments rather than by degradation. Although recent work indicates some turnover of higher molecular weight DOC by microbial respiration[23,24] or by photochemical degradation,[29,30] still the residence time of this DOC fraction in the water column is on a time scale of weeks to thousands of years.

There is an ongoing scientific debate over the role that natural organic compounds play in complexing metal ions in aquatic systems.[31–33] An imposing body of experimental evidence supports the argument that some metal ions are largely, if not mostly, bound to organic ligands. Determinations of trace metal speciation in natural waters are based on the nonreactivity of the metals in chemical or biological assays; this nonreactivity is generally attributed to metal complexation by dissolved organic ligands. Thus the analytical method employed must be responsive only to some definable fraction of the total (dissolved) metal, ideally the free metal ion alone or with its inorganic complexes. For example, the dependence of copper toxicity on the free cupric ion concentration (discussed

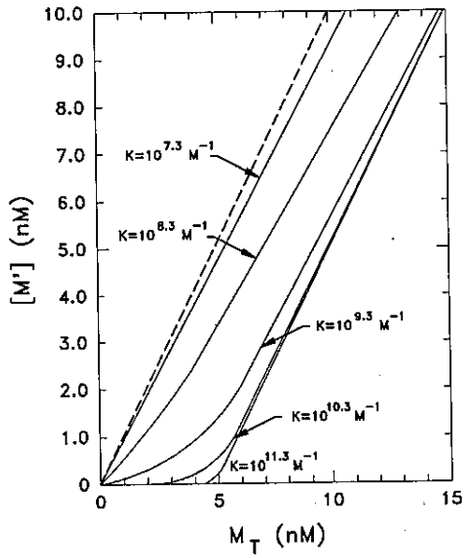

Figure 6.9 Voltammetric titration of a 5-nM ligand of variable metal binding strength. Only the inorganic form of the metal, M′, is assumed to be measured by reaction at the electrode surface. The effective complexation constant K is defined as $K = [MY]/[M'][Y_T - [MY]]$.

in Section 6) has been used as the basis for bioassays. In these assays, however, copper must be added to the water sample in order to observe any deleterious effect on the organisms. In almost all cases, such a metal titration is necessary because of the detection limit of the analytical method. Estimations of the ambient free metal ion concentrations are then obtained by modeling the metal titration and extrapolating to ambient total metal concentrations as discussed in Sidebar 6.1.

According to such estimations, the extent of metal complexation in natural waters can be close to 100% for reactive metals such as copper. Recently, significant complexation of lead, mercury, and even the less reactive metals zinc and cadmium has also been reported (see references from Table 6.10). Table 6.10 lists some of the reported values for trace metal complexation in both fresh- and seawater. This table is meant to provide an introduction to the substantial literature on metal complexation rather than a comprehensive review.

It can also be argued that very few important metal complexes have been directly demonstrated to exist and that, in evaluating reported metal complexation, certain limitations and assumptions of the analytical methods must be considered. The necessity for data modeling and extrapolating in the case of strongly complexed metals has already been mentioned. The attribution of the nonreactivity of metals strictly to organic complexation (or organometallic compounds) neg-

SIDEBAR 6.1

Electrochemical Measurements of Metal Complexation

Although bioassays have been used with some success and chromatographic techniques now show promise, the overwhelming majority of the analytical data on metal complexation in natural waters has been obtained with electrochemical methods. These electrochemical methods fall into two categories: potentiometric and voltammetric. Potentiometric methods involve the use of ion-sensitive electrodes, which exhibit a logarithmic response to free metal ion activity. An example of potentiometric data on copper complexation by humic substances is shown later (Figure 6.18). Although ion-sensitive electrodes have excellent sensitivity for free metal ion activities, the measurements require fairly high *total* metal concentrations ($\geq 10^{-7}$ M), usually in excess of those present in natural waters. In addition, for some metals, measurements cannot be made in high-chloride media, such as seawater.[50]

In voltammetric methods, the current generated when metals are oxidized or reduced at an electrode surface is measured. In direct application, the measured signal is linearly related to the concentration of labile metal—which may include weak organic complexes as well as inorganic complexes of the metal. The sensitivity of such direct measurements is usually insufficient for environmental applications. Thus voltammetric techniques applied in natural waters include an electrochemical preconcentration step, which dramatically increases sensitivity. For example, a widely used preconcentration technique consists of plating the metal by reduction at a hanging mercury electrode before measuring it in an oxidative "stripping" step (reverse polarography). Recent applications of such methods in their multifarious variations have allowed determination of labile metals at concentrations down to 0.2 nM.[44] now ~3pM level for Co

In some cases this sensitivity is good enough to obtain direct measurement of labile metal concentrations in natural water. In many cases, however, the reactive metal concentrations are still too low and a titration of the water sample with added metal is then performed. The shape of such a titration curve in the presence of a ligand at 5×10^{-9} M concentration is shown in Figure 6.9. This figure assumes that the added metal has reached equilibrium with the ligand before measurement and that the metal–ligand complex is strictly unreactive at the electrode surface. Neither assumption is necessarily always correct (see Section 5). As seen in Figure 6.9, the ligand concentration L_T can in principle be obtained by extrapolation of the linear portion of the graph and the ligand's strength, K,

(*continued*)

deduced from its curvature (various linearizations of the graph can be used to simplify the data reduction). Thus in a simple system the inorganic (viz. "reactive") metal concentration can be calculated from knowledge of L_T, K, and M_T. In complex systems containing several ligands of varying concentrations and strengths, the data-fitting problem is much more complicated. In all cases the validity of the calculated inorganic metal concentration depends on the assumption that the ligand controlling it is the one characterized by the titration. For example one must assume that the unmeasurable leftmost point in Figure 6.9 is determined by the 5-nM ligand, not by another much stronger 1-nM ligand.

TABLE 6.10 Extent of Organic Complexation of Metals in Surface Waters

Metal	Percent Complexed	Water Type	Method	Reference
Cu	100	Oceanic	Electrochemical	34
	> 99	Coastal	Electrochemical	35
	> 95		Electrochemical	36
	> 99.9		Ligand competition	37
	> 99.9		Ligand competition	38
	> 99		Bioassay	35, 39
Zn	> 98	Oceanic	Electrochemical	40
	> 95		Electrochemical	41
	60–95	Estuarine	Electrochemical	42
	14	Riverine	Sorption	43
Pb	50–70	Oceanic	Electrochemical	44
Hg	2–89[a]	Freshwaters	Atomic fluorescence	45
Al	≃ 40	Freshwaters	Ion-exchange chromatography	46
Cd	0	Oceanic	Electrochemical	47
	0		Radiotracer addition and chromatography	48
	70		Electrochemical	49
Mn	0	Oceanic	Radiotracer addition and chromatography	48

[a]For Hg, "organic complexation" includes organomercury compounds (cf. Section 4.5).

lects the possible importance of colloidal species. Usually, the "dissolved" metal fraction is operationally defined by filtration or other physical methods of separation that do not exclude colloids. More importantly, equilibrium between (dissolved) metal and ligand species on the analytical time scale of titration experiments is usually assumed. Possible artifacts arising from this assumption are discussed in Section 5 on complexation kinetics. In addition, competition among metals has been considered only in a few cases.[37,44]

The greatest difficulty in predicting trace metal speciation from field measurements stems from a lack of information about naturally occurring complexing agents. Modeling requires information on ligand concentrations and stability constants, yet field measurements of trace metal speciation provide these parameters only indirectly. Direct information on the distribution and structures of naturally occurring metal complexes is a crucial link between measuring and modeling trace metal speciation in natural waters.

In the absence of such information, we may gain some quantitative understanding of the effects of organic complexation on trace metals in natural waters by making equilibrium calculations of model systems. As we shall see, the identifiable fraction of marine DOC cannot contribute much to metal complexation. Even the amino acids, which have the most interesting complexing properties, are not present in sufficient concentrations to affect metal speciation in most natural waters. We therefore focus on the following three categories of aquatic organic ligands:

1. Well-defined, strong complexing agents, such as EDTA and NTA, that are introduced into the aquatic environment through human activities.
2. Strong ligands produced by the planktonic biota. These may be present at only trace concentrations but exhibit much higher affinities for metals than the metabolites listed in Table 6.9. The information concerning these ligands originates mostly from culture studies in which high concentrations can be obtained. Extrapolation of these results to natural waters is of course problematic.
3. Humic substances isolated from a variety of aquatic systems and whose coordination properties have been characterized on concentrated samples by an assortment of methods.

Let us then examine each of these categories and obtain some quantitative estimates of organic complexation, recognizing that the question must ultimately be resolved through direct analysis, not model calculations.

4.1 Trace Metal Complexation by Strong (Anthropogenic) Chelating Agents

Metal complexation by strong artificial chelating agents such as NTA $[N(CH_2COO^-)_3]$ or EDTA (see Figure 6.7) is probably the best studied topic in aquatic coordination chemistry, and the effects of these chelating agents in complex mixtures have been thoroughly analyzed. EDTA has been and continues to be used for a wide range of industrial, pharmaceutical, and agricultural applications.[51,52] Because of its widespread use and limited biodegradation, EDTA has been found in groundwaters, sewage effluents, freshwaters, including drinking water, and estuarine waters.[53–56] Of particular concern is the mobilization of trace metals in groundwater due to the presence

of EDTA. The use of EDTA in decontamination of nuclear facilities has been implicated in radionuclide migration in groundwater.[57,58]

The effect of EDTA on trace metal speciation is examined in the following example. According to the data of Table 6.3, copper is one of the metals expected to be most complexed by EDTA. For comparison purposes let us consider both copper and cadmium.

Example 5. Complexation of Copper and Cadmium by EDTA in Seawater
Measured concentrations of EDTA in the Mississippi River are in the range of 1–10 nM, attaining the upper limit of the range downstream of major urban inputs. In the United State municipal sewage contains typically 100–500 nM. (In countries where EDTA is used to replace phosphates in some cleaning products, the concentration is higher.) Thus, $10^{-7}\,M$ EDTA is a reasonable upper limit to the possible ligand concentration in a harbor or estuary. To the recipe of our seawater model (Example 2), let us then add typical surface seawater concentrations of copper ($10^{-8.5}\,M$) and cadmium ($10^{-9}\,M$) and $10^{-7}\,M$ EDTA:

$$Y_T = 10^{-7}\,M$$
$$Cu_T = 10^{-8.5}\,M$$
$$Cd_T = 10^{-9}\,M$$

Recall that at pH = 8.1,

$$[OH^-] = 10^{-5.7}$$
$$[CO_3^{2-}] = 10^{-4.5}$$
$$[SO_4^{2-}] = 10^{-2.0}$$
$$[Cl^-] = 10^{-0.26}$$
$$[Ca^{2+}] = 10^{-2.0}$$
$$[Mg^{2+}] = 10^{-1.3}$$

The relevant EDTA constants are obtained from Table 6.3 after appropriate ionic strength corrections*:

$HY^{3-}; \log \beta'_1 = 10.1$	$CaY^{2-}; \log \beta_1 = 10.0$	$CuY^{2-}; \log \beta_1 = 18.1$
$H_2Y^{2-}; \log \beta'_2 = 16.0$	$MgY^{2-}; \log \beta_1 = 8.2$	$CdY^{2-}; \log \beta_1 = 15.8$

*Ionic strength corrections according to the Davies equation have dubious validity for ions of charge 3 and 4. However, as seen in the example and as is discussed below, the results of the calculations are controlled by the ratios K_{Cu}/K_{Ca} and K_{Cd}/K_{Ca}, which are unaffected by the ionic strength corrections.

To simplify the problem, let us recall the results of Example 4:

$$\Sigma \text{inorganic Cu species} = [Cu'] = 10^{1.14}\,[Cu^{2+}]$$
$$\Sigma \text{inorganic Cd species} = [Cd'] = 10^{1.56}\,[Cd^{2+}]$$

The mole balance equations for copper and cadmium thus simplify to:

$$TOTCu = [Cu'] + [CuY^{2-}] = [Cu^{2+}](10^{1.14} + 10^{18.1}[Y^{4-}])$$
$$= Cu_T = 10^{-8.5} \quad (40)$$
$$TOTCd = [Cd'] + [CdY^{2-}] = [Cd^{2+}](10^{1.56} + 10^{15.8}[Y^{4-}])$$
$$= Cd_T = 10^{-9.0} \quad (41)$$

The free ligand concentration is obtained from the EDTA mole balance equation:

$$TOTY = [HY^{3-}] + [H_2Y^{2-}] + [CaY^{2-}] + [MgY^{2-}] + [CuY^{2-}] + [CdY^{2-}]$$
$$= Y_T = 10^{-7} \quad (42)$$

The last two terms can obviously be neglected since Cu_T and $Cd_T \ll Y_T$:

$$TOTY = [Y^{4-}](10^{10.1}[H^+] + 10^{16.0}[H^+]^2 + 10^{10.0}[Ca^{2+}] + 10^{8.2}[Mg^{2+}])$$
$$= 10^{-7} \quad (43)$$
$$TOTY = [Y^{4-}](10^{2.0} + 10^{-0.2} + 10^{8.0} + 10^{6.9}) = 10^{-7} \quad (44)$$

Note that the first two terms are also negligible and that EDTA is predominantly in the calcium form. As a result,

$$[Y^{4-}] = 10^{-8.0} \times 10^{-7} = 10^{-15.0} \quad (45)$$

Substituting into the copper and cadmium mole balances,

$$TOTCu = [Cu^{2+}](10^{1.14} + 10^{3.1}) = 10^{-8.5} \quad (46)$$
$$TOTCd = [Cd^{2+}](10^{1.56} + 10^{0.8}) = 10^{-9.0} \quad (47)$$

The concentrations of free, total inorganic, and organically-complexed metals are:

$[Cu^{2+}] = 10^{-11.6}$;	$[Cu'] = 10^{-10.5}$;	$[CuY^{2-}] = 10^{-8.5}$
$[Cd^{2+}] = 10^{-10.6}$;	$[Cd'] = 10^{-9.1}$;	$[CdY^{2-}] = 10^{-9.9}$

The copper is thus totally bound to EDTA, but only some 12% of the cadmium is in the organic complex form. In this example, there is no competition between

the two trace metals for complexation with the organic ligand since EDTA is present in large excess.

* * *

Example 5 illustrates several important points concerning organic complexation of trace metals in natural waters. First and foremost, weak complexing agents, such as amino acids or other identifiable organic compounds listed in Table 6.9, cannot, at their ambient concentrations in natural waters, affect metal speciation. Even the strong ligand EDTA at the relatively high concentration of $10^{-7}\,M$ can only slightly affect the speciation of cadmium in seawater. If the affinity and concentration of the ligand were somewhat smaller, say, a factor of 10 each, even copper, one of the most reactive trace metals, would be present largely as inorganic species. For organic complexation to be important in the speciation of a trace metal, it is thus necessary that the ligand exhibit a very high specificity for the metal (see next example) or that the ligand concentration and effective binding constant be quite high.

In addition to higher organic ligand concentrations and lesser competition from inorganic ligands, a reason to expect organic complexation of trace metals to be more important in freshwater than in seawater is the dominant role of the major divalent cations, Ca^{2+} and Mg^{2+}, on the organic ligand speciation in seawater. As seen in Example 5, while copper is effectively 100% bound with EDTA, EDTA itself is 100% bound with calcium, which is itself 100% free. This is possible of course because of the wide differences in total concentrations: $Cu_T \ll Y_T \ll Ca_T$. The result is a large decrease in the apparent binding strength of EDTA for the metals:

$$[CuY^{2-}] = K_{Cu}[Cu^{2+}][Y^{4-}] \tag{48}$$

$$[CuY^{2-}] = \frac{K_{Cu}}{K_{Ca}[Ca^{2+}]}[Cu^{2+}]Y_T \tag{49}$$

therefore

$$K_{Cu}^{app} = \frac{K_{Cu}}{K_{Ca}[Ca^{2+}]} = 10^{-8}\,K_{Cu} \tag{50}$$

In other words, the complexation of copper by EDTA is controlled by the equilibrium of the reaction:

$$CaY^{2-} + Cu^{2+} = CuY^{2-} + Ca^{2+}; \qquad K = \frac{K_{Cu}}{K_{Ca}} \tag{51}$$

which is pushed to the left by a large calcium concentration. Although sometimes the magnesium rather than the calcium complex is dominant, this result is applicable to many organic ligands in seawater, and it affects the complexation of all trace metals. In freshwaters, where the calcium and magnesium concentrations are 1–3 orders of magnitude smaller, the effective binding constants

are increased accordingly. In some cases, depending on the particular ligand and the pH, the ligand speciation may in fact depend directly on its acid–base chemistry. This is often the case for weak ligands. Even for EDTA the calcium and magnesium complexes become unimportant in soft, acidic waters (e.g., where pH = 4, $[Ca^{2+}] = 10^{-4}$, $I = 0\,M$):

$$TOTY = [Y^{4-}](10^{11.1}[H^+] + 10^{17.8}[H^+]^2 + 10^{21.0}[H^+]^3 + 10^{12.4}[Ca^{2+}]) \tag{52}$$

The ligand speciation is then dominated by the species H_2Y^{2-} and H_3Y^-. At low ligand concentrations, however, when the metal–ligand concentration ratio exceeds unity for some metals, the ligand speciation is dominated by the corresponding complexes. Figure 6.10 illustrates what happens to EDTA and to various trace metals when a freshwater is titrated with EDTA. In this example EDTA at very low concentrations is present chiefly in the nickel complex. When nickel itself becomes titrated as the EDTA concentration exceeds that of nickel, the copper and zinc complexes become prevalent. Finally, when those two

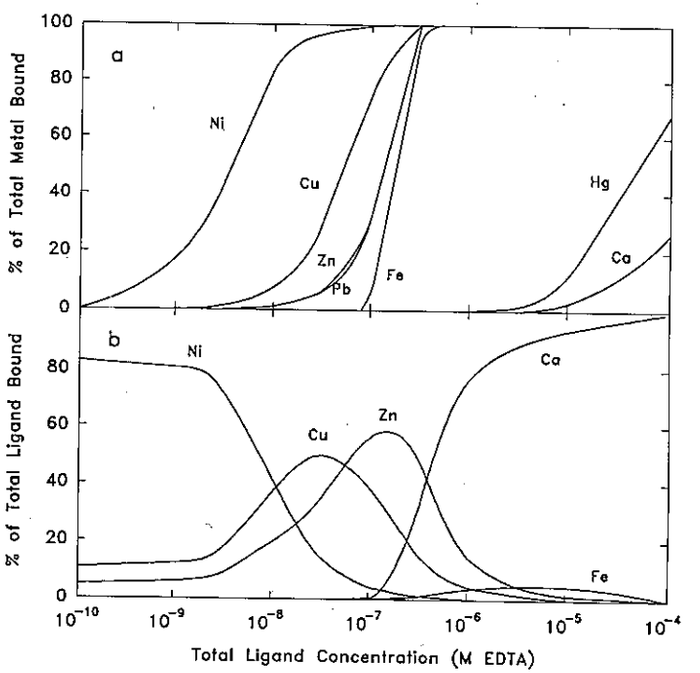

Figure 6.10 Calculated titration of a model freshwater with EDTA. (*a*) Speciation of the metals; (*b*) EDTA speciation. The pH is fixed at 8.10 and the total concentrations are as follows: $Ca_T = 3.7 \times 10^{-4}\,M$; $Mg_T = 1.6 \times 10^{-4}\,M$; $K_T = 6.0 \times 10^{-5}\,M$; $Na_T = 2.8 \times 10^{-4}\,M$; $Fe(III)_T = 5.0 \times 10^{-7}\,M$; $Cu_T = 5 \times 10^{-8}\,M$; $Hg_T = 10^{-9}\,M$; $Zn_T = 1.5 \times 10^{-7}\,M$; $Ni_T = 5 \times 10^{-9}\,M$; $Pb_T = 10^{-9}\,M$; $C_T = 10^{-3}\,M$; $[SO_4]_T = 10^{-4}\,M$; $Cl_T = 2 \times 10^{-4}\,M$.

metals are themselves titrated ($Y_T > Cu_T + Zn_T = 50 + 150\,nM$), EDTA becomes controlled by its calcium complex. Besides Ni, Cu, and Zn, the other three metals included in this model calculation, Hg, Pb, and Fe, also become bound to EDTA although they never account for a sizeable fraction of the ligand. Lead and zinc are titrated simultaneously. Lead, in contrast to zinc, does not affect the ligand speciation because of its low total concentration; zinc is present in 150-fold excess of lead. Iron, which is controlled by its amorphous hydroxide precipitate, becomes organically bound only when the free EDTA increases markedly upon titration of the zinc. Mercury is the last of the trace metals to be titrated.

4.2 Trace Metal Complexation by Strong Biogenic Chelating Agents

Practically all aquatic microorganisms release metabolites into their growth medium, including a variety of compounds whose affinity for metals ranges from that of simple amino acids up to that of fairly strong chelating agents. But, as argued before, unless these compounds have unusual metal binding strength or specificity, they are unlikely to affect metal speciation in natural waters. Aquatic microorganisms, however, synthesize two families of strong metal complexing agents: transport ligands to acquire essential trace metals and detoxifying (or buffering) ligands to defend themselves against the toxicity of others.

Transport Ligands. For the most part we do not know the nature of the metal transport ligands in phytoplankton and bacteria. But we know that they are normally membrane-bound and exhibit high affinity and specificity for the target metals. (This is clearly a necessity to acquire trace metals from oligotrophic waters.) In the case of iron, three types of transport ligands may be important. The catechol and hydroxamate siderophores of terrestrial bacteria (Figure 6.11) are also produced by heterotrophic marine bacteria, cyanobacteria (blue green algae), fungi, and marine dinoflagellate phytoplankton.[59–63] In the organisms that have been studied so far, siderophores are produced under iron-limited growth conditions and then released to the medium. (Such release may not be typical of organisms living in dilute media such as the high seas.) The iron–siderophore complexes are then taken up through an active (i.e., ATP-requiring) process involving specific membrane proteins.[64,65] The detailed structures and the exact properties of several of these siderophores have been characterized and one of them, desferriferrioxamine B, is included in Table 6.3. Siderophores have been isolated from soils[66] and chemical and biological assays have indicated their presence in algal mats[67] and in lakewater during a blue-green algal bloom.[68] It has been suggested that siderophore production by blue-green algae may suppress the growth of competing species, which are unable to utilize the iron–siderophore complex for growth, thus fostering the bloom of blue-green algae.[68] In the next example, we use the well-characterized trihydroxamate siderophore desferriferrioxamine B as a model compound to

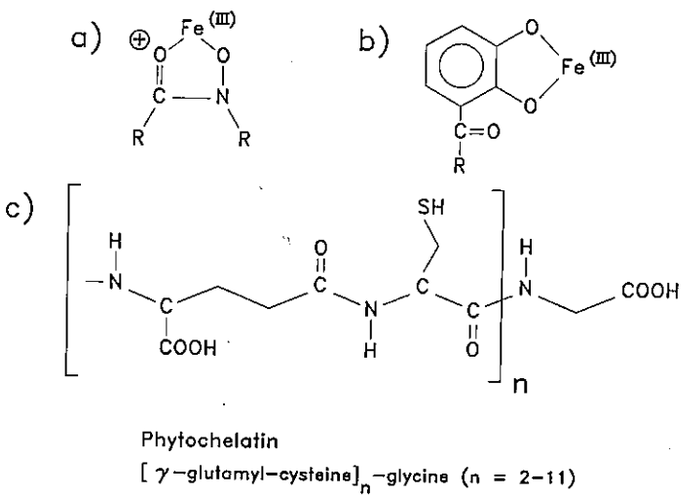

Figure 6.11 Complexing functionalities of some biogenic ligands: (*a*) hydroxar siderophores; (*b*) catechol siderophores; (*c*) phytochelatins. Only partial structures shown for the siderophores. The side-chain moieties (indicated by R-) are, in n siderophores, quite substantial and often include additional complexing functional grc of the types illustrated. For example, desferriferrioxamine B, the siderophore that app in Table 6.3, is a hexadentate ligand with three of the hydroxamate functional grc shown in *a*. For detailed structures see Neilands, 1981.[59]

examine the situation created by the presence of complexing agents with v high affinity and specificity for a particular metal.

Example 6. Complexation of Iron(III) and Copper by a Trihydroxam Siderophore in Freshwater Consider the effect of adding desferriferrioxam B to the freshwater system of Example 1 containing $10^{-6}\,M$ Fe(III) a $10^{-7}\,M$ Cu. (Recall that at pH = 8.1, $[OH^-] = 10^{-5.9}$, $[CO_3^{2-}] = 10^{-}$ $[SO_4^{2-}] = 10^{-4.0}$, $[Cl^-] = 10^{-3.2}$, $[Ca^{2+}] = 10^{-3.5}$, and $[Mg^{2+}] = 10^{-4}$ Desferriferrioxamine B is a hexadentate ligand with three hydroxamates an terminal amine which is protonated somewhere below pH = 11. We thus u the symbol Y^{2-} to indicate the ligand with all hydroxamates deprotonat The relevant organic complexation constants are given in Table 6.3:

$HY^-; \log\beta_1 = 10.1$	$CaY^{2-}; \log\beta_1 = 3.5$	$FeY^+; \log\beta_1 = 31.9$
$H_2Y; \log\beta_2 = 19.4$	$MgY^{2-}; \log\beta_1 = 5.2$	$FeHY^{2+}; \log\beta_{11} = 32.6$
$H_3Y^+; \log\beta_3 = 27.8$		$CuY^{2-}; \log\beta_1 = 15.0$
		$CuHY^+; \log\beta_{11} = 24.1$
		$CuH_2Y^{2+}; \log\beta_{12} = 27.$

At a pH of 8.1, in the absence of chelating agents, iron is precipitated as $Fe(OH)_3(s)$ (see Example 1 in Chapter 5), and the free ferric ion concentration is given by

$$[Fe^{3+}] = 10^{3.2}[H^+]^3 = 10^{-21.1} \tag{53}$$

The free cupric ion concentration in the absence of a chelator has been calculated as 3% ($10^{-1.5}$) of the total inorganic copper in Example 3:

$$[Cu^{2+}] = 10^{-1.5}[Cu'] = 10^{-8.5}$$

The mole balance equation for desferriferrioxamine at low ligand concentration, low enough not to affect $[Fe^{3+}]$ or $[Cu^{2+}]$, can then be simplified:

$$\begin{aligned} TOTY = [Y^{2-}](1 &+ 10^{10.1}[H^+] + 10^{19.4}[H^+]^2 + 10^{27.8}[H^+]^3 \\ &+ 10^{3.5}[Ca^{2+}] + 10^{5.2}[Mg^{2+}] + 10^{31.9}[Fe^{3+}] \\ &+ 10^{32.6}[H^+][Fe^{3+}] + 10^{15}[Cu^{2+}] + 10^{24.1}[H^+][Cu^{2+}] \\ &+ 10^{27}[H^+]^2[Cu^{2+}]) = Y_T \end{aligned} \tag{54}$$

All terms are negligible compared to the FeY^+ concentration:

$$TOTY = [FeY^+] = 10^{31.9}[Fe^{3+}][Y^{2-}] = 10^{10.8}[Y^{2-}] = Y_T \tag{55}$$

Given the enormous affinity of the organic ligand for the ferric ion, as long as $Y_T < Fe_T$, the speciation problem is simple: the ligand is entirely bound to iron; the free feric ion is controlled by precipitation of $Fe(OH)_3(s)$; and the copper remains chiefly in the copper carbonate complex ($K_{CO_3}[CO_3^{2-}] = 10^{1.4}$).

As soon as the hydroxamate is in excess of Fe_T, however, it completely dissolves the iron, and the high affinity of the ligand for copper becomes important for copper speciation. Consider, for example, $Y_T = 10^{-5.8}\,M$. In addition to FeY^+, the major species at pH = 8.1 are clearly H_2Y and H_3Y^+:

$$TOTY = [H_2Y] + [H_3Y^+] + [FeY^+] = Y_T = 10^{-5.8} \tag{56}$$

At this point a reasonable assumption to be verified subsequently is that all the iron is bound to the organic ligand:

$$[FeY^+] = Fe_T = 10^{-6} \tag{57}$$

therefore

$$[H_2Y] + [H_3Y^+] = Y_T - Fe_T = 10^{-6.23} \tag{58}$$

and

$$\begin{aligned} [Y^{2-}](10^{19.4}[H^+]^2 + 10^{27.8}[H^+]^3) &= 10^{-6.23} \\ [Y^{2-}](10^{3.2} + 10^{3.5}) &= 10^{-6.23} \\ [Y^{2-}] &= 10^{-9.9} \end{aligned} \tag{59}$$

We can verify that the iron is indeed dissolved:

$$[FeY^+] = 10^{31.9}[Y^{2-}][Fe^{3+}] = Fe_T = 10^{-6} \tag{60}$$

therefore

$$[Fe^{3+}] = 10^{-28.0} < 10^{-21.1}$$

The mole balance for copper is now written:

$$TOTCu = [Cu'] + [CuY] + [CuHY^+] = Cu_T = 10^{-7} \tag{61}$$

$$TOTCu = [Cu^{2+}][10^{1.5} + 10^{15.0}[Y^{2-}] + 10^{24.1}[H^+][Y^{2-}]] = 10^{-7}$$

$$TOTCu = [CuHY^+] = 10^{6.1}[Cu^{2+}] = 10^{-7} \tag{62}$$

therefore

$$[Cu^{2+}] = 10^{-13.1}$$

The copper becomes immediately complexed by the hydroxamate, and its free concentration is lowered by a factor of approximately one million. Thus, siderophores can alleviate copper toxicity to algae. Note, however, that this is possible only if the organic ligand is in excess of the iron, a situation that may not be commonly encountered in natural waters. In seawater, as illustrated in Example 5, the major cations would affect (slightly) the complexing ability of the organic ligand toward copper since MgY is one of the major ligand species in seawater (once the iron is entirely complexed). In the most probable situation where iron siderophores are present at very low concentrations, lower than that of trace metals, their expected effect on metal speciation is a simple stoichiometric binding of Fe(III).

* * *

Detoxifying Ligands. The other major family of strong biogenic chelating agents, the metal detoxifying molecules, are synthesized by bacteria, plants, and animals in response to metal toxicity. They consist of cysteine-rich polypeptides and include two major types, the phytochelatins of plants and the metallothioneins of animals. Phytochelatins are small polypeptides (Figure 6.11) produced enzymatically by all plants.[69] In microscopic algae they seem to play a metal buffering role even when the algae are not under metal stress.[70] Metallothioneins are small proteins (mw $\simeq$ 6000–7000) with high cysteine content and no aromatic amino acids.[71] They bind several metal ions per molecule and are ubiquitous throughout the animal kingdom. Both phytochelatins and metallothioneins are highly soluble and may thus represent a sizeable source of

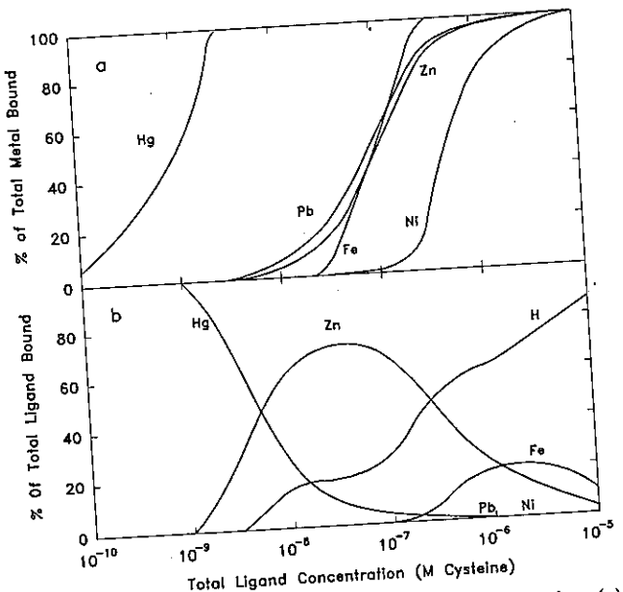

Figure 6.12 Calculated titration of a model freshwater with cysteine. (*a*) Speciation of the metals. (*b*) Cysteine speciation. Same conditions as Figure 6.10 except that Cu(II), which is reduced by cysteine, has been omitted.

strong, unspecific metal complexing agents in water upon cell lysis. Cysteine is included in Table 6.3 to exemplify lower limits on the binding strength of these compounds.

Because detoxifying ligands, like EDTA, are strong unspecific chelators, their effect on metal speciation is very similar to that discussed in Section 4.1. The major difference stems from the different relative metal affinities of the "softer" S in the thiols of the phytochelatins and metallothioneins compared to the "harder" O in the carboxylate of EDTA. For example, Figure 6.12 is the result of complexation calculations identical to those of Figure 6.10, in which EDTA has been replaced by cysteine as a model thiol chelator. Owing to its very high affinity for the thiol group, Hg^{2+} is readily titrated by cysteine. However, because (in this example!) the more abundant zinc controls the cysteine speciation at low ligand concentrations (compared to the less abundant nickel in the case of EDTA), the other trace metals never influence the ligand speciation. Nickel, whose affinity for thiols is relatively poor, is the last metal titrated. [Note that Cu(II) which is reduced to Cu(I) in the presence of cysteine is not included in the calculations.]

* * *

In the preceding discussion, the problem of trace metal complexation has been kept simple by considering only one organic ligand at a time. The problem appears much more complicated when one has to consider several metals and several ligands together. Determining the extent of competition among metals for the same ligand and among ligands for the same metal in a complex mixture seems formidable, and computer programs have been used extensively for this purpose.

In fact, examination of the results of such computer calculations shows that the problems are often not as difficult as they may appear at first and that competition among metals for the same ligand seldom occurs. A few rules of thumb can be given:

1. Like the hydrogen ion (H^+), major cations (Ca^{2+}, Mg^{2+}) do not really "compete" with trace metals for strong ligands, they merely decrease the ligand's apparent affinities for the metals (recall the $K_{Cu}/K_{Ca}[Ca^{2+}]$ factor in Example 5).
2. Trace metals do not compete with each other for the same ligand as long as the ligand is in large excess of the metals ($L_T > M_T$'s). This is the situation most often considered.

Table 6.11 presents the results of a computer calculation for a model freshwater system containing citrate, glycine, cysteine, and NTA, all in excess of all the trace metals but iron. Except for mercury, which has a very high affinity for cysteine, and iron, which is partly present as the hydroxide solid, the reactive trace metals are found chiefly as NTA complexes. Most of the NTA itself is present as the calcium complex. A series of hand calculations such as those presented in Examples 5 and 6 would have yielded the same result ponderously but easily.

4.3 Complexation by Humic Compounds

As mentioned previously, a major fraction of the dissolved organic matter in natural waters is composed of refractory humic compounds, polymers of variable composition. Although their overall structure, particularly their three-dimensional conformation, may be complicated and ill-defined, humic compounds appear to contain reasonably simple and consistent functional groups for coordination: carboxyl, alcohol, and phenol.[72,73] Humic substances have substantially different chemistry in the open ocean and in fresh or coastal waters. In the open ocean where organic matter is almost entirely autochthonous (formed in situ), humic compounds are formed by condensation, polymerization, and partial oxidation of smaller molecules such as triglycerides, sugars, or amino acids, and they exhibit little aromatic character.[74] This is illustrated in Figure 6.13, which shows a hypothetical pathway of formation of marine humates from polyunsaturated triglycerides, leading to crosslinked aliphatic acids.[75] Near land, by contrast, the DOC is largely allochthonous (imported from foreign sources) and derived from the decaying material of higher plants, particularly

TABLE 6.11 Results of an Equilibrium Computation for a Freshwater System Containing Four Organic Ligands[a]

	Total Conc	Free Conc	CO_3	SO_4	Cl	F	NH_3	PO_4	SiO_2	CIT	GLY	NTA	CYST	OH
		→	3.00	4.50	3.50	5.50	5.50	5.00	4.00	5.00	5.00	5.00	5.00	—
		→	6.15	4.56	3.50	5.51	7.50	11.84	12.51	17.00	7.84	9.97	10.51	7.00
	↓	↓				7.56	10.62	5.51s	—	5.88	9.19	5.18	—	8.28
Ca	3.00	**3.02**	4.82	5.54	—	7.35	10.91	7.70	—	7.17	7.58	6.67	10.08	7.77
Mg	3.50	**3.51**	5.30	5.93	—	—	—	—	—	—	—	11.26	—	—
Na	3.50	**3.50**	8.58	7.49	—	—	—	—	—	7.59	14.94	6.66	5.75	8.70
Fe(III)	5.00	17.80	—	18.56	20.10	17.47	—	16.53	14.14					**5.10s**
							13.36	9.64	—	9.61	10.82	7.71	12.62	9.72
Mn(II)	6.50	**6.55**	7.86	9.07	9.08	—	11.86	12.85	—	7.65	9.32	**6.01**	—	11.12
Cu(II)	6.00	10.15	9.86	12.68	13.18	14.49	—	—	—	27.06	13.67	10.86	—	12.87
Ba	7.00	**7.00**	—	—	—	—	12.56	15.88	—	9.41	11.12	**6.01**	—	9.62
Cd	6.00	7.56	10.76	10.08	9.19	12.10	14.36	12.65	—	13.25	11.72	**7.01**	8.82	11.62
Zn	7.00	9.05	—	11.57	13.18	13.39	14.05	—	—	10.38	10.91	**6.50**	10.63	11.01
Ni	6.50	9.24	—	11.76	12.37	13.78	30.40	—	—	—	28.76	27.33	**9.00**	24.18
Hg	9.00	32.91	—	35.34	26.10	36.95	—	—	—	11.56	12.21	**7.10**	7.70	10.50
Pb	7.00	10.34	9.35	12.46	12.27	—	15.05	—	—	27.20	12.41	**7.51**	10.12	11.81
Co(II)	7.50	9.55	—	11.87	12.68	—	13.43	—	—	17.85	13.13	—	—	13.83
Ag	9.00	**9.13**	—	12.72	9.59	—	—	5.48	6.03s	**5.07**		8.03		9.18
Al	5.00	13.95	—	15.70	—	12.16	—	6.07	4.01	7.32	5.00	6.66	5.19	—
H	—	7.00	3.01	9.49	—	9.58	5.50							

Source: Morel et al. (1973).[33]

[a]*Note*: CIT = citrate, GLY = Glycine, NTA = nitrilotriacetate, CYST = cysteine. Numbers are negative logarithms of molar concentrations in solution. The presence of a solid is indicated by s. A dash signifies the absence of a computable species. Bold-face numbers indicate the major species or solid for each metal.

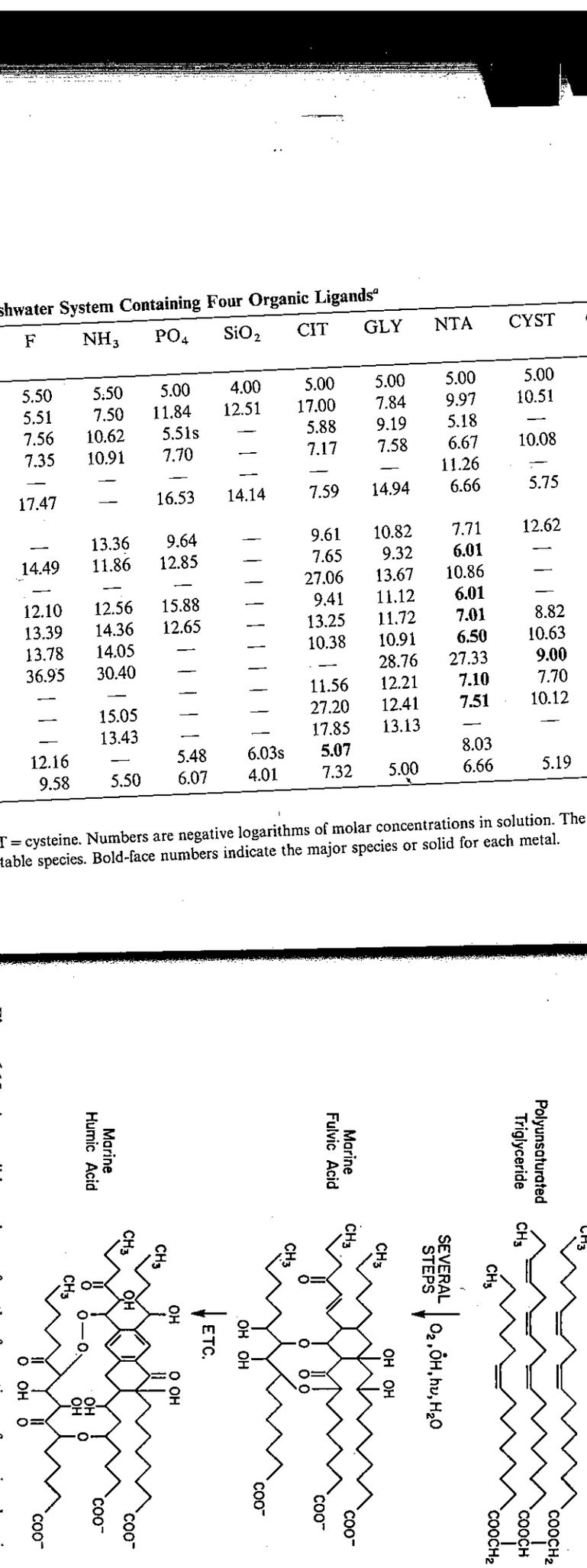

Figure 6.13 A possible pathway for the formation of marine humic acids from a triglyceride. From Harvey et al., 1983.[75]

lignins[73,76] (Figure 6.14). The resulting terrigenous humic compounds retain a relatively high degree of aromaticity from their precursors[77] (Figure 6.15). Thus carboxylic and alcoholic functional groups are characteristic of all humates but phenolic groups are found predominantly in the humic compounds near land.

The total number of titratable acid groups in humic substances is typically in the range of 10 to 20 meq $(gC)^{-1}$. Terrigenous humic compounds are usually close to 50% carbon by weight. Using calorimetric techniques it has been estimated that 60–90% of these acid groups are carboxyl groups and the rest phenolic groups.[78] Chelation of carboxyl and phenolic groups in close proximity to each other is generally considered to be the major mode of metal complexation by such humates. Thus, compounds such as malonate, phthalate, salicylate, or catechol serve as convenient model compounds for the coordinative properties of humic acids (Figure 6.16).

Convenient though they may be for didactic or illustrative purposes, model compounds do not provide an accurate image of the complications involved in

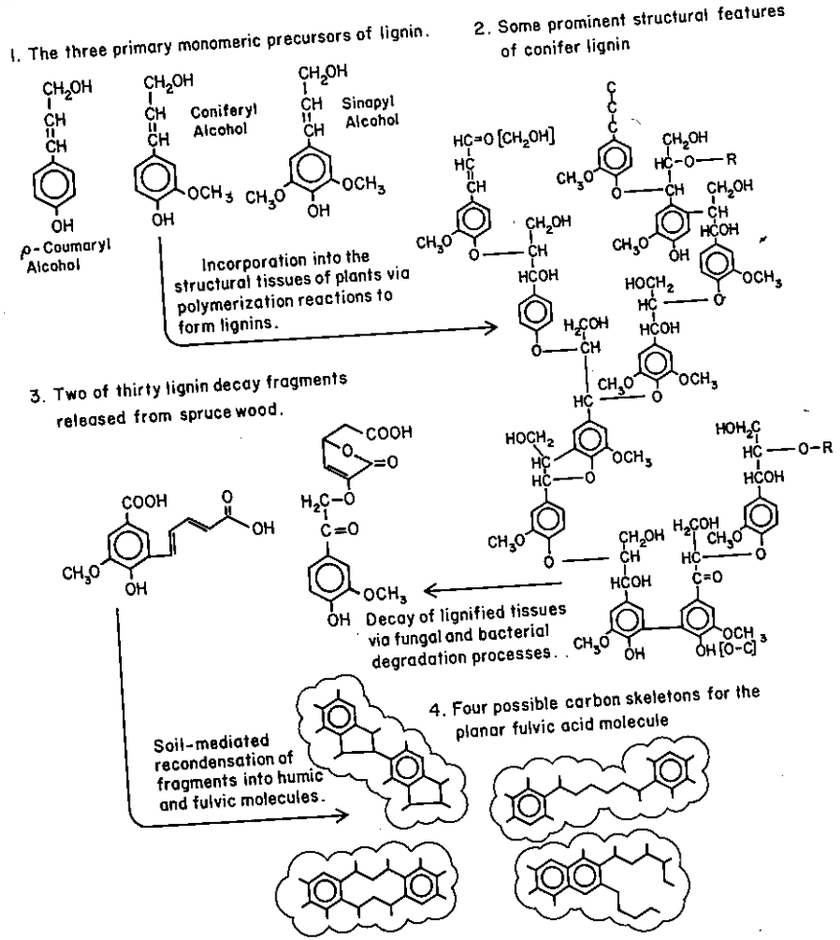

Figure 6.14 A possible schematic pathway for the formation of terrigenous humic acids from lignins. Based on Aiken et al. (1985)[73] and Crawford (1981).[76]

studying the coordinative properties of humic substances. Reduction of data from typical acid–base titrations or metal-coordination experiments with humates usually do not yield a simple set of discrete constants; the titration curves are "smeared" and the resulting constants vary continuously with the experimental conditions. There are three principal causes for this confusing state of affairs:

1. As a result of chemical and steric differences in their neighboring groups, coordination sites on humates may well have a continuous range of affinities for metals including H^+.

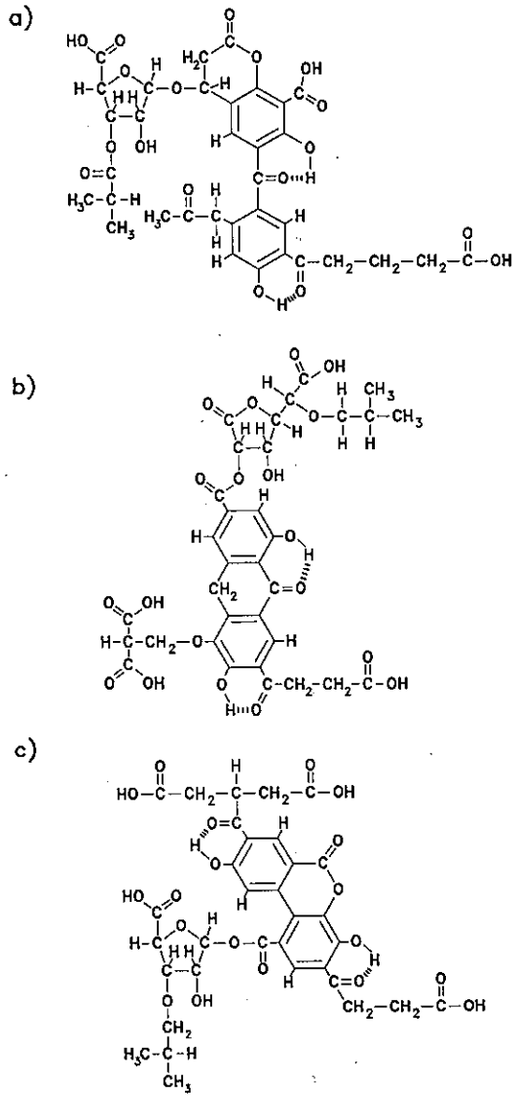

Figure 6.15 Three proposed structures for terrigenous humic acids. After Leenheer in reference 72.

2. Conformational changes resulting from electrostatic interactions among the various functional groups on a single molecule may make the coordination properties of the molecule highly dependent on the extent of cation binding and on the ionic strength of the solution.

3. Electrostatic attraction and repulsion from neighboring ionized groups

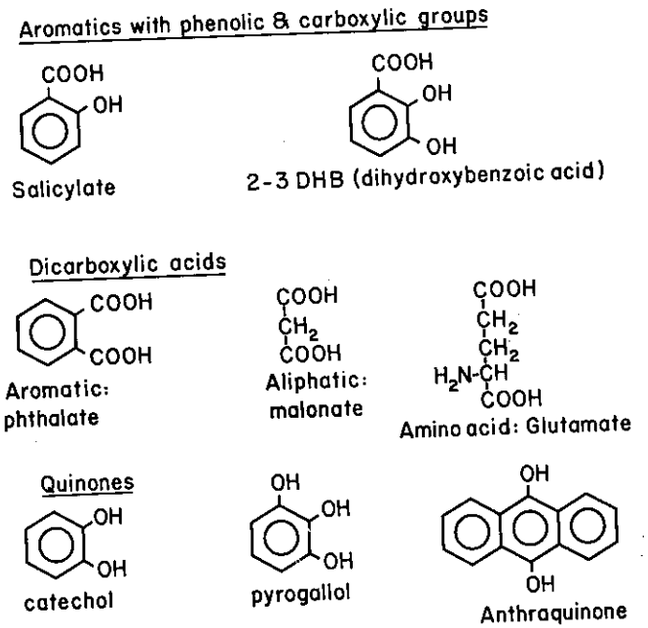

Figure 6.16 Model compounds with appropriate functionalities for humic acids.

may affect markedly the metal affinity of a given group, thus making the free energy of complexation, and hence the complexation constant, dependent on the extent of cation complexation of the ligand, particularly its protonation (and on ionic strength).

Three different approaches have been taken to model the complicated coordination chemistry of such complex mixtures of complex molecules. The easiest and most common is to fit titrimetric data with an ad hoc set of well-defined discrete ligands. Though simple, this approach has the fundamental weakness of being strictly an empirical data fitting procedure without power of prediction or extrapolation. This weakness is not ameliorated by the second approach in which humates are modeled as a mixture of ligands with a continuous (Gaussian) distribution of acidity or metal binding constants. Here we take a third approach and assume that the coordination properties of humates can be described by a superposition of the individual affinities of a few well-defined ligands and the coulombic attraction of neighboring groups. The idea is to capture in such a model enough of the fundamental physical–chemical processes controlling humate chemistry to obtain true predictive capability.

Polyelectrolyte effects. As noted in Chapter 2, coulombic forces are effective over relatively large distances and affect the free energies of ions even in dilute

solutions. When a cation reacts with an acidic functional group of a molecule with multiple functional groups (a "polyanion" such as a humic acid or a protein), the chemical free energy of interaction is augmented by the long-range coulombic attraction emanating from all the neighboring, nonreacting, negative sites. This so-called polyelectrolyte effect which can strengthen greatly the binding of metal ions by polyanions has been well studied in physical-biochemistry. Its role in the chemistry of humic compounds is beginning to be understood. A simple quantitative treatment of coulombic effects in polyion binding is obtained by the same blending of thermodynamics and electrostatics and the very same starting equation involved in the Debye–Hückel theory.[79]

The free energy of reaction between a metal M^{n+} and the functional group L^{m-}

$$M^{n+} + L^{m-} \rightleftharpoons LM^{(n-m)+}$$

is the sum of the *chemical free energy* due to the reaction with the functional group itself and the *coulombic free energy* due to electrostatic interactions between M^{n+} and all the charges on the polyanion.

$$\Delta G^{\circ} = \Delta G^{\circ}_{\text{chem}} + \Delta G^{\circ}_{\text{coul}} \tag{63}$$

In the Debye–Hückel theory, the coulombic term was calculated as the work necessary to charge the molecule from zero to $-Ze$ ($=ZF$ per mole) in an ionic atmosphere. In the case of a polyelectrolyte, the coulombic work involved in reacting with M^{n+} can be taken as the product of the charge increase because of the reaction ($=nF$) and an average potential (Ψ_0) at the surface of the polyelectrolyte.

$$\Delta G^{\circ}_{\text{coul}} = nF\Psi_0 \tag{64}$$

(Recall that F is the Faraday constant, 96,500 C).

In terms of equilibrium constants,

$$K = e^{-\Delta G^{\circ}/RT} = K_{\text{chem}} \cdot K_{\text{coul}} \tag{65}$$

where

$$K_{\text{chem}} = e^{-\Delta G^{\circ}_{\text{chem}}/RT} \tag{66}$$

$$K_{\text{coul}} = e^{-\Delta G^{\circ}_{\text{coul}}/RT} = e^{-nF\Psi_0/RT} = P^n \tag{67}$$

The convenient parameter P is the inverse of the exponential of the nondimensional average surface potential, Ψ_0.

The issue then is to calculate what the average electrical potential, Ψ_0, at the binding site might be. For this purpose, the polyion is represented as an impenetrable sphere of uniform surface charge density. The distribution of

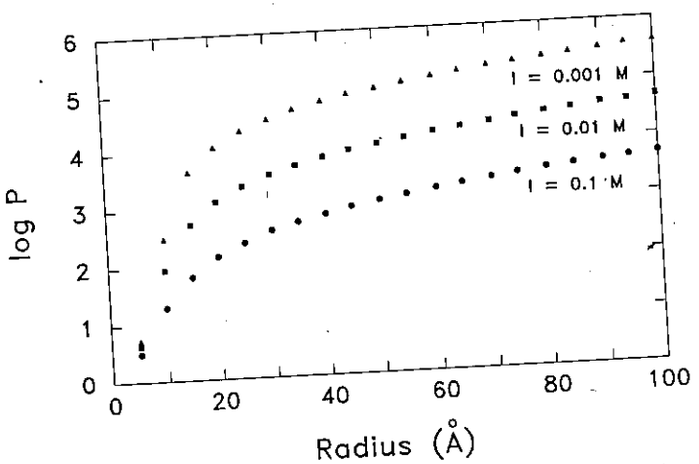

Figure 6.17 Coulombic factor ($\log P = -2.3\,F\Psi_0/RT$) for an impenetrable sphere as a function of its radius and the ionic strength. The total charge is assumed to be proportional to R^3 so that the surface charge density increases proportionally to R. A charge density of 9.2 μC cm^{-2} was chosen for $R = 7.7$ Å. After Bartschat et al., 1992.[79]

co- and counterions from the surrounding electrolyte is represented as a continuously varying charge in a medium of uniform dielectric constant.

As discussed in Chapter 2 for the Debye–Hückel theory, the Poisson–Boltzmann equation then describes the relationship between the variations in potential and the concentration of co- and counterions in the medium. With the appropriate boundary conditions (see Sidebar 6.2), we can solve this equation to obtain the potential Ψ as a function of distance from the spherical polyelectrolyte. More importantly, we also obtain the value of the surface potential Ψ_0 as a function of the surface charge density, the radius (R) of the polyelectrolyte, and the concentration of co- and counterions in solution (Figure 6.17). As may be expected, these surface potentials approach the Debye–Hückel values at small radii and the values for infinite flat plates (see Gouy–Chapman theory in Chapter 8) at large radii.

To calculate the extent of binding of cations by polyanions requires an iterative procedure since the equilibrium constant, $K = K_{chem} \cdot K_{coul}$, depends on the surface charge of the polyanion, which itself depends on the extent of binding of cations, including protons. A general approach to such calculations will be presented in Chapter 8 dealing with binding at the surface of solids. In the following section we describe a simple model of humates, discuss the general features of their acid–base and complexometric titrations (from experimental data and corresponding model calculations), and study how to calculate by hand the extent of metal complexation by humates in the simple and typical case of low metal to ligand ratios.

SIDEBAR 6.2

Solutions to the Poisson–Boltzmann Equation
II. COULOMBIC EFFECTS ON OLIGOELECTROLYTES

Our humic acid model is the same as the Debye–Hückel model for small ions introduced in Chapter 2 and is based on the spherically symmetrical form of the Poisson–Boltzmann equation:

$$\frac{d^2\Psi}{dr^2} + \frac{2}{r}\frac{d\Psi}{dr} = \frac{-1}{\varepsilon\varepsilon_0}\sum Z_i F(S_i)_0 e^{-Z_i F\Psi/RT} \qquad \text{(i)}$$

There are two important differences, however.

First, if the model is to be applicable to oligoelectrolytes (which have a larger charge number and a larger surface charge density than small ions), we cannot assume that the potentials are small enough to justify the linearization step used in the Debye–Hückel theory. We instead have to solve equation (i) numerically. The result is Ψ as a function of r (the distance from the center of the sphere) for a given bulk ionic composition, molecular radius R, and charge on the molecule (Q^-).[79]

Second, we make an approximation which spares us from having to integrate our numerical solution of Ψ over the charge of the molecule as we did in Chapter 1.

Consider a reaction between a polyion of charge Q^- and a small ion of charge Z^+:

$$A^{Q^-} + M^{Z^+} \rightarrow A\text{–}M^{Z-Q}$$

The apparent (conditional) equilibrium constant for this reaction is

$$K_{app} = \frac{[A\text{–}M^{Z-Q}]}{[A^{Q^-}][M^{Z^+}]} = \frac{\{A\text{–}M^{Z-Q}\}}{\{A^{Q^-}\}\{M^{Z^+}\}}\frac{\gamma_Q\gamma_Z}{\gamma_{Z-Q}} = K_{int}\gamma_Z\frac{\gamma_Q}{\gamma_{Z-Q}} \qquad \text{(ii)}$$

Thus, it is the ratio of polyion activity coefficients γ_Q/γ_{Z-Q} and the simple Debye–Hückel activity coefficient for the small ion that will appear as the corrections to K_{int} in the equilibrium expression. One can define this ratio as an effective activity coefficient:

$$\ln\gamma_{eff} = \ln\frac{\gamma_Q}{\gamma_{Z-Q}} = \ln\gamma_Q - \ln\gamma_{Z-Q}$$

(*continued*)

$$= \frac{-1}{kT} \int_{-Qe}^{(Z-Q)e} \Psi_0(q)\,dq \qquad \text{(iii)}$$

If Q is much larger than Z, $\Psi_0(q)$ remains approximately constant over the range of the integral, so that

$$\ln \gamma_{\text{eff}} = \frac{-Ze}{kT} \Psi_0(Q) \qquad \text{(iv)}$$

The "local" activity of a small ion at the surface of the oligoelectrolyte is then given by the "bulk" activity multiplied by a Boltzmann factor,

$$P = \exp\left(-\frac{Ze}{kT}\Psi_0\right)$$

given in Figure 6.17. A physical interpretation of the Boltzmann factor is that it represents the work required to bring the small ion from an infinite distance to the surface of the oligoelectrolyte. This interpretation is often used to derive the expression for γ_Z, but it is only strictly correct when the oligoelectrolyte does not come close to being neutralized by the reaction with the small ion. In reality, it is not a "local" activity coefficient which we use to correct the equilibrium constants, but a ΔG_{coul}, and if the charge on the oligoelectrolyte changes enough so that the ionic atmosphere also rearranges itself significantly, the former is not a good approximation of the latter.

A Simple Model Humate. A simple model of a humic acid is presented in Table 6.12. It consists of a mixture of three ligands, acetate, malonate, and catechol, distributed among two size groups, 75% in molecules of molecular weight 700 daltons ($R = 7.7$ Å) and 25% in molecules of molecular weight 5000 daltons ($R = 15$ Å). Such relatively low molecular weight compounds may be termed "oligoelectrolytes" to distinguish them from true polyelectrolytes such as proteins. The types and concentrations of the ligands have been chosen to be consistent with available structural data and to approximate titrimetric data with H^+ and Cu^{2+}. The total concentration of carboxylic acid groups [$6\,\text{meq}\,g^{-1} \simeq 12\,\text{meq}\,(\text{gC})^{-1}$] is in the middle range of reported values. As discussed above, the molecules are considered as impenetrable spheres with their ionizable functional groups producing a uniform charge distribution on the surface—the maximum charge is $4.3\,\text{eq}\,\text{mol}^{-1}$ for the small size range and $32\,\text{eq}\,\text{mol}^{-1}$ for the large size range.[79]

Acid–Base Properties of Humates. In Chapter 4 we showed a typical acid-base

TABLE 6.12 A Model Humate

Two size groups

$R = 7.7$ Å ($Z = 4.3\,\text{eq}\,\text{mol}^{-1}$; mw $\simeq 700$)
75% of all functional groups

$R = 15$ Å ($Z = 32\,\text{eq}\,\text{mol}^{-1}$; mw $\simeq 5000$)
25% of all functional groups

Three ligands

"Acetate"	$4 \times 10^{-3}\,\text{mol}\,g^{-1}$	HL_0	$pK_a = 3.8$
"Malonate"	$10^{-3}\,\text{mol}\,g^{-1}$	H_2L_1	$pK_{a1} = 4.5$
		HL_1^-	$pK_{a2} = 4.5$
		CuL_1	$pK_{Cu} = 5.1$
"Catechol"	$5 \times 10^{-4}\,\text{mol}\,g^{-1}$	H_2L_2	$pK_{a1} = 9.4$
		HL_2^-	$pK_{a2} = 12.6$
		CuL_2	$pK_{Cu} = 14.7$

titration of a humic acid sample (Figure 4.13) and the influence of ionic strength. The oligoelectrolyte model described above accounts for the observed ionic strength effects (though it has not been designed to fit the data of Chapter 4 and may, in particular, lack sufficiently strong acid groups). Both the distribution of the pK_a's and the coulombic polyelectrolyte effect contribute to the smeared aspect of the titration curve in which no clear inflection point can be distinguished. The importance of the polyelectrolyte effect which is due to a gradual decrease in the coulombic attraction of protons can be quantified by expressing the mass law for the deprotonation of an acid site.

$$HL = H^+ + L^-$$

$$\frac{[H^+][L^-]}{[HL]} = K_a \cdot P^{-1} \qquad (68)$$

where K_a is the intrinsic (chemical) acidity constant of the site and P^{-1} ($= e^{F\Psi_0/RT}$) is the coulombic term. The increase in the value of P with increasing pH—hence the increase in the apparent pK of the acid site: $pK_a^{\text{app}} = pK_a + \log P$—is given in Table 6.13 for each of the two sizes of the model humate molecules. Because the smaller humates account for 75% of the acid groups, they dominate the acid–base titrations. The magnitude of the ionic strength effects is thus chiefly a reflection of the dependence of P on I as given in Table 6.13.

Metal Binding by Humates. Much of the experimental data on metal binding by humates concerns copper. The effects of pH and ionic strength on copper

TABLE 6.13 Calculated Values of the Electrostatic Factor P as a Function of pH and Ionic Strength[a]

	$I = 0.01\ M$		$I = 0.1\ M$	
pH	$\log P_S$	$\log P_L$	$\log P_S$	$\log P_L$
2.7	0.061	0.158	0.045	0.105
2.8	0.074	0.185	0.054	0.124
2.9	0.089	0.215	0.065	0.147
3.0	0.105	0.248	0.078	0.172
3.1	0.124	0.284	0.093	0.199
3.2	0.146	0.323	0.110	0.230
3.3	0.169	0.364	0.128	0.262
3.4	0.195	0.408	0.149	0.297
3.5	0.223	0.454	0.171	0.335
3.6	0.252	0.502	0.195	0.374
3.7	0.284	0.551	0.221	0.415
3.8	0.317	0.603	0.248	0.458
3.9	0.352	0.656	0.276	0.502
4.0	0.387	0.710	0.305	0.547
4.1	0.424	0.766	0.335	0.594
4.2	0.462	0.823	0.365	0.641
4.3	0.501	0.880	0.397	0.689
4.4	0.540	0.939	0.428	0.737
4.5	0.580	0.998	0.460	0.785
4.6	0.620	1.057	0.492	0.834
4.7	0.661	1.117	0.523	0.883
4.8	0.701	1.178	0.555	0.931
4.9	0.742	1.238	0.587	0.980
5.0	0.782	1.298	0.617	1.028
5.1	0.823	1.359	0.648	1.075
5.2	0.863	1.419	0.677	1.122
5.3	0.902	1.479	0.705	1.168
5.4	0.941	1.539	0.731	1.214
5.5	0.979	1.598	0.755	1.259
5.6	1.016	1.656	0.778	1.302
5.7	1.051	1.714	0.798	1.345
5.8	1.084	1.772	0.815	1.386
5.9	1.115	1.828	0.831	1.425
6.0	1.144	1.884	0.844	1.463
6.1	1.171	1.939	0.854	1.499
6.2	1.194	1.993	0.863	1.533
6.3	1.215	2.045	0.871	1.564
6.4	1.233	2.097	0.877	1.593
6.5	1.248	2.147	0.881	1.618
6.6	1.261	2.196	0.885	1.641
6.7	1.271	2.243	0.888	1.661
6.8	1.280	2.288	0.891	1.678

(continued)

TABLE 6.13 *(Continued)*

	$I = 0.01\ M$		$I = 0.1\ M$	
pH	$\log P_S$	$\log P_L$	$\log P_S$	$\log P_L$
6.9	1.287	2.331	0.893	1.692
7.0	1.293	2.372	0.894	1.704
7.2	1.302	2.446	0.897	1.722
7.4	1.307	2.508	0.898	1.734
7.6	1.311	2.557	0.899	1.741
7.8	1.313	2.593	0.900	1.746
8.0	1.314	2.619	0.900	1.749
8.2	1.315	2.637	0.901	1.751
8.4	1.316	2.648	0.901	1.752
8.6	1.317	2.655	0.902	1.753
8.8	1.317	2.660	0.903	1.754
9.0	1.318	2.663	0.904	1.754

[a]The fulvic acid parameter of Bartschat et al. (1992)[79] were used to obtain values of P for the small (P_S) and large (P_L) size classes.

titration of humic acids are shown in Figure 6.18. The oligoelectrolyte model described in Table 6.12 accounts reasonably well for these effects, particularly at low total copper concentrations, in the range of Cu_T/L_T representative of some natural waters. As one expects, pH has a dramatic effect on the extent of binding as is the case for any weak acid ligand whose apparent affinity for a

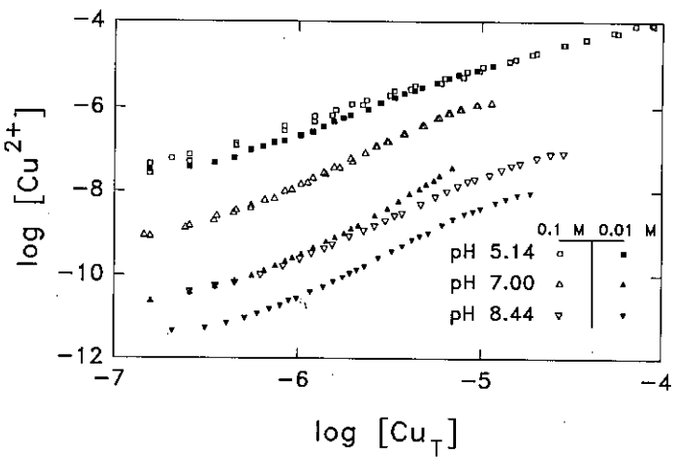

Figure 6.18 Copper-sensitive electrode titrations of humic acids at various pH's and ionic strengths. Note the characteristic shapes of such potentiometric titration curves (contrast these log–log graphs to those in Figure 6.9). Data from Cabaniss as reported in Bartschat et al., 1992.[79]

metal increases with pH. This effect is exacerbated by the increase in coulombic attraction of the metal ion to the binding sites as the humates become deprotonated as can be seen by writing the mass law equation for copper binding:

$$Cu^{2+} + L^{2-} = CuL$$

$$\frac{[CuL]}{[Cu^{2+}][L^{2-}]} = K_{Cu} \cdot P^2 \tag{69}$$

where K_{Cu} is the intrinsic (chemical) copper-binding constant of the site. As pH increases, the coulombic term P increases and so does the apparent binding constant.

Both the high apparent affinity of the humates for copper and its large (and pH-dependent) sensitivity to ionic strength are due to polyelectrolyte effects. At low Cu_T/L_T ratios, the larger humates, whose copper affinities are most enhanced by coulombic attraction, account for the bulk of copper binding. Because the coulombic term P for these molecules (at high pH) is inversely proportional to I (see Figure 6.17), the effective affinity for copper binding increases dramatically at low ionic strength. The actual dependency of the free cupric ion concentration, $[Cu^{2+}]$, on I (at a given pH, L_T, and Cu_T) depends on the stoichiometry of H^+ exchange at a specific binding site. If $H_\alpha L^{n-}$ is the dominant protonated form of the site, the reaction with copper is written:

$$Cu^{2+} + H_\alpha L^{n-} \rightleftharpoons CuL^{(n+\alpha-2)-} + \alpha H^+$$

$$K_{coul} = P^{2-\alpha} \propto I^{2-\alpha} \tag{70}$$

Thus the effect of I on K_{coul} may lead to a dependency of the apparent copper affinity on I that is anywhere between null ($\alpha = 2$) or up to a square function ($\alpha = 0$). Though it is complicated by the multiplicity of binding sites, Figure 6.18 illustrates that the maximum ionic effect ($\alpha = 0$) is observed at pH = 7.

Example 7. Cu Complexation by Humates in Freshwater To get a better quantitative understanding of these questions, let us reconsider the issue of copper speciation in a freshwater at pH = 8.1 that we now assume to contain $10\,mg\,L^{-1}$ of humic acids. We have already calculated the ratio of free to inorganic copper in Example 3 and found $[Cu^{2+}]/[Cu'] = 10^{-1.5}$. Following the usual methodology, we can write the mole balance for copper as

$$TOTCu = [Cu'] + [CuL_{0S}] + [CuL_{0L}] + [CuL_{1S}] + [CuL_{1L}] + [CuL_{2S}] + [CuL_{2L}] = Cu_T \tag{71}$$

In our model humic acid, the acetate-type ligand (L_0) is much weaker than the other two, and despite its somewhat higher concentration it can have no sizable effect on copper speciation at the low metal to ligand ratio of this example. We thus neglect the species CuL_{0S} and CuL_{0L} and limit our calculation to the other two ligands, malonate (L_1) and catechol (L_2). As in all the previous examples, we first need to calculate the speciation of these ligands. Ignoring the possible complexation by Ca^{2+} and Mg^{2+} we can write the mole balance for the malonate-type ligands in the small humates, L_{1S}, as

$$TOTL_{1S} = [L_{1S}^{2-}] + [HL_{1S}^{-}] + [H_2L_{1S}] + [CuL_{1S}] = [L_{1S}]_T = 0.75 \times 10^{-3}\,mol\,g^{-1} \times 10^{-2}\,g\,L^{-1} = 10^{-5.12}\,M \tag{72}$$

Because copper is assumed to be in trace quantities, it has a negligible effect on the ligands. We can thus ignore $[CuL_{1S}]$ in the mole balance. We can also calculate the coulombic factor P a priori for a given pH and ionic strength. According to Table 6.13, at a pH = 8.1 and $I = 0.01\,M$ the relevant value of P for small humates is

$$\log P_S = 1.32$$

The mass laws for the acid–base reactions of the malonate-type ligands in the small humates can then be written

$$\frac{[L_{1S}^{2-}]}{[HL_{1S}^{-}]} = \frac{K_{a2}}{[H^+] \cdot P} = \frac{10^{-4.5}}{10^{-8.1} \cdot 10^{+1.3}} \gg 1$$

$$\frac{[HL_{1S}^{-}]}{[H_2L_{1S}]} = \frac{K_{a1}}{[H^+] \cdot P} = \frac{10^{-4.5}}{10^{-8.1} \cdot 10^{+1.3}} \gg 1$$

Thus, the completely deprotonated ligand is the dominant species:

$$TOTL_{1S} \simeq [L_{1S}^{2-}] = [L_{1S}]_T = 10^{-5.12} \tag{73}$$

Similar calculations show that L_{1L}^{2-} is also the dominant species for malonate-type ligands in the larger humates [despite the larger shift in apparent pK_a ($= pK_a + \log P = pK_a + 2.63$) due to coulombic effects] and that H_2L_{2S} and H_2L_{2L} are the dominant species for the catechol-type ligands, in both size classes:

$$[L_{1L}^{2-}] = [L_{1L}]_T = 0.25 \times 10^{-5.0} = 10^{-5.60} \tag{74}$$

$$[H_2L_{2S}] = [H_2L_{2S}]_T = 0.75 \times 10^{-5.3} = 10^{-5.42} \tag{75}$$

$$[H_2L_{2L}] = [H_2L_{2L}]_T = 0.25 \times 10^{-5.3} = 10^{-5.90} \tag{76}$$

The mole balance equation for copper can then be written:

$$TOTCu = Cu_T = [Cu^{2+}]\Big[10^{1.5} + 10^{5.1} \times P_S^2 \times 10^{-5.12} + 10^{5.1} \times P_L^2 \times 10^{-5.60} + 10^{14.7} P_S^2 \times \frac{10^{-9.4}}{P_S[H^+]} \times \frac{10^{-12.6}}{P_S[H^+]} \times 10^{-5.42} + 10^{14.7} \times P_L^2 \times \frac{10^{-9.4}}{P_L[H^+]} \times \frac{10^{-12.6}}{P_L[H^+]} \times 10^{-5.90}\Big] \quad (77)$$

Introducing $P_S = 10^{1.32}$, $P_L = 10^{2.63}$ (Table 6.13), and $[H^+] = 10^{-8.1}$:

$$TOTCu = [Cu^{2+}][10^{1.5} + 10^{2.62} + 10^{4.76} + 10^{3.48} + 10^{3.00}] \quad (78)$$

Thus the copper is 99.9% bound to humates, the free cupric ion is decreased more than three orders of magnitude compared to the purely inorganic case

$$\frac{[Cu^{2+}]}{Cu_T} = 10^{-4.79}$$

and the malonate-type ligand in the large humic compounds, L_{1L}, accounts for 93% of the copper in solution.

* * *

Example 7 provides an extreme case of metal complexation by humates since the humic acid content of the system is relatively large, the ionic strength is low, and the pH is high. The apparent complexation constants would decrease by more than one order of magnitude per pH unit at this ionic strength (see Figure 6.18). Nonetheless, it is clear that humic compounds may control the speciation of some trace metals in waters of high humic content. According to Example 7, some four orders of magnitude decrease in the product $K_{Cu}L_{1L}$ is necessary for the metal–humate complex to be unimportant. If the model ligands malonate and catechol are truly representative of the relative metal affinities of all complexing sites on humates, metals such as Cd^{2+}, Ni^{2+}, or Zn^{2+} should have humate affinities roughly 10 times less than that of copper. Depending on the pH and the humic content of the water, the complexation of such metals by humic material may thus vary from 0% (pH < 7, DOC < 1 mg L^{-1}) to 100% in situations such as that of Example 7.

An important difference between the oligoelectrolyte theory and the Debye–Hückel theory is the role that divalent background electrolyte ions play in determining the charge-potential relationship. In the linear approximation of the Debye–Hückel theory, the effects of all the ions in the background electrolyte are accounted for by one parameter, the ionic strength of the solution.

In the oligoelectrolyte theory, the nonlinearity of the equations results in a proportionally much greater effect of di- and trivalent ions on the surface potential. The relative role of each counterion in neutralizing the surface potential can be calculated by comparing the relative *surface concentrations* of metal ions of charge number z^+:

$$[M^{z+}]_{surface} = P^z \cdot [M^{z+}]_{bulk} \quad (79)$$

For example, in a medium of 0.1 M ionic strength, a concentration of 1 mM Ca^{2+} will dominate the coulombic interactions of moderate size polyacids.[79] Thus, the divalent cations Ca^{2+} and Mg^{2+}, which are abundant in natural waters, can diminish the tendency of humates to complex trace metals both by competing for specific functional groups and by decreasing (shielding) the coulombic attraction of neighboring ionized groups (the oligoelectrolyte effect).

4.4 Conditional Stability Constants

In earlier sections of this chapter, we have introduced various apparent or effective stability constants for complexation reactions. Often researchers who deal with metal complexation in natural waters find it convenient to describe the thermodynamics of the reactions with conditional stability constants that are applied to some analytical fraction of the reactants and products. Thus these constants are only valid under a specified set of conditions. To avoid confusion, let us briefly review the different types of conditional constants and provide a systematic terminology for them.

Consider the complexation reaction

$$M^{2+} + L^- = ML^+$$

The thermodynamic constant for this reaction is written

$$K = \frac{\{ML^+\}}{\{M^{2+}\}\{L^-\}} \quad \text{(thermodynamic constant)} \quad (80)$$

In Chapter 2 we defined the corresponding concentration constant that we are using throughout the text:

$${}^cK = \frac{[ML^+]}{[M^{2+}][L^-]} \quad \text{(concentration constant)} \quad (81)$$

This is a conditional constant valid for a particular ionic strength, and it includes implicitly all unspecific long-range (mostly electrostatic) interactions among ions, namely, activity coefficients.

Going one step further, in Section 2 of this chapter we defined apparent constants for carbonate species in seawater, including in the constants all the specific and unspecific interactions among the major ions:

$$K^{app} = \frac{[\sum ML^+]}{[M^{2+}][\sum L^-]} \qquad \text{(apparent constant)} \tag{82}$$

The symbol $\sum$ indicates that all complexes formed with the major metals, $Na^+, K^+, Ca^{2+}, Mg^{2+}$, are included in the formulation. The domain of validity of such apparent constants is of course restricted to solutions with similar major ion composition. For dilute solutions such as freshwaters, ${}^cK = K^{app}$.

To study organic complexation of metals it is convenient to introduce yet another type of conditional constant, an effective constant that includes the acid–base speciation of the ligand ($[\sum H_xL] = [L] + [HL] + [H_2L] + [H_3L] + \cdots$):

$$K^{eff} = \frac{[ML]}{[M^{2+}][\sum H_xL]} \qquad \text{(effective constant)} \tag{83}$$

Such a constant is of course highly pH dependent and is obtained simply by introducing the ligand ionization fractions in the mass law expression. It can be generalized slightly by considering also all the various acid–base species of the complex (e.g., $[\sum ML] = [ML^+] + [MHL^{2+}] + [MOHL] + \cdots$):

$$K^{eff} = \frac{[\sum ML]}{[M^{2+}][\sum H_xL]} \tag{84}$$

Over a limited pH range the $[H^+]$ dependency of such a constant can often be made explicit:

$$K^{eff} = K_x^{eff}[H^+]^x \tag{85}$$

where K_x^{eff} is constant over some pH range; see Section 4.1. In our study of inorganic speciation, we have used effective constants as the product $\beta\alpha^m$ (see Section 3).

We can combine the notion of apparent constant with that of effective constant to obtain an overall conditional constant that includes the interactions of the ligand with all major cations, H^+, Ca^{2+}, Mg^{2+}:

$$K^{cond} = \frac{[\sum ML]}{[M^{2+}] \times L_T} \tag{86}$$

In cases where the calcium or magnesium complexes of the ligand are dominant, $K^{cond} = K^{app}$; in cases where the acid–base species dominate the ligand speciation, $K^{cond} = K^{eff}$.

In general, the inorganic metal speciation is *not* included in the expressions of conditional constants and the free metal ion concentration $[M^{2+}]$ appears in all the foregoing mass law expressions. In situations where the complex is a sizeable fraction of the ligand, only the unbound ligand should appear in the denominator of the mass law expression:

$$K^{cond} = \frac{[\sum ML]}{[M^{2+}][L_T - \sum ML]} \tag{87}$$

Conditional constants are the most directly attainable quantities in complexation experiments where the measured concentrations are simply the fractions of bound and free metal:

$$K^{cond} = \frac{[M \cdot \text{bound}]}{[M \cdot \text{free}][L_T - M \cdot \text{bound}]} \tag{88}$$

Although such constants may have little thermodynamic meaning and only a limited range of applicability, they are very convenient to use. In addition, for humates whose thermodynamic constants are difficult to define, they provide a direct link between experimental data and calculations, without an intervening and often misunderstood extrapolation procedure. When using conditional constants one should always remember the particular conditions of applicability and be wary that different authors may include implicitly different factors in their constants (e.g., acid–base chemistry or major ion complexation). As noted earlier, internal consistency in thermodynamic data is as important as the absolute values of the individual constants. Often, to increase the range of applicability of conditional constants, particularly for humates, a pH dependency is given explicitly:

$$K^{cond} = K_x^{cond}[H^+]^x = \frac{[H^+]^x \times [\sum ML]}{[M^{2+}][L_T - \sum ML]} \tag{89}$$

In this case, the exponent x reflects not only the acid–base chemistry of the ligand and the complex over a certain pH range, but also the pH dependency of the electrostatic effects on the metal affinity for the ligand; that is, the value of x can be interpreted as the average number of protons released per bound metal ion, or it can be a more generalized fitting parameter.

4.5 Organometallic Compounds

There is one class of coordination compounds that cannot be addressed satisfactorily within the framework of complexation equilibria. These are the

organometallic compounds, in which the ligand bonds to the metal through carbon atoms (excluding the inorganic ligand CN^-). Although organometallic compounds may be formed with almost any metal, only a few metals, notably mercury and tin, form organometallic compounds that are stable in water. The metalloids arsenic and selenium also form compounds that are chemically similar to organometallic compounds and are stable in water. Other organometallic compounds are hydrolyzed by reactions such as

$$RM + H_2O \longrightarrow RH + M^+ + OH^-$$

The "ligand" in an organometallic compound is a carbanion R^-, that is, an organic anion with a carbon atom bearing the negative charge. These species are extremely reactive and organometallic compounds have a strong covalent character. Dissociation of an organometallic compound, as in the complexation equilibrium

$$RM = R^- + M^+$$

would result in immediate reaction of the carbanion with water (or protons).

Concern over environmental contamination by organomercury and organotin compounds arises because of their toxicity and because they tend to become concentrated in the biota. These compounds are directly introduced into the environment through their use as biocides.[80,81] Organometallic species are also produced by enzymatic methylation of cationic metals or by their reaction with biogenic methylating agents, such as methyl iodide.[82,83] Organometallic

TABLE 6.14 Occurrence of Organometallic Compounds in the Environment

Element	Compound	Concentration (M)	Sampling Site	Ref.
Hg	Monomethylmercury	$< 0.5–2.8 \times 10^{-13}$	Equatorial Pacific (subthermocline)	84
		$< 0.02–3.2 \times 10^{-12}$	Freshwaters	85
		8.0×10^{-14}	Coastal seawater	85
	Dimethylmercury	$0.3–6.7 \times 10^{-13}$	Equatorial Pacific	84
Sn	Monobutyltin	up to 1.4×10^{-8}	Freshwaters	86
	Dibutyltin	up to 7.8×10^{-9}		86
	Tributyltin	up to 1.4×10^{-8}		86
	"organotin"[a]	$(2.8–6.7) \times 10^{-10}$	Rivers	87
		$(0.25–4.7) \times 10^{-9}$	Harbors	87
		$(1.3–7.6) \times 10^{-9}$		88
As	Methylarsonate	4×10^{-10}	Baltic Sea	89
		$(< 0.1–8.6) \times 10^{-9}$	Lakes	90
	Dimethylarsenate	$(0.77–6.15) \times 10^{-9}$	Baltic Sea	89
		$(0.4–33) \times 10^{-9}$	Lakes	90

[a]Includes tri- and dibutylated species.

compounds are widely distributed in the aquatic environment, both freshwater and marine (see Table 6.14).

The occurrence and reactions of organometallic compounds can be quite significant in the biogeochemical cycles and mass balances of some metals in natural waters. An important feature of many organometallic compounds in this regard is their volatility. Aquatic systems may be a source of Hg, Sn, As, and Se to the atmosphere through the volatilization of methylated species.[83,91,92] Reactions involving organometallic compounds, however, may be better addressed in the context of reactions of organic rather than inorganic species.[93]

5. COMPLEXATION KINETICS

The preceding discussion of complexation reactions is based on equilibrium arguments. All reactions that are considered to take place in the system are also considered to have reached equilibrium. In many cases, complexation of metals by ligands is indeed rapid relative to other processes of interest, and equilibrium models then provide a good representation of complexation phenomena in natural waters. Here, however, we wish to consider the general question of whether complexation kinetics, that is, the rates of formation or dissociation of metal–organic complexes, may affect the overall rates of biogeochemical processes or the analytical determination of metal speciation in natural waters.[94]

The ambient trace metal speciation in a natural water is, as we have seen, determined by the mixture of metals and complexing agents present and also by the pH, ionic strength, and major ion composition. Changes in one or more of these parameters may result from the physical mixing that occurs at stream confluences, upwelling of deep ocean water, or input of sewage effluents to surface waters. Such changes may also be effected by biogeochemical processes, such as uptake of metals or release of complexing agents by microorganisms, changes in pH of surface waters due to photosynthesis, or photochemical reactions. Clearly one question concerning complexation kinetics is how quickly the metal and ligand species distributions change in response to such perturbations.

This question may be particularly important in analytical determinations of trace metal speciation where the initial composition of the water sample is often significantly perturbed by the additions of either metals or ligands or both (see Table 6.10 for references) and the equilibration time between the perturbation and the analytical measurement tends to be short. In metal titrations, the equilibration time between metal additions and the analytical measurement can affect the measured concentration of inorganic (labile) metal[44,95] (see Figure 6.19). As discussed below, the stronger ligands may, in some cases, react more slowly with added metals than weaker ligands; this effect depends on the initial ligand speciation. When the sample is titrated with a metal, the final

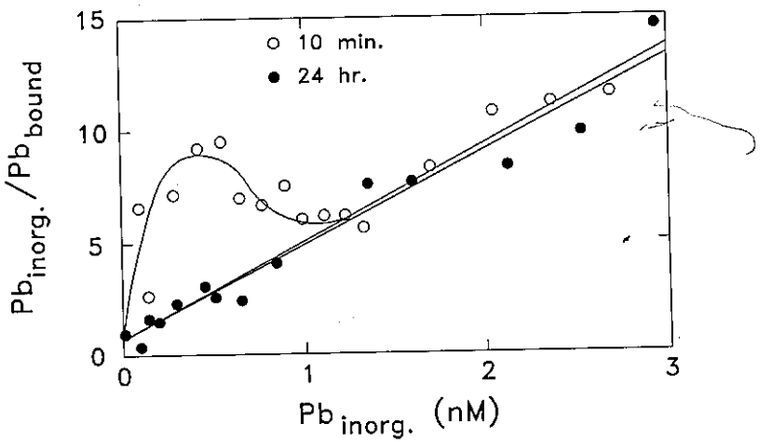

Figure 6.19 Ratios of inorganic-to-bound lead as a function of inorganic lead observed in a titration experiment after 10 min (open circles) or 24 h (closed circles) equilibration time. Because equilibration of added lead is incomplete after 10 min, increasing lead complexation (decreasing ratio of inorganic-to-bound lead) is observed over time. From Capodaglio et al. (1990).[44]

composition of the sample (e.g., the total metal concentration at each step of the titration) uniquely determines the equilibrium metal and ligand speciation but *not* the path to equilibrium. Since the fastest reactions do not necessarily result in formation of the thermodynamically favored complexes, attainment of equilibrium speciation may be slow on an analytical time scale.

When perturbation of metal and ligand speciation occurs as a result of biogeochemical processes, such as biological metal uptake, sorption, or chemical or photochemical transformation, the rates of these processes may be linked to the rates of complexation reactions. For example, as we shall see in the next section, if a metal occurs predominantly as an organic complex and the intact complex is not transported into the cells, then the kinetics of complex dissociation may, under some conditions, limit the rate at which the metal can be accumulated by microorganisms.

To evaluate the importance of complexation kinetics in natural or laboratory systems, it is necessary to consider the pathways both for the complexation reactions and for any co-occurring biogeochemical processes. From the reaction pathways, the intermediate species whose low or transient concentrations determine the rates of reactions may be identified. In the following discussion, we examine the effects of initial speciation and reaction pathways on the kinetics of copper complexation by humic acid and EDTA.

Humic acids exhibit a natural fluorescence which is decreased (quenched) when the humic acid is associated with Cu(II) ions.[96] As shown in Figure 6.20,

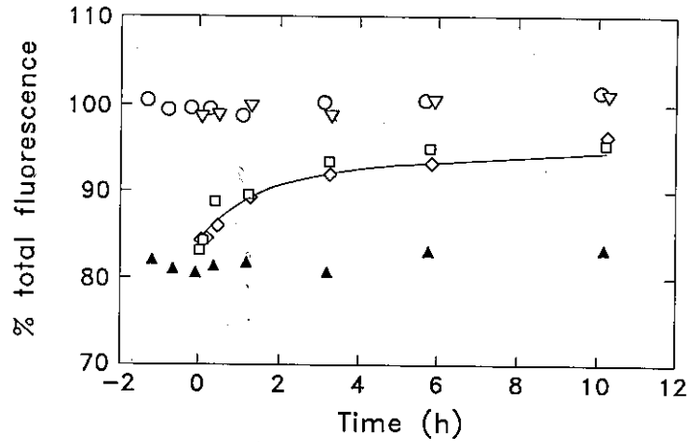

Figure 6.20 Reaction of copper with a mixture of EDTA and humic acid. Percent fluorescence of the humic acid is shown over time after addition of copper at $t = 0$ to the ligand mixture in the absence of calcium (▽) or with 0.01 M calcium (□, ◇). For reference, the percent fluorescence over time of the ligand mixture in the absence of copper (○) and of humic acid and copper in the absence of EDTA (▲) with 0.01 M Ca are shown. (——) calculated values obtained by assuming pseudoequilibrium between inorganic copper and humate binding sites and reaction of inorganic copper with CaEDTA as described in Section 5.3. From Hering and Morel (1989).[97]

the quenching of humate fluorescence (i.e., formation of humate–Cu complexes) when Cu(II) is added to a mixture of humic acid and EDTA is strongly dependent on the calcium concentration.[79] In the absence of calcium, no decrease in fluorescence is observed, indicating rapid formation of the thermodynamically favored CuEDTA species. With 10^{-2} M calcium, however, the initial decrease in fluorescence indicates formation of Cu–humate complexes; the slow recovery of the fluorescence over time corresponds to exchange of copper between the humic acid and EDTA.

We have already seen in Example 5 that calcium can have little effect on the equilibrium copper speciation in these systems. Why then does it have such a dramatic effect on the rate at which the equilibrium speciation is attained?

The presence or absence of calcium determines the initial EDTA speciation. Without calcium, *complex formation* between the protonated EDTA species and the added copper is rapid. At high calcium concentrations, however, reaction of the added copper with the dominant CaEDTA complex involves a slower *metal-exchange* reaction and formation of Cu–humate complexes is kinetically favored. Subsequent reequilibration requires a *double-exchange* reaction, that is, both a *ligand exchange* in which EDTA replaces the humate in the copper complex and a *metal exchange* in which copper replaces calcium in the EDTA complex. Then to understand these experimental observations, we must

understand the mechanisms and rates of the reactions, complex formation and dissociation, as well as metal, ligand, and double exchange.

5.1 Kinetics of Complex Formation and Dissociation

Observed rates of complex formation are generally consistent with a mechanism in which formation of an outer-sphere complex between the metal and ligand, with the stability constant K_{os}, is followed by a rate-limiting loss of water from the inner coordination sphere of the metal, with the water loss rate constant k_{-w}:

$$M(H_2O)_6^{2+} + L^{n-} \overset{K_{os}}{\rightleftharpoons} M(H_2O)_6,L^{(2-n)+}$$

$$M(H_2O)_6,L^{(2-n)+} \xrightarrow{k_{-w}} M(H_2O)_5L^{(2-n)+} + H_2O$$

Then the rate constant for complex formation, k_f, can be written (omitting coordinated waters) as:

$$\frac{d[ML^{(2-n)+}]}{dt} = k_f[M^{2+}][L^{n-}] \tag{90}$$

where

$$k_f = K_{os}k_{-w} \tag{91}$$

The stability constant for the outer-sphere complex, K_{os}, is primarily dependent on the charges of the reacting species and the ionic strength of the medium. This term can be calculated as shown in Sidebar 6.3. Experimentally determined values of K_{os} (which may be obtained for relatively slow-reacting species) are in agreement with calculated values. For 3+ ions, observed values of K_{os} range from approximately $10\,M^{-1}$ for complexes with 1− ions to approximately 3×10^3 for complexes with 3− ions.[98]

The rate constant for water-loss, k_{-w}, is characteristic of the reacting metal (Table 6.15). For many metals, the magnitude of k_{-w} can be explained by the electrostatic interaction between the metal cation and the coordinated water molecules, which is related to the charge and, inversely, to the size of the metal cation as shown in Figure 6.21. The particular inertness of some metals, such as Cr^{3+}, Rh^{3+}, Co^{3+}, and Ni^{2+}, relative to other metals has been attributed to unfavorable changes in ligand field stabilization energy (LFSE) during complex formation (c.f. Section 1.2). A ligand field activation energy (LFAE) can be derived by comparing the LFSE of the initial 6-coordinate octahedral complex with the LFSE of the 5-coordinate square pyramidal complex that results from dissociation of a coordinated water molecule.[4] This change in LFSE is most unfavorable for $d^3(Cr^{3+})$, $d^8(Ni^{2+})$, and (strong field) d^6 (Rh^{3+}) configurations.

The rate of water loss can be significantly accelerated by metal hydrolysis; this effect is especially important for slow-reacting metals[101] such as Cr(III),

SIDEBAR 6.3

Stability Constants for Outer-Sphere Complexes (K_{os})

A theoretical expression for K_{os}, derived from statistical considerations and including both the electrostatic interaction of the ions and the effect of ionic strength on those interactions,[98,99] is given by

$$K_{os} = \frac{4000\pi\mathcal{N}a^3}{3}\exp\left[\frac{-z_M z_L e^2}{4\pi\varepsilon_0\varepsilon\mathbf{k}Ta}\right]\exp\left[\frac{z_M z_L e^2\kappa}{4\pi_0\varepsilon\mathbf{k}T(1+\kappa a)}\right] \tag{i}$$

where κ is the Debye–Hückel ion atmosphere parameter[100]

$$\kappa^2 = \frac{2000e^2\mathcal{N}I}{\varepsilon_0\varepsilon\mathbf{k}T} \tag{ii}$$

These equations are written for SI units with the constants e (elementary charge) in C, $\mathbf{k}$ (Boltzmann constant) in $J\cdot K^{-1}$, $\mathcal{N}$ (Avogadro constant) in mol^{-1}, ε_0 (vacuum permittivity) $8.854 \times 10^{-12}\,J^{-1}C^2\,m^{-1}$, and T (absolute temperature) in K. The relative permittivity of the medium, ε, is 78.54 for water at 25°C. The parameter a is the distance of closest approach of the ions (usually 5×10^{-10} m). In the table below, values of K_{os} are calculated for different values of the product of the charges on the ions ($z_M z_L$) for ionic strengths (I) of both 0 and 0.1.

	$\log K_{os}$			$\log K_{os}$	
$z_M z_L$	$I=0$	$I=0.1$	$z_M z_L$	$I=0$	$I=0.1$
0	−0.50	−0.50			
−1	0.12	−0.93	+1	−1.12	−0.91
−2	0.74	0.32	+2	−1.74	−1.32
−3	1.36	0.72	+3	−2.36	−1.73
−4	1.98	1.13	+4	−2.98	−2.13
−6	3.22	1.95	+6	−4.22	−2.95
−8	4.46	2.76	+8	−5.46	−3.76
−9	5.08	3.17	+9	−6.08	−4.17
−12	6.94	4.39	+12	−7.94	−5.40

TABLE 6.15 Rate Constants for Water Exchange[a]

Metal Ion	k_{-w} (s^{-1})	Range of Reported Values	Ref.
Pb^{2+}	7×10^9		
Hg^{2+}	2×10^9		
Cu^{2+}	1×10^9	$(0.2–5) \times 10^9$	
Ca^{2+}	6×10^8	$(> 0.5–9) \times 10^8$	
Cd^{2+}	3×10^8	$(> 1–5) \times 10^8$	
La^{3+}	1×10^8	$(0.8–2) \times 10^8$	
Zn^{2+}	7×10^7	$(3–50) \times 10^7$	
Mn^{2+}	3×10^7	$(0.4–5) \times 10^7$	
Fe^{2+}	4×10^6	$(1–4) \times 10^6$	101
Co^{2+}	2×10^6	$(0.2–2) \times 10^6$	
Mg^{2+}	3×10^5	$(1–5) \times 10^5$	
Ni^{2+}	3×10^4	$(1–4) \times 10^4$	
Fe^{3+}	2×10^2	$(2–200) \times 10^2$	
Ga^{3+}	8×10^2	$(8–20) \times 10^2$	101
Al^{3+}	1	0.2–16	
Cr^{3+}	5×10^{-7}	$(4–6) \times 10^{-7}$	
Rh^{3+}	3×10^{-8}		
Fe^{3+}	2×10^2		101
$FeOH^{2+}$	1×10^5		101
$Fe(OH)_2^+$	10^7 (est)		102
$Fe(OH)_4^-$	10^9 (est)		102

[a]Unless otherwise noted, reference is to Margerum et al. (1978).[98] Values for k_{-w} assigned based on most current reference, most reliable method, or as average for narrow ranges of reported values.

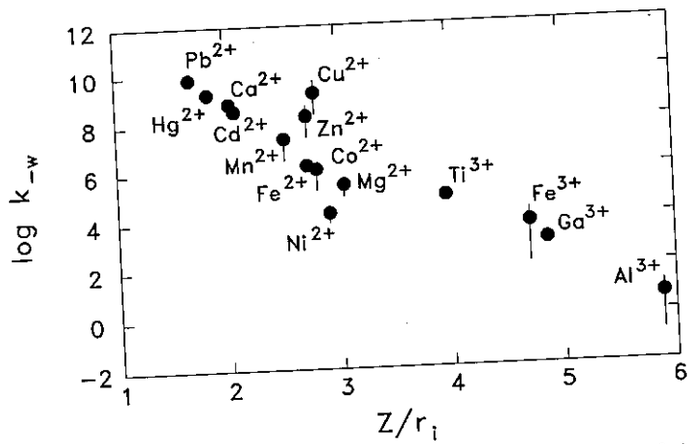

Figure 6.21 Water-loss rate constants for metal cations as a function of the ratio of the charge to the ionic radius of the metal ion. Rate constants from Margerum et al. (1978).[98] Adapted from Crumbliss and Garrison (1988).[101]

Al(III), and Fe(III) (see Table 6.15). Complexation by other inorganic ligands (e.g, Cl^-, NH_3, CO_3^{2-}) does not generally influence the rate of water loss from the metal as strongly as complexation by hydroxide. In practice, it may often be convenient to define an apparent rate constant for complex formation (k'_f) that includes the contribution of various inorganic metal species, thus

$$k'_f[M'] = k_{f0}[M^{2+}] + k_{f1}[MOH^+] + k_{f2}[MCl^+] + k_{f3}[MCO_3^0] + \cdots \tag{92}$$

where [M′] is the concentration of all inorganic metal species. This apparent rate constant must, of course, vary with pH and ionic strength.

The above mechanism for complex formation also holds for the reaction of metals with multidentate ligands if the rate-limiting step for complexation is the formation of the first metal–ligand bond. The effects of ligand structure, other than charge, are unfortunately difficult to generalize. Ligand protonation decreases the rate of complex formation often more than can be accounted for based on the change in ligand charge (see Margerum et al.[98] for further discussion).

Rate constants for complex dissociation can be related to formation rate constants through detailed balancing:

$$M + L \underset{k_b}{\overset{k_f}{\rightleftharpoons}} ML$$

$$k_b = k_f/K \tag{93}$$

If the formation rate constants for a reaction of a single metal with a series of ligands show little variation (being, as discussed above, mostly dependent on k_{-w}), then the dissociation rate constants should show an inverse correlation with the stability constant K. We have already seen an example of this correlation in Chapter 3 (Figure 3.16).

5.2 Kinetics of Metal- and Ligand-Exchange Reactions

Both metal- and ligand-exchange reactions involve three reacting species. For reaction of an initial complex ML with an incoming metal or ligand X, the rate of the overall reaction

$$ML + X \longrightarrow \begin{cases} XL + M \text{ (metal exchange)} \\ \text{or} \\ MX + L \text{ (ligand exchange)} \end{cases}$$

can be described by the rate expression

$$\frac{-d[ML]}{dt} = k_{ex}[ML][X] \tag{94}$$

This overall exchange reaction can proceed through two general pathways: a *disjunctive pathway*, involving complete dissociation of the initial complex, and an *adjunctive* pathway, involving direct attack of the incoming species on the initial complex.[94,103] For the metal-exchange reaction $ML + M^* \rightarrow M^*L + M$, these may be written:

Disjunctive mechanism	Adjunctive mechanism
$ML \rightleftharpoons M + L$	$M^* + ML \rightleftharpoons M^*LM$
$M^* + L \longrightarrow M^*L$	$M^*LM \longrightarrow M^*L + M$

where charges and protonated ligand species are omitted for simplicity. Analogous pathways can be written for ligand-exchange reactions. The rate law for the overall reaction then reflects the contributions of both of these pathways. When pseudoequilibrium can be assumed for the first step in the disjunctive pathway (which will usually be valid when the outgoing metal, M is in large excess), the overall rate of metal exchange is

$$\frac{-d[ML]}{dt} = \frac{-d[M^*]}{dt} = \frac{d[M^*L]}{dt} = k_{dis}\frac{[ML][M^*]}{[M]} + k_{adj}[ML][M^*]$$
$$= k_{ex}[ML][M^*] \qquad (95)$$

where k_{dis} is the rate constant for the disjunctive pathway and k_{adj} is the rate constant for the adjunctive pathway. These *stoichiometric* mechanisms can then

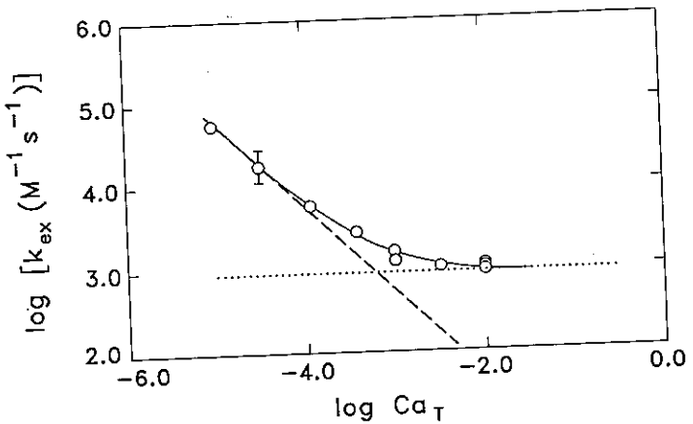

Figure 6.22 Rate constants for the metal-exchange reaction of Cu(II) with CaEDTA at pH = 8.2 as a function of (excess) calcium for rate $= -d[Cu]/dt = k_{ex}[Cu][CaEDTA]$, where $k_{ex} = (k_{dis}/[Ca] + k_{adj})$. Data (○) are shown with empirically derived contributions of the adjunctive pathway (···) and disjunctive pathway (– – –) to the observed rate constant (———). Adapted from Hering and Morel (1988).[103]

be distinguished by the dependence of the observed rate constant k_{ex} on the concentration of the outgoing metal M:

$$k_{ex} = \frac{k_{dis}}{[M]} + k_{adj} \qquad (96)$$

The variation in k_{ex} as a function of [M] is shown in Figure 6.22 for the reaction of Cu(II) with CaEDTA. The kinetic inhibition of formation of the CuEDTA complex at high calcium concentration is part of the explanation for the data shown in Figure 6.20.

The rate constants k_{dis} and k_{adj} are dependent on the ligand structure and, for k_{dis}, on pH. The disjunctive rate constant is determined by the rate constant for reaction of the incoming metal with the steady-state concentration of the free or protonated ligand intermediate. It is thus inversely proportional to the conditional equilibrium constant for the initial metal complex. The adjunctive rate constant is more dependent on ligand structure since either formation or dissociation of the intermediate dinuclear complex M*LM can be rate limiting. When the incoming metal M* is a transition metal and the outgoing metal M an alkaline earth metal, the formation of the dinuclear complex is more likely to be limiting. The adjunctive rate constant can be rationalized on the basis of the rate stability of the (outgoing) metal complex with a ligand fragment (corresponding to a partially dissociated complex), and the rate of reaction of

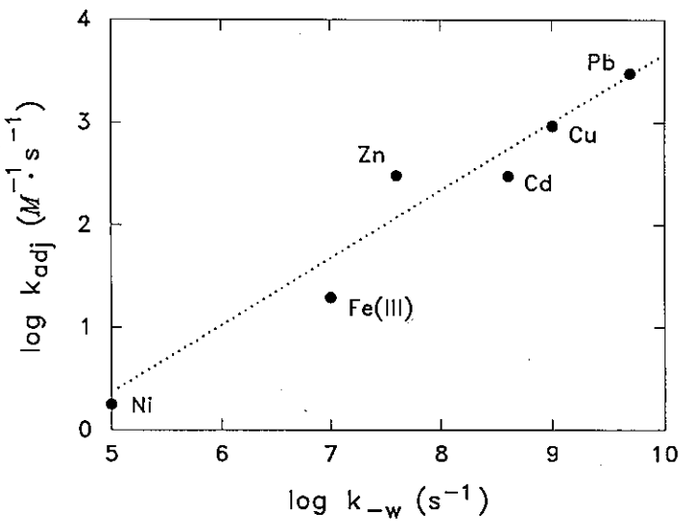

Figure 6.23 Correlation between adjunctive rate constants (k_{adj}) for reactions of CaEDTA with various metals in seawater and the water-loss rate constants of the metals (k_{-w}). From Hudson (1989).[104]

the incoming metal with this partially dissociated complex.[98,103] On this basis a correlation between the adjunctive rate constant for reactions of a specific complex with various metals and their water loss rate constants is expected.[104] Such a correlation for the reaction of CaEDTA is shown in Figure 6.23.

5.3 Kinetics of Double-Exchange Reactions

The overall double-exchange reaction

$$ML + M^*L^* \longrightarrow ML^* + M^*L$$

involves four reacting species in simultaneous metal- and ligand-exchange reactions. The overall reaction may be either "ligand-initiated"

$$ML \rightleftharpoons M + L$$
$$L + M^*L^* \longrightarrow M^*L + L^*$$

or "metal-initiated"

$$ML \rightleftharpoons M + L$$
$$M + M^*L^* \longrightarrow ML^* + M^*$$

Both of these pathways are disjunctive with respect to the complex ML and may be either adjunctive or disjunctive with respect to the reaction of the intermediate free M or L with the complex M*L*. The complete dissociation of both initial complexes is an unlikely pathway unless both are weak, as may be the case for alkaline earth metal complexes. Double-exchange reactions of transition metals often involve coordination chain mechanisms (e.g., further reaction of L*, produced by a "ligand-initiated" pathway, with initial complex ML) and the overall rates may be strongly dependent on trace concentrations of reactants that promote or terminate coordination chain mechanisms.[98]

* * *

Now we can understand why calcium has such a dramatic effect on the overall rate of formation of CuEDTA species when a competing ligand (i.e., humic acid) is present as shown in Figure 6.20. At high calcium concentrations, reaction of CaEDTA with added copper by a disjunctive pathway is not kinetically favored and reaction by an adjunctive pathway is slow compared to the formation of Cu–humate complexes. Thus because EDTA speciation in seawater is dominated by Ca, EDTA is effectively a much slower-reacting ligand than, in this case, humic acid. Once the Cu–humate complexes are formed, equilibrium can only be attained through slow double-exchange reactions. Note that this corresponds to the conditions chosen arbitrarily in the illustration of

pseudoequilibrium in Chapter 3 where the stronger ligand was assigned a slower rate constant for complex formation than the weaker ligand. The experimental data in Figure 6.20 can be modeled by assuming a "metal-initiated" double-exchange in which inorganic copper (in pseudoequilibrium with humate binding sites) reacts with CaEDTA. In this model, the formation of CuEDTA is taken to proceed via the same pathways, in which CaEDTA reacts with inorganic copper, whether or not humates and Cu–humate complexes are present. Then, since copper complexation by humates markedly decreases the inorganic copper concentration [Cu′], the rate of formation of CuEDTA

$$\frac{-d[\text{CuEDTA}]}{dt} = \left[\frac{k_{\text{diss}}}{[\text{Ca}^{2+}]} + k_{\text{adj}}\right][\text{Cu}'][\text{CaEDTA}] \qquad (97)$$

is slow in the presence of humates.

This example illustrates the somewhat counterintuitive point that the availability of multiple reaction pathways can, in some instances, decreases the rate at which the equilibrium distribution of ligand and metal species is attained. The most facile complexation reactions may not be the ones that lead most directly to the ultimate equilibrium distribution. Although the equilibrium speciation is determined by the lowest free energy of the system, the predominant path to this lowest energy state may not be the most direct one. As we have seen, slow complexation kinetics are most likely to be observed in systems containing mixtures of strong and weak ligands and high concentrations of alkaline earth metals or mixtures of competing transition metals.

The extrapolation of rates and mechanisms of complexation reactions to natural waters is hampered because of limited knowledge of the structure and reactivity of naturally occurring ligands. Certain principles, however, should still hold. The initial speciation of both metals and ligands in a system subject to some perturbation can profoundly influence the reaction pathways through which equilibrium is reestablished. In this way, species that have only little effect on the final equilibrium speciation can have a dramatic effect on the rate at which that equilibrium is attained. In estimating the rates of complexation reactions in natural waters and their effects on the overall rates of biogeochemical processes, the relative and absolute concentrations of all reacting species and the most probable reaction pathways under the natural conditions of interest must be considered.

6. TRACE METALS AND MICROORGANISMS

As mentioned early in this chapter, the complexation of trace metals in natural waters modulates their effects on the aquatic biota. The growth of all organisms is dependent on the acquisition of the proper quantities of many trace elements. Some trace metals such as iron, zinc, manganese, and copper are required for growth, but too high a concentration of these metals or others produce toxic

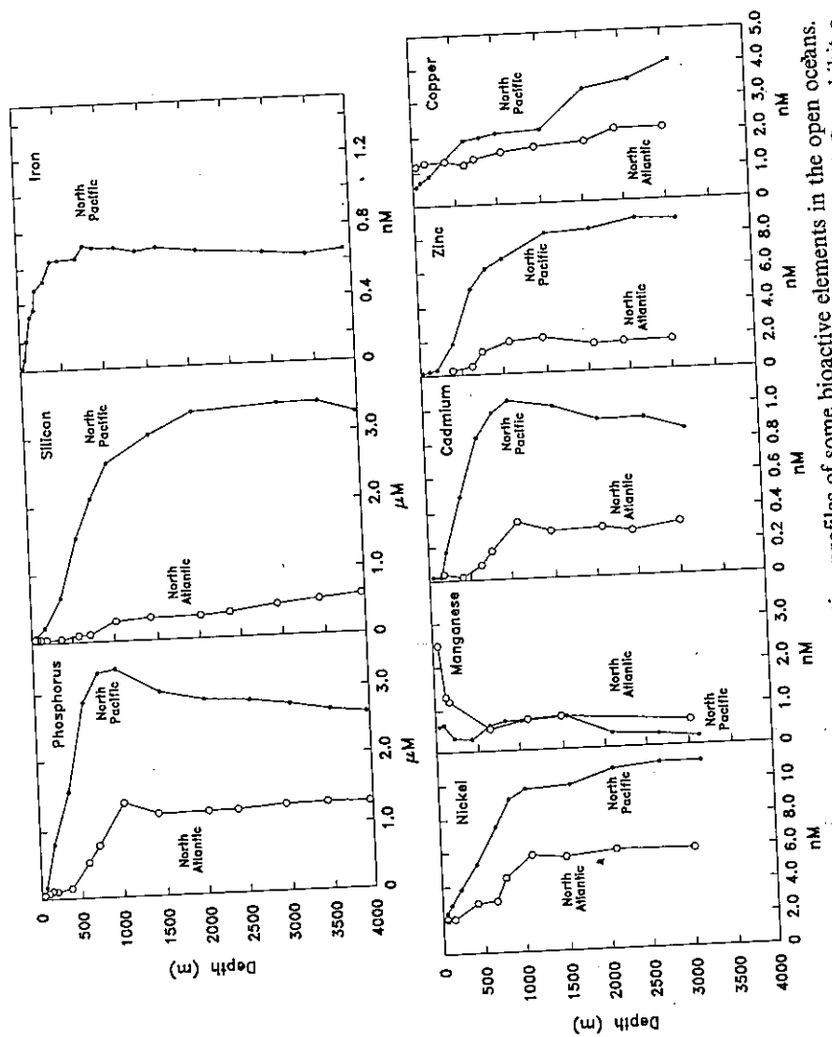

Figure 6.24 Dissolved concentration profiles of some bioactive elements in the open oceans. Like the major algal nutrients P and Si, the trace elements Ni, Cd, Zn, and Cu exhibit a characteristic surface depletion resulting from algal uptake. The dissolved concentration of Mn shows a surface maximum due to photoreductive dissolution of particulate Mn(IV) and bacterial oxidation of Mn(II) at depth. Iron from Martin et al. 1989;[106] others from Bruland and Franks, 1983.[105]

effects. Whereas higher organisms maintain a finely poised *internal milieu* for the proper operation of the various physiological tasks of the individual cells, aquatic microorganisms, particularly unicellular organisms such as phytoplankton and bacteria, must function in an *external milieu* whose chemistry is governed both by abiotic geochemical processes and by the action of the organisms themselves. Biological uptake of essential trace elements from the photic zone of lakes and oceans can be clearly seen in characteristic surface depletion.[105,106] As seen in Figure 6.24 both major nutrients N, P, and Si, and the trace nutrients Fe, Zn, Ni, Cu, and Cd are scavenged from oceanic surface waters. In addition to depleting surface concentrations through uptake, microorganisms can also influence trace metal chemistry by releasing complexing agents (see Section 4.2) and by inducing redox transformation (see Chapter 7). In this section we examine the kinetics of trace metal uptake by microorganisms, a process that is chiefly one of coordination chemistry and which controls both essential trace element availability and trace element toxicity.

Trace Element Uptake. Some compounds, including some trace metal complexes, are sufficiently lipid soluble that they can diffuse at significant rates through the lipid-bilayer membrane that is the major barrier between the inside of a unicellular organism and its external milieu. Passive diffusion governs the uptake of the dichloro-mercuric complex, $HgCl_2$, which is very toxic to aquatic microorganisms. In most cases, however, trace metal ions and their complexes have very low solubility in lipids and consequently very slow diffusion rates through cell membrances. Uptake of such trace metals is then catalyzed by a two-step process consisting first of chemical binding to a membrane uptake site, followed by transfer through the cell membrane and delivery to the inside of the cell. The steady-state kinetic description of such an uptake process is known as the Michaelis–Menten equation, as discussed in Chapter 3:

$$\rho = \frac{[\mathrm{M}]}{K_\mathrm{M} + [\mathrm{M}]}\rho_{\max} \tag{98}$$

TABLE 6.16 Michaelis–Menten Uptake Kinetics

Reaction	$\mathrm{M} + \mathrm{L} \underset{k_{-L}}{\overset{k_L}{\rightleftharpoons}} \mathrm{ML} \xrightarrow{k_{in}} \mathrm{M}_{cell}$
Uptake rate	$\rho = \dfrac{\rho_{\max}[\mathrm{M}]}{K_\mathrm{M} + [\mathrm{M}]}$
Maximum uptake rate	$\rho_{\max} = \mathrm{L}_T k_{in}$
Half-saturation constant	$K_\mathrm{M} = \dfrac{k_{-L} + k_{in}}{k_L}$

The maximum uptake rate ρ_{max} (mol L^{-1} $cell^{-1}$ s^{-1}) and the half saturation constant K_M(mol L^{-1}) are related to the concentration of uptake sites and the reaction rate constants as shown in Table 6.16. At low concentrations of the metal, $[M] < K_M$, the uptake rate is linearly related to [M]. At high concentrations, $[M] > K_M$, when most of the uptake ligands are bound to M, the uptake rate becomes saturated ($\rho = \rho_{max}$) and independent of [M]. Under normal circumstances, trace metal uptake ligands are far from saturated in natural waters: most of the ligands are free and available to react with the rare metals in the water. This is the case we shall focus on in the following discussion. The uptake rate is then a linear function of the metal concentration:

$$\rho = \frac{[M]}{K_M}\rho_{max} \tag{99}$$

Importance of Trace Metal Speciation. Coordination with transport sites on the surface of microorganisms is only one of the possible reactions for a trace metal in a natural water. The diagram of Figure 6.25 exemplifies a situation in which a coordination reaction with an organic chelating agent Y in excess dominates the speciation of a trace metal M which is taken up by cells via a cellular ligand L.[107] Although we shall consider only two dissolved species, M and MY, the following discussion applies to any set of species, dissolved or precipitated. In particular, M may represent the sum of all inorganic dissolved species of a given metal (denoted M') and MY may be a solid phase, such as an oxide or a hydroxide rather than an organic chelate.

The concentration of M, which depends on the relative rates of formation and dissociation of the competing complexes MY in solution and ML on the cells' surfaces, will reach a steady state after some characteristic time as discussed in Chapter 3 (see Figure 3.8).

Three possible limiting cases are shown on Figure 6.25: (A) The reactions with the ligands L and Y may be fast enough that the trace metal is in a condition of pseudoequilibrium in the medium; (B) the rate of binding to the surface ligand L may limit the metal uptake rate; (C) the rate of dissociation of the complex MY may limit the metal uptake rate.

A. Consider first a surface binding reaction that is reversible and reaches a pseudoequilibrium with M ($k_{in} \ll k_{-L}$, thus $k_L/k_{-L} = K_M$, the half saturation constant). This may be the case for a necessary metal that is relatively abundant or for a toxic metal transported adventitiously by the cells. At low cell concentrations the concentration of cellular ligands L is also low and the total concentration of M is determined by its equilibrium with Y. As depicted in Figure 6.25, both coordination reactions are then at pseudoequilibrium and the uptake rate, which is determined by the free metal concentration [M], is slow compared to all complexation and dissociation reactions.

B. The second limiting case is obtained for metal uptake systems that are largely irreversible ($k_{in} \gg k_{-L}$) as is observed for the transport of essential

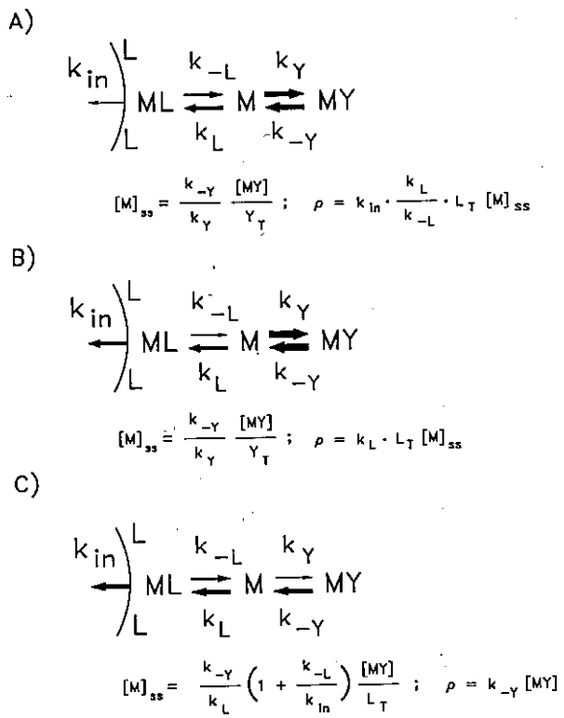

Figure 6.25 Limiting cases for the kinetics of biological uptake of a trace metal M in the presence of a chelator Y. (*a*) Pseudo-equilibrium between M and Y and between M and the surface uptake ligand L. (*b*) Pseudo-equilibrium between M and Y (fast kinetics) and quasi-irreversible uptake of M (slow). (*c*) Steady state between dissociation of the complex MY and quasi-irreversible uptake of M. The magnitudes of the fluxes are indicated by the widths of the arrows.

elements present as low concentrations in the medium. At low cell concentrations, the free metal concentration is again determined by pseudoequilibrium with the dominant ligand Y (compare A and B). However, the cell surface complex ML is then controlled by a steady state between binding and internalization, not pseudoequilibrium, and the uptake rate is simply the rate of formation of the surface complex. This case is characteristic of limiting trace elements in aquatic systems.

C. The third limiting case is characteristic of systems with high cell (and total cellular ligands) concentrations or with slow-dissociating ligands, Y, in the medium. The rate of uptake then becomes limited by the rate of dissociation of the complex MY. The free metal concentration decreases along with the uptake rate of individual cells as the concentrations of cells and total cellular ligands increase (the concentration of L per cell being constant). If the rate of dissociation from the surface ligand is much faster than the rate of internalization,

the cellular ligand and the metal remain at pseudoequilibrium as in the first case discussed above.

The Importance of Free Metal Concentrations. The conditions illustrated by cases A and B are those most relevant to natural waters where the ambient cell concentrations are usually modest and to laboratory cultures where the trace metals are extensively buffered by chelation. In both of those cases, the free concentration of the metal [M] determines its rate of uptake.

In case A this is true regardless of reaction mechanisms since pseudoequilibrium is achieved among all parties. The uptake rate is proportional to the concentration of the surface complex [ML], which depends on the free metal ion concentration [M]; [M] itself can be calculated from its equilibrium with the ligand Y ("thermodynamic control"). Thus the dependence of the biological response—the uptake rate or, as a result of limitation or toxicity, the growth rate—on the free metal ion concentration [M] does not signify that the free metal ion is the only species available (or toxic) to the organism. In an equilibrium system, the extent of all complexation reactions, including those that control the uptake rate, are determined by the free metal ion concentration regardless of reaction mechanisms. The free metal ion concentration merely provides a thermodynamic measure of the reactivity of the metal. The same result would obtain even if the chelated metal MY were "available"; that is, if a fast (adjunctive) metal exchange reaction occurred between MY and L.[108]

In contrast, in case B the importance of the free metal concentration results from the reasonable assumption that the exchange of the metal between the chelator Y and the uptake ligand L proceeds via dissociation of the complex MY (disjunctive process). Then it is the steady state concentration of the fast reacting metal species that determines the reaction rate with the transport ligands and, hence the uptake rate ("kinetic control"). Typically all the inorganic metal species may be considered to react rapidly and the relevant concentration is then their sum, denoted [M']. As seen in Section 5.8, an effective reaction rate constant, k'_L, can be determined for M' at given pH and major ion concentrations.

Because in most experiments the total metal and the total ligand concentrations are varied but the pH and major ion concentrations are kept constant, [M'] is proportional to [M]. Thus one cannot easily distinguish between "thermodynamic control" and "kinetic control" of the uptake. Figure 6.26*a* illustrates how in the presence of various complexing agents, the uptake of iron by microscopic algae is indeed dependent on the free iron concentration. In this case, we know from short-term studies of the reaction kinetics that the uptake is kinetically controlled as shown in Figure 6.26*b*, which depicts the individual reaction rates of iron in a typical experiment.

Metal Competition and Toxicity. No ligand, not even an uptake ligand, can be totally specific for a trace metal. Thus one expects that the binding of another metal to the uptake ligand for an essential metal may competitively inhibit its

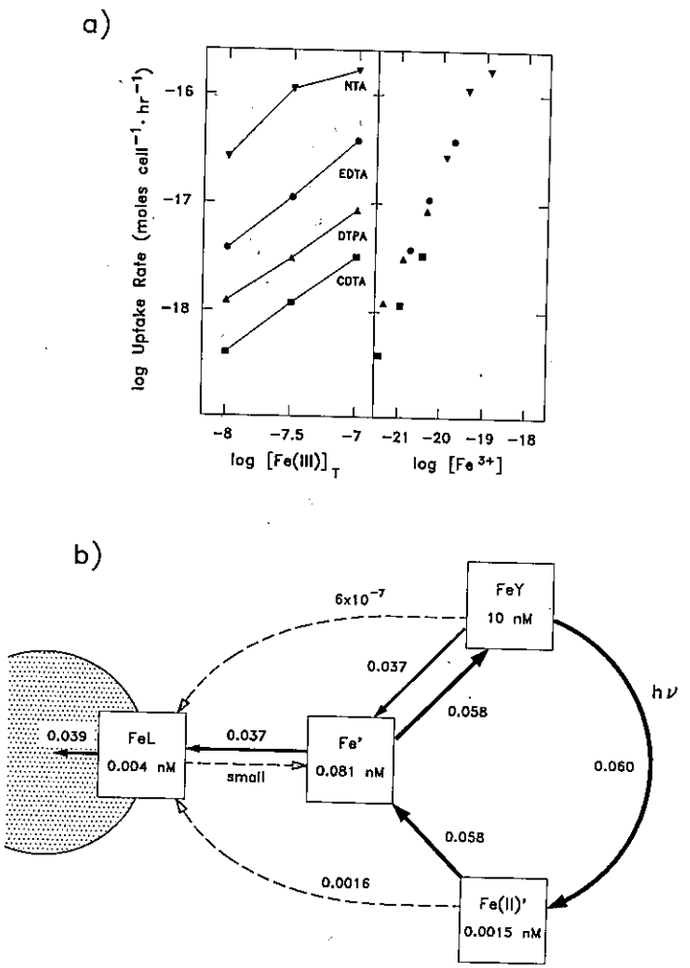

Figure 6.26 Kinetics of iron uptake in laboratory cultures of the marine diatom *Thalassosira weissflogii*. (*a*) Uptake rates at varying iron concentrations in the presence of 10^{-5} *M* of various chelating agents (1.4×10^7 cells L^{-1}). The uptake rate is a unique function of the free ferric ion concentration. Symbols indicate the organic ligand used to control iron speciation: (▼) NTA, (●) EDTA, (▲) DTPA, (■) CDTA. After Anderson and Morel, 1982.[108] (*b*) Measured and estimated rates of individual processes in an iron-limited culture containing 10^{-8} *M* iron and 10^{-5} *M* EDTA in the presence of 10^7 cells L^{-1} and with white-light illumination (ca. 100 μmol quanta $m^{-2}s^{-1}$). Both the thermal dissociation of FeEDTA and its photoreduction and reoxidation contribute to the formation of the dissolved inorganic Fe(III) pool which is responsible for the uptake. After Hudson and Morel, 1990.[107]

uptake. The extent of such inhibition can be simply calculated by considering the fraction of uptake ligand bound to the competing metal M* assumed to be at (pseudo)equilibrium with the ligand:

$$\text{percent of inhibition} = \frac{[M^*L]}{L_T} \tag{100}$$

If only a small fraction of the transport ligands is bound to the target metal M, this ratio can be written

$$\text{percent of inhibition} = \frac{K^*[M^*]}{1 + K^*[M^*]} \tag{101}$$

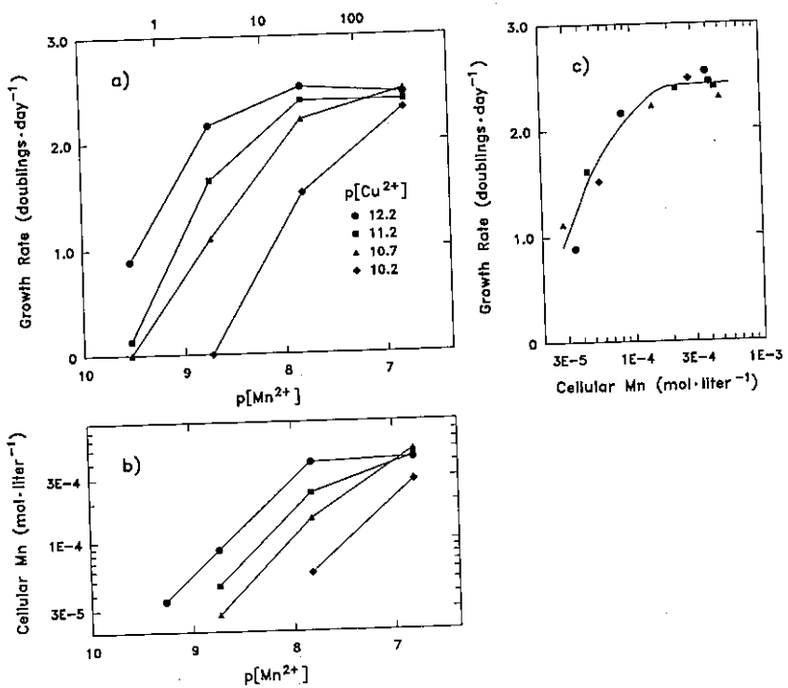

Figure 6.27 The relation between growth rate, free manganese ion concentration, cellular manganese concentration, and free cupric ion concentration in manganese-limited cultures of *Thalassosira pseudonana*. Increasing $[Mn^{2+}]$ or decreasing $[Cu^{2+}]$ increases the growth rate (A). In either case this is a reflection of an increasing intracellular concentration of the limiting nutrient manganese (B). The growth rate is a unique function of the intercellular manganese concentration (C), demonstrating that the toxicity of copper is the result of its inhibition of manganese uptake. After Sunda and Huntsman.[109]

Thus the uptake inhibition—and hence the inhibition of growth rate if M is limiting—is a function of the free concentration of the competing metal [M*] and of its affinity for the transport site.

An example of such competitive inhibition of manganese uptake by copper in a marine phytoplankton is illustrated in Figure 6.27. Under manganese-limited conditions, increasing copper decreases the growth rate. This is because the growth rate depends solely on the manganese content of the cells and as the copper concentration is increased, the cellular manganese is decreased. Additional manganese in the medium reverses the toxicity of copper.[109] Such antagonism between copper and manganese is thought to cause the low productivity of newly upwelled waters which contain low dissolved manganese and, presumably, low concentrations of chelating agents to reduce the inorganic concentration and hence the toxicity of copper.[110]

In the example of Figure 6.27, at a given manganese concentration, the growth rate is only a function of $[Cu^{2+}]$. This situation is a rather general one and may result from competitive inhibition of uptake of an essential metal (Mn) or from competitive inhibition of its assimilation or utilization. Thus, through proper calibration, the growth rate (or other appropriate measure of toxicity) of a microorganism can be used as a measure of the free concentration of toxic metals. This is the basis of the bioassay techniques that have been utilized to quantify metal chelation in natural waters.

Kinetic Control of Growth Rate. At steady state, the cellular concentration of a limiting element M is determined by a balance between the uptake rate and the rate of cell division:

$$\rho = \mu Q \tag{102}$$

where μ is the specific growth rate (in inverse time) and Q the cellular concentration of M (the "quota" expressed in mol cell^{-1}).

As illustrated above for iron, the acquisition of limiting trace metals is usually determined by a kinetically controlled uptake process involving uptake ligands in large excess (Case B in Figure 6.25). The uptake rate is then simply the rate of reaction of the metal with the uptake ligands:

$$\rho = k'_L[M']L_T \tag{103}$$

Thus from Equations 102 and 103 we obtain the growth rate as a simple expression of chemical kinetics:

$$\mu = \frac{1}{Q}k'_L[M']L_T \tag{104}$$

As discussed in Section 5.1, the effective complexation rate constant k'_L (applicable

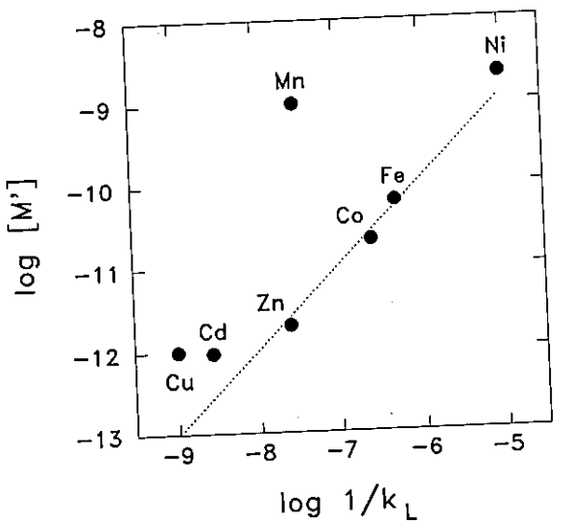

Figure 6.28. Apparent relationship between the concentration of inorganic metals in surface ocean water and their complexation rate constants. (Adapted from Morel et al., 1991[111] as corrected in Hudson and Morel, 1992.[112])

to the total inorganic metal concentration [M′]) is characteristic of the metal and fixed for a given pH and ionic medium. For any organism, the cellular parameters Q and L_T are adjustable within limits: for a given volume (or cellular mass) there is a minimum requirement of the essential metal M; for a given surface area there is a maximum concentration of uptake ligands that can be fit in the membrane without compromising its integrity. When these physiological limits are approached, Equation 104 provides an expression of the maximum growth rate attainable for a given inorganic concentration [M′] of the limiting trace metal. Equation 104 also shows how low the inorganic concentration of a trace element may get as a result of uptake by an organism growing at a given rate.[111,112]

If we postulate that for all essential trace elements there is a constant relationship between the maximum number of uptake ligands and the minimum cellular quota, then Equation 104 predicts an inverse relationship between [M′] and k'_L. Though the available data on inorganic trace metal concentrations in seawater are very few and still questionable, they seem indeed to follow such inverse dependence on complexation rates (Figure 6.28). If this is correct it would support the contention that many elements are, on average, limiting the growth of microorganisms in the sea. Complexation kinetics may be one of the keys to marine ecology.

REFERENCES

1. J. Burgess, *Metal Ions in Solution*, Ellis Horwood-Wiley, New York, 1978.
2. F. A. Cotton and G. Wilkinson, *Advanced Inorganic Chemistry*, 3rd ed., Wiley Interscience, New York, 1972, 1145 pp.
3. J. J. Christensen and R. M. Izatt, *Handbook of Metal–Ligand Heats*, Marcel Dekker, New York, 1983, 783 pp.
4. J. E. Huheey, *Inorganic Chemistry*, 3rd ed., Harper and Row, New York, 1983, 936 pp.
5. J. Burgess, *Ions in Solution*, Ellis Horwood, Chichester, 1988, 191 pp.
6. A. E. Martell and R. M. Smith, *Critical Stability Constants*, Vol. 1, *Amino Acids*, Plenum, New York, 1974; R. M. Smith and A. E. Maltell, Vol. 2, *Amines*, Plenum, New York, 1975; A. E. Martell and R. M. Smith, Vol. 3, *Other Organic Ligands*, Plenum, New York, 1977; R. M. Smith and A. E. Martell, Vol. 4, *Inorganic Ligands*, Plenum, New York, 1976.
7. M. Whitfield, *Limnol. Oceanogr.*, **19**, 235 (1974).
8. C. F. Baes, Jr. and R. E. Mesmer, *The Hydrolysis of Cations*, Wiley, New York, 1976.
9. W. G. Sunda and P. J. Hanson, in *Chemical Modeling in Aqueous Systems*, E. A. Jenne, Ed., ACS Symposium Series 93, American Chemical Society, Washington, DC, 1979.
10. J. Sainte Marie, A. E. Torma, and A. O. Gübeli, *Can. J. Chem.*, **42**, 662 (1964).
11. J. J. Morgan, in *Principles and Application in Water Chemistry*, S. D. Faust and J. V. Hunter, Eds., Wiley, New York, 1967.
12. W. Stumm and J. J. Morgan, *Aquatic Chemistry*, 2nd ed., Wiley, New York, 1981, p. 332.
13. L. G. Sillén and A. E. Martell, *Stability Constants of Metal–Ion Complexes*, Special Publications Nos. 17 and 25, Chemical Society, London, 1964 and 1971.
14. H. Irving and R. J. P. Williams, *J. Chem. Soc.*, 3192 (1953).
15. F. A. Cotton and G. Wilkinson, *Basic Inorganic Chemistry*, Wiley, New York, 1976, 579 pp.
16. H. D. Holland, *The Chemistry of the Atmosphere and Oceans*, Wiley, New York, 1978.
17. R. M. Garrels and M. E. Thompson, *Am. J. Sci.*, **57**, 260 (1962).
18. K. S. Johnson and R. M. Pytkowicz, *Mar. Chem.*, **8**, 87 (1979).
19. R. A. Horne, *Marine Chemistry*, Wiley, New York, 1969.
20. W. Stumm and J. J. Morgan, *Aquatic Chemistry*, 2nd ed., Wiley, New York, 1981, p. 364.
21. J. Boulègue, J. P. Ciabrini, C. Fouillac, G. Michard, and G. Ouzounian, *Chem. Geol.*, **25**, 19 (1979).
22. J. Boulègue and G. Michard, in *Chemical Modeling in Aqueous Systms*, E. A. Jenne, Ed., ACS Symposium 93, American Chemical Society, Washington, DC, 1979.
23. Y. Sugimura and Y. Suzuki, *Mar. Chem.*, **24**, 105 (1988).
24. J. R. Toggweiler, *Nature*, **334** 468 (1988).

25. J. Buffle, *Complexation Reactions in Aquatic Systems*, Ellis Horwood, Chichester, 1988, 692 pp.
26. E. M. Thurman, Organic Geochemistry of Natural Waters, Martinus Nijhoff/Dr. W. Junk Publishers, Dordrecht, 1985, 497 pp.
27. C. M. Burney, K. M. Johnson, D. M. Lavoie, and McN. Sieburth, *Deep Sea Res.*, **26**, 1267 (1979).
28. R. Benner, J. D. Pakulski, M. McCarthy, J. I. Hedges, and P. G. Hatcher, *Science*, **255**, 1561 (1992).
29. R. J. Kieber, X. Zhou, and K. Mopper, *Limnol. Oceanogr.*, **37**, 1503 (1990).
30. K. Mopper and X. Zhou, *Science*, **250**, 661 (1990).
31. W. Stumm and P. A. Brauner, in *Chemical Oceanography*, 2nd ed., E. K. Duursma and R. Dawson, Eds., Academic, London, 1975.
32. R. F. C. Mantoura, in *Marine Organic Chemistry*, E. K. Duursma and R. Dawson, Eds., Elsevier, Amsterdam, 1981.
33. F. M. M. Morel, R. E. McDuff, and J. J. Morgan, in *Trace Metals and Metal–Organic Interactions in Natural Waters*, P. C. Singer, Ed., Ann Arbor Science, Ann Arbor, MI, 1973.
34. K. H. Coale and K. W. Bruland, *Limnol. Oceanogr.*, **33**, 1084 (1988).
35. J. G. Hering, W. G. Sunda, R. L. Ferguson, and F. M. M. Morel, *Mar. Chem.*, **20**, 299 (1987).
36. D. L. Huizenga and D. R. Kester, *Mar. Chem.*, **13**, 281 (1983).
37. W. G. Sunda and A. K. Hanson, *Limnol. Oceanogr.*, **32**, 537 (1987).
38. J. W. Moffett and R. G. Zika, *Mar. Chem.*, **21**, 301 (1987).
39. W. G. Sunda and R. L. Ferguson, in *Trace Metals in Sea Water*, C. S. Wong, E. Boyle, K. W. Bruland, J. D. Burton, and E. D. Goldberg, Eds., Plenum, New York, 1983.
40. K. W. Bruland, *Limnol. Oceanogr.*, **34**, 269 (1989).
41. J. R. Donat and K. W. Bruland, *Mar. Chem.*, **28**, 301 (1990).
42. C. M. G. van den Berg, A. G. A. Merks, and E. K. Duursma, *Est. Coast. Shelf Sci.*, **24**, 784 (1987).
43. C. M. G. van den Berg and S. Dharmvanij, *Limnol. Oceanogr.*, **29**, 1025 (1984).
44. G. Capodaglio, K. H. Coale, and K. W. Bruland, *Mar. Chem.*, **29**, 221 (1990).
45. G. A. Gill and K. W. Bruland, *Environ. Sci. Technol.*, **24**, 1392 (1990).
46. C. T. Driscoll, J. P. Baker, J. J. Bisogni, and C. L. Schofield, in *Acid Precipitation: Geological Aspects*, O. Bricker, Ed., Butterworths, Boston, 1984.
47. J. C. Duinker and C. J. M. Kraemer, *Mar. Chem.*, **5**, 207 (1977).
48. W. G. Sunda, *Mar. Chem.*, **14**, 365 (1984).
49. K. W. Bruland, *Limnol. Oceanogr.*, **36**, 1555 (1991).
50. J. C. Westall, F. M. M. Morel, and D. N. Hume, *Anal. Chem.*, **51**, 1792 (1979).
51. J. L. Means, T. Kucak, and D. A. Crerrar, *Environ. Poll. (ser. B)*, **1**, (1980).
52. J. Gardiner, *Wat. Res.*, **10**, 507 (1976).
53. J. L. Means, D. A. Crerar, and J. O. Duguid, *Science*, **200**, 1477 (1978).
54. W. Giger, H. Ponusz, A. Alder, D. Baschnagel, D. Renggli, C. Schaffner, EAWAG Jahresbericht, EAWAG/ETH, Zurich, 1987.

55. A. C. Alder, H. Siegrist, W. Gujer, and W. Giger, *Water Res.*, **24**, 733 (1990).
56. H.-J. Brauch and S. Schullerer, *Vom Wasser*, **69**, 155 (1987).
57. J. M. Cleveland and T. F. Rees, *Science*, **212**, 1506 (1981).
58. R. W. D. Killey, J. O. McHugh, D. R. Champ, E. L. Cooper, and J. L. Young, *Environ. Sci. Technol.*, **18**, 148 (1984).
59. J. B. Neilands, *Ann. Rev. Biochem.*, **50**, 715 (1981).
60. B. F. Matzambe, G. Müller-Matzambe, and K. M. Raymond, *Phys. Bioinorg. Chem.*, Series 5, 3 (1989).
61. C. G. Trick, R. J. Andersen, A. Gillam, and P. J. Harrison, *Science*, **219**, 306 (1983).
62. C. M. Brown and C. G. Trick, *Arch. Microbiol.*, **157**, 349 (1992).
63. C. G. Trick and A. Kerry, *Curr. Microbiol.*, **24**, 241 (1992).
64. J. B. Neilands, *Ann. Rev. Microbiol.*, **36**, 285 (1982).
65. K. N. Raymond and C. J. Carrano, *Accts. Chem. Res.*, **12**, 183 (1979).
66. P. E. Powell, G. R. Cline, C. P. P. Reid, and P. J. Szaniszlo, *Nature*, **287**, 833 (1980).
67. M. Estep, J. E. Armstrong, and van Baalen, *App. Environ. Microbiol.*, **30**, 186 (1975).
68. T. P. Murphy, D. R. S. Lean, and C. Nalewajko, *Science*, **192**, 900 (1976).
69. E. Gill, E. L. Winnacker, and M. H. Zenk, *Science*, **30**, 674 (1985).
70. W. Gekeler, E. Grill, E.-L. Winnacker, and M. H. Zenk, *Arch. Microbiol.*, **150**, 197 (1988).
71. Y. Kojima and J. H. R. Kagi, *Metallothioneins TIBS*, **4**, (1978).
72. R. C. Averett, J. A. Leenheer, D. M. McKnight, and K. A. Thorn, Eds., *Humic Substances in the Sunwannee River, Georgia: Interactions, Properties and Proposed Structures.* U.S. Geological Survey Open File Report 87–557, 1989.
73. G. R. Aiken, D. M. McKnight, R. L. Wilson, and R. MacCarthy, Eds., *Humic Substances in the Soil, Sediment, and Water*, Wiley, New York, 1985.
74. D. H. Stuermer and G. R. Harvey, *Mar. Chem.*, **6**, 55 (1978).
75. G. R. Harvey, D. A. Boran, L. S. Chesal, and J. M. Tokar, *Mar. Chem.*, **12**, 119 (1983).
76. R. L. Crawford, *Lignin Biodegradation and Transformation*, Wiley, New York, 1981.
77. M. A. Wilson, P. F. Barron, and A. H. Gillam, *Geochim. Cosmochim. Acta*, **45**, 1743 (1981).
78. E. M. Perdue, *Geochim. Cosmochim. Acta*, **42**, 1351 (1978).
79. B. M. Bartschat, S. E. Cabaniss, and F. M. M. Morel, *Environ. Sci. Technol.*, **26**, 284 (1992).
80. T. C. Hutchinson and K. M. Meema, Eds., *Lead, Mercury, Cadmium, and Arsenic in the Environment, SCOPE 31*, John Wiley and Sons, Chichester, 1987, 360 pp.
81. K. Fent, *Mar. Environ. Res.*, **28**, 477 (1989).
82. C. C. Gilmour, J. H. Tuttle, and J. C. Means, in *Marine and Estuarine Geochemistry*, A. C. Sigleo and A. Hattori, Eds., Lewis, Chelsea, MI, 1985, pp. 239–258.
83. O. F. X. Donard, F. T. Short and J. H. Weber, *Can. J. Fish. Aq. Sci.*, **44**, 140 (1987).
84. R. P. Mason and W. F. Fitzgerald, *Nature*, **347**, 457 (1990).
85. N. Bloom, *Can. J. Fish. Aq. Sci.*, **46**, 1131 (1989).
86. R. J. Maguire, R. J. Tkacz, Y. K. Chan, G. A. Bengert, and P. T. S. Wong, *Chemosphere*, **15**, 253 (1986).

87. J. J. Cleary and A. R. D. Stebbing, *Mar. Poll. Bull.*, **18**, 238 (1987).
88. C. L. Alzieu, J. Sanjuan, J. P. Itreil, and M. Borel, *Mar. Poll. Bull.*, **17**, 494 (1986).
89. M. O. Andrea and P. N. Froelich, Jr., *Tellus*, **36B**, 101 (1984).
90. L. C. D. Anderson and K. W. Bruland, *Environ. Sci. Technol.*, **25**, 420 (1991).
91. J. P. Kim and W. F. Fitzgerald, *Science*, **231**, 1131 (1986).
92. J. T. Byrd and M. O. Andreae, *Science*, **218**, 565 (1982).
93. P. J. Craig, Ed., *Organometallic Compounds in the Environment*, Longman, Essex, 1986, 368 pp.
94. This discussion is based on J. G. Hering and F. M. M. Morel, in *Aquatic Chemical Kinetics*, W. Stumm, Ed., Wiley-Interscience, New York, 1990, pp. 145–171.
95. C. J. M. Kraemer, *Mar. Chem.*, **18**, 335 (1986).
96. S. E. Cabaniss and M. S. Shuman, *Anal. Chem.*, **60**, 2418 (1988).
97. J. G. Hering and F. M. M. Morel, *Geochim. Cosmochim. Acta*, **53**, 611 (1989).
98. D. W. Margerum, G. R. Cayley, D. C. Weatherburn, and G. K. Pagenkopf, in *Coordination Chemistry*, Vol. 2, A. E. Martell, Ed., ACS Monograph 174, Washington, DC, 1978, pp. 1–220.
99. J. N. Israelachvili, *Intermolecular and Surface Forces*, 2nd. ed., Academic Press, London, 1992, p. 33.
100. P. C. Hiemenz, *Principles of Colloid and Surface Chemistry*, 2nd ed., Dekker, New York, 1986, p. 691.
101. A. L. Crumbliss and J. M. Garrison, *Comments Inorg. Chem.*, **8**, 1 (1988).
102. W. Schneider, Personal Communication.
103. J. G. Hering and F. M. M. Morel, *Environ. Sci. Technol.*, **22**, 1469 (1988).
104. R. J. M. Hudson, "The Chemical Kinetics of Iron Uptake by Marine Phytoplankton," Ph.D. Thesis, Massachusetts Institute of Technology, Cambridge, MA, 1989.
105. K. W. Bruland and R. P. Franks, in *Trace Metals in Seawater*, C. S. Wong, E. Boyle, K. W. Bruland, J. D. Burton, and E. D. Goldberg, Eds., Plenum, New York, 1983.
106. J. H. Martin, R. M. Gordon, S. Fitzwater, and W. W. Broenkow, *Deep Sea Res.*, **36**, 649 (1989).
107. R. J. M. Hudson and F. M. M. Morel, *Limnol. Oceanogr.*, **35**, 1002 (1990).
108. M. A. Anderson and F. M. M. Morel, *Limnol. Oceanogr.*, **27**, 789 (1982).
109. W. G. Sunda and S. A. Huntsman, *Limnol. Oceanogr.*, **28**, 924 (1983).
110. W. G. Sunda, R. T. Barber, and S. A. Huntsman, *J. Mar. Res.*, **39**, 567 (1981).
111. F. M. M. Morel, R. J. M. Hudson, and N. M. Price, *Limnol. Oceanogr.*, **36**, 1742 (1991).
112. R. J. M. Hudson and F. M. M. Morel, *Deep Sea Res.*, (in press) (1992).

PROBLEMS

6.1 **a.** Using the same major ion composition as in Example 1, calculate the inorganic speciation of nickel and mercury in freshwater at pH = 8.1.

b. Maintaining C_T constant, calculate the effect of pH (from 5 to 12) on the inorganic speciation of nickel and mercury.

c. At what pH's would the carbonate or hydroxide solids precipitate given $[Ni]_T = [Hg]_T = 10^{-7}\,M$?

6.2 Consider the usual approximate stoichiometric reaction of photosynthesis: $CO_2 + H_2O \rightarrow$ "CH_2O" $+ O_2$. Note that this reaction changes both C_T and pH. Assuming the system to be closed to the atmosphere, discuss quantitatively the effect of an algal bloom on the formation of carbonate and bicarbonate trace metal complexes [e.g., $CuCO_3$(aq) and $CuHCO_3^+$].

6.3 What is the effect of major ion associations in seawater on (a) pH (at equilibrium with the atmosphere), and (b) carbonate and bicarbonate trace metal complexes.

6.4 **a.** Redo Example 6 of Chapter 5 adding $Ca_T = 10^{-3}\,M$ and $[NTA]_T = 10^{-4}\,M$ to the recipe of the system and letting $CaCO_3$(s) supersaturate.

b. How much NTA would have to be added at any pH to avoid precipitation of the iron [$Y_T = Y_T$(pH)]?

c. Redo parts a and b for $CaCO_3$(s) precipitation.

6.5 Consider a seawater culture medium containing $[EDTA]_T = 5 \times 10^{-5}\,M$, $Fe(III)_T = 10^{-8}\,M$ and $Cd_T = 10^{-10}\,M$. ($I = 0.5\,M$, $Ca_T = 10^{-2}\,M$, and pH = 8.2.)

a. Calculate the speciation and the free concentrations of EDTA, Fe, and Cd.

b. $4 \times 10^{-5}\,M$ $CdCl_2$ is added to the system. Calculate the new speciation and new free concentrations. What would the result have been if $4 \times 10^{-5}\,M$ CdEDTA had been added to the system?

c. The algae in the cultures (10^6 cells L^{-1}) have on their surface an iron-transport molecule characterized by $X_T = 10^{-16}$ mol cell^{-1}; $K_{Fe} = 10^{19}$; $K_{Cd} = 10^8$. How much Fe and Cd is bound to the cells before and after $CdCl_2$ addition? What is the net effect of the Cd addition on the Fe transport rate?

6.6 A lake with the simple composition

$$Na_T = Ca_T = Mg_T = K_T = Cl_T = [SO_4]_T = [CO_3]_T = 10^{-3}\,M$$

contains an organic complexing agent Y, characterized by

$$\begin{aligned} HY &= H^+ + Y^- && pK_a = 6.0 \\ CuY^+ &= Cu^{2+} + Y^- && pK = 7.0 \\ CaY^+ &= Ca^{2+} + Y^- && pK = 2.0 \\ MgY^+ &= Mg^{2+} + Y^- && pK = 2.0 \end{aligned}$$

a. Consider no solid phase but all the relevant complexes. Calculate the copper speciation at pH = 7.0 ($Cu_T = 10^{-7}\,M$; $Y_T = 10^{-6}\,M$). Calculate the copper speciation as a function of pH.

b. Consider now that $Cu_T = 10^{-6}\,M$ and that copper carbonates and/or hydroxide may precipitate (same inorganic and organic species as in part a). Calculate the critical pH('s) of precipitation of the solid(s) in the absence of organic ligand. What solid(s) should form as pH varies from 6 to 12? Sketch a major Cu species diagram on a $\log Y_T$ versus pH graph.

CHAPTER 7

OXIDATION–REDUCTION

The geochemical cycles of elements are driven in part by oxidation–reduction reactions. Some mineral phases such as metal sulfides are dissolved through oxidation by oxygen, others such as iron oxides through reduction in anoxic environments; conversely, some solutes are ultimately precipitated as reduced sulfides or as oxides. Although significant, this auxiliary role of redox chemistry in the exogenic cycle of elements is not our major focus in this chapter. As unstable chemical entities fueled by a continual diet of decomposing compounds, sustained by a constant energy flux from oxidation reactions, we are motivated by more than pure academic curiosity to study redox chemistry; it is a simple, or not so simple, matter of life and death. Life is by nature a redox process and a majority of redox processes on the earth are life dependent. From our point of view the subject of the redox cycles of elements thus takes on an importance disproportionate to the relatively small elemental fluxes that are involved.

Fueling all the redox cycles on the earth's surface is one fundamental, thermodynamically unfavorable process, photosynthesis. Using solar energy through specialized pigments and organelles, plants reduce inorganic carbon to organic matter and produce oxygen, thus increasing the Gibbs free energy of the earth:

$$CO_2(g) + H_2O \longrightarrow \text{“}CH_2O\text{”} + O_2(g); \qquad \Delta G^\circ = +478\,\text{kJ mol}^{-1} \qquad (1)$$

With very few exceptions, this energy capturing process drives all other redox reactions: organic matter is the ultimate reductant; oxygen, the ultimate oxidant.